



Acquisition of 3D Topography

Automated 3D road and building reconstruction
using airborne laser scanner data and topographic maps

Sander Oude Elberink

ACQUISITION OF 3D TOPOGRAPHY
AUTOMATED 3D ROAD AND BUILDING RECONSTRUCTION USING
AIRBORNE LASER SCANNER DATA AND TOPOGRAPHIC MAPS

Sander Oude Elberink
March 2010



International Institute for Geo-information Science and Earth Observation,
Enschede, The Netherlands

ITC dissertation number 167
ITC, P.O. Box 6, 7500 AA Enschede, The Netherlands

ISBN 978-90-6164-287-9
Cover designed by SOESET © 2010
Printed by Optima Grafische Communicatie B.V.
Copyright © 2010 by Sander Oude Elberink

This dissertation is published under the same title in the series Publications on Geodesy
74, Netherlands Geodetic Commission, Delft, the Netherlands, with ISBN 978 90 6132
318 1.

More information: info@ncg.knaw.nl, www.ncg.knaw.nl

ACQUISITION OF 3D TOPOGRAPHY
AUTOMATED 3D ROAD AND BUILDING RECONSTRUCTION USING
AIRBORNE LASER SCANNER DATA AND TOPOGRAPHIC MAPS

DISSERTATION

to obtain
the degree of doctor at the University of Twente,
on the authority of the rector magnificus,
prof.dr. H. Brinksma,
on account of the decision of the graduation committee,
to be publicly defended
on Friday March 26, 2010 at 13.15 Hrs

by

Sander Jakob Oude Elberink

born on April 24th 1976

in Almelo, The Netherlands

This thesis is approved by
Prof. dr. ir. M.G. Vosselman, promotor

Acknowledgements

Niet vergeten om der eben bij stille te staon
Niet vergeten eben knippen met de vingers
Niet vergeten dit moment in't geheugen op te slaon
Zo van oja, dat was mooi

...
Daniël Lohues, *Oja, dat was mooi*, Allenig III, 2009.

When something good happens, snap your fingers, do not forget to memorise this moment. That is a free translation of what singer songwriter Lohues sings in his song “Oja, dat was mooi”. Looking back at the past four years, many good things have happened. I would like to thank the ones who definitively contributed to making these good things happen.

George. Thank you for calling my attention to this great PhD opportunity, and keeping the challenge high during the whole period. I enjoyed every inch of this research project.

Pu. We started our journey on the same day in 2005, with the same destination in mind. Thanks for the support and discussions along the way. I can't think of a better PhD buddy than one who reaches the destination on the same day. Thanks and congratulations in advance.

Being part of an inspiring team makes PhD life easier. I would like to express my thanks to all EOS colleagues and the project partners of RGI project 011 ‘3D Topography’.

Lizet. I keep on memorising good moments ever since we are together. Living with you is the biggest joy in my life. Thank you for making me smile when I think about our future.

Table of Contents

Part I: Introduction to acquisition of 3D topography	1
1 Introduction	3
1.1 3D Topography	4
1.2 Scope and limitations.....	6
1.3 Input data.....	6
1.4 Research problems.....	7
1.5 Goal and objectives.....	8
1.6 Importance	9
1.7 Thesis outline.....	9
2 Use of 3D topography	11
2.1 Introduction.....	12
2.2 User requirements	13
2.2.1 Municipality of Den Bosch.....	13
2.2.2 Survey Department of Rijkswaterstaat	13
2.2.3 Water board “Hoogheemraadschap de Stichtse Rijnlanden”	15
2.2.4 Topographic Service of the Dutch Cadastre.....	15
2.3 Re-using 3D models	16
2.3.1 Municipality of Den Bosch.....	18
2.3.2 Survey Department of Rijkswaterstaat	19
2.3.3 Water board “Hoogheemraadschap de Stichtse Rijnlanden”	19
2.3.4 Topographic Service of the Dutch Cadastre.....	19
2.3.5 Availability and distribution	19
2.3.6 Data fusion	19
2.3.7 Generalization and filtering	20
2.3.8 3D Represents as-is situation.....	20
2.4 Role of use cases in research project.....	20
2.5 Recent developments in using 3D topography	21
2.6 Conclusions.....	22
Part II: 3D Roads	25
3 3D Reconstruction of roads.....	27
3.1 Introduction.....	28
3.2 Related work	29
3.2.1 Road reconstruction from aerial images.....	29
3.2.2 2D Road mapping from laser data	29
3.2.3 3D Reconstruction from laser data	30
3.3 Proposed approach	30
3.4 Data sources	32
3.4.1 Airborne laser scanner data.....	33
3.4.2 Pre-processing laser data.....	33
3.4.3 2D Topographic map data.....	34
3.4.4 Pre-processing 2D map	34
3.5 Fusion of map and laser data	35
3.5.1 Research problems on fusing map and laser data	35
3.5.2 Proposed fusion algorithm	36
3.6 3D Reconstruction of polygons.....	39

3.6.1	Polygon boundaries.....	39
3.6.2	Additional polygons.....	40
3.6.3	Assumptions on boundaries.....	41
3.6.4	Surfaces.....	42
3.7	Results.....	43
3.7.1	Interchange “Prins Clausplein”.....	43
3.7.2	Interchange “Waterberg”.....	45
3.8	Discussion.....	47
3.8.1	Parameter settings.....	47
3.8.2	Topological correctness.....	49
4	Quality analysis on 3D roads.....	51
4.1	Error propagation.....	52
4.1.1	Quality of plane at map point location.....	52
4.1.2	Quality of laser block.....	53
4.1.3	Quality of plane model.....	53
4.2	Reference data.....	56
4.2.1	Height differences between reference data and 3D model.....	57
4.3	Testing of predicted quality.....	60
4.4	Discussion.....	62
Part III: 3D Buildings.....		65
5	Building shape detection.....	67
5.1	Introduction.....	68
5.1.1	Real buildings vs 3D model representation.....	69
5.1.2	Real buildings vs appearance in input data.....	70
5.1.3	Appearance in input data vs 3D model representation.....	70
5.2	Related work.....	71
5.2.1	2D Mapping of building outlines.....	71
5.2.2	3D Reconstruction of buildings.....	72
5.3	Research problems.....	73
5.3.1	Problems on roof shape detection.....	74
5.3.2	Problems on scene complexity.....	77
5.4	Proposed approach.....	78
5.5	Information from map data.....	80
5.6	Features from laser data.....	81
5.6.1	Segmentation of laser scanner data.....	81
5.6.2	Intersection lines.....	82
5.6.3	Step edges.....	83
5.6.4	Roof topology graph.....	85
5.7	Target graphs.....	86
5.8	Target based graph matching.....	87
5.9	Complete matching results.....	89
5.10	Incomplete matching results.....	90
6	3D Building Reconstruction.....	93
6.1	Introduction.....	94
6.2	Components of a roof boundary.....	95
6.3	Approach 1: Combine features from complete match results.....	96
6.4	Extension of horizontal intersection lines.....	98
6.5	Outer boundaries of roof faces.....	100

6.5.1	Flat roof faces.....	100
6.5.2	Eave construction.....	101
6.5.3	Gutter construction.....	101
6.6	Dormers and step edges.....	102
6.6.1	Simple dormers.....	102
6.6.2	Step edges.....	103
6.6.3	Step edges for map subdivision.....	104
6.7	Reconstruction of walls.....	105
6.8	Approach 2: reconstructed targets.....	106
6.8.1	Parameterised target models.....	107
6.8.2	Use of map data.....	110
6.8.3	Limitations.....	111
6.8.4	Potential use.....	111
6.9	Summary.....	114
7	Results and evaluation.....	115
7.1	Introduction.....	116
7.2	Results.....	119
7.2.1	Approach 1: Combined features.....	119
7.2.2	Approach 2: Reconstructed targets.....	123
7.3	Evaluation.....	127
7.3.1	Laser data features.....	128
7.3.2	Evaluation on target based matching.....	133
7.3.3	Reconstructed models.....	138
7.3.4	Problematic situations.....	146
7.3.5	Performance in time.....	150
7.4	Potential for nation wide 3D building database.....	151
7.5	Summary.....	152
Part IV:	Conclusions and recommendations.....	153
8	Conclusions and recommendations.....	153
8.1	Conclusions.....	154
8.1.1	3D Topographic object reconstruction.....	154
8.1.2	3D Road reconstruction.....	154
8.1.3	3D Building reconstruction.....	155
8.2	Recommendations.....	157
	List of publications.....	159
	Bibliography.....	160
	Summary.....	165
	Samenvatting.....	168
	ITC Dissertation List.....	172
	Curriculum Vitae.....	173

Part I: Introduction to acquisition of 3D topography

Part I contains two chapters:

- 1 Introduction
- 2 Use of 3D Topography

1 Introduction

1.1 3D Topography

In the last decades the 3D representation of topographic objects becomes more and more visible in professional and consumer applications. The major advantage of 3D representation is that it better approximates the real world situation, in relation with traditional 2D maps. Examples are the usage of 3D city models as a communication tool between city planners and citizens. Several municipalities, such as Berlin and Rotterdam, have decided to capture their city in a detailed 3D city model. It is expected that many organisations will follow. The quality of those models is directly related to the time spent on building those models. That is because building up those 3D models is still time-consuming, as it can not be done automatically in a reliable manner.

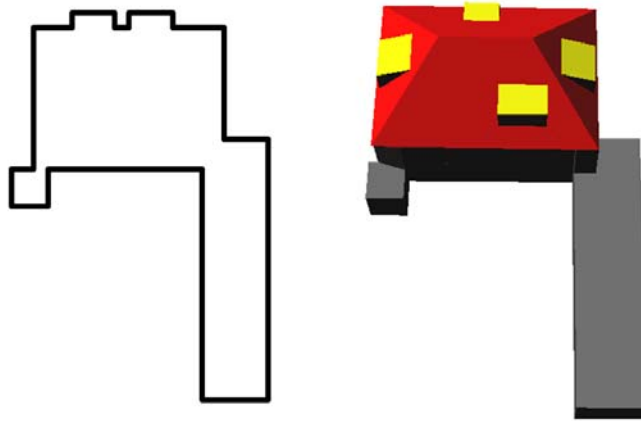


Figure 1-1 Building in 2D topographic map (left) and in 3D representation (right).

This research is part of project ‘3D Topography’, which is funded by the Dutch Ministry of Economic affairs under the BSIK/RGI (Space for Geo-information) program. This BSIK/RGI project aims to develop methods for acquiring, storing and querying three-dimensional (3D) topographic data, as a feasibility study for a future national 3D topographic database. As in various countries and communities different understandings of the term topography exist, we start with describing our interpretation of the term 3D topography. Topographic maps describe objects in terms of geometry, semantics, land use or other specific attributes for that map. 3D topography is a digital three-dimensional representation of the objects in topographic maps. These objects can represent buildings (see Figure 1-1), roads, and bodies of water but can also define ownership boundaries.

Our research focuses on the automation in acquiring 3D topographic objects. To accomplish an automated approach, we make use of existing 2D topographic maps which we upgrade to 3D using detailed height information. Upgrading also includes adding 3D substructures to objects, e.g. four dormers in Figure 1-1. In our case, we assume laser scanner data is the best data source for a reliable and highly automated

processing strategy. Use is made of data from national topographic databases and (potential) national elevation models.

Acquiring 3D objects is a challenging task as it deals with real world 3D objects that have different appearances when looking from different viewing angles. If we place the 3D topography acquisition task in the centre of our research field we see that our activities are located between how topographic objects exist in reality, how they are captured and how they appear in a modelled/virtual world. The approaches of reconstructing 3D objects should be able to capture real objects and represent them in a virtual model.

- Real topographic objects. The term ‘real’ in this sense means *the state of topographic objects as they exist* at a certain time and place, independent from the way how the data is acquired or modelled.
- Input data. The term input data describes the data that is input for our reconstruction approach. For laser scanning companies and map producers the data can be seen as output. Our research touches their work field in the sense that we use their output data (laser point clouds and topographic maps) as input data for our reconstruction algorithm. Manufacturers are constantly improving their sensors and systems to acquire data. We need to be aware of specifications of the raw data acquisition technique(s) in order to correctly process that data into information.
- 3D model. This field describes the (desired) output of the reconstruction algorithm.

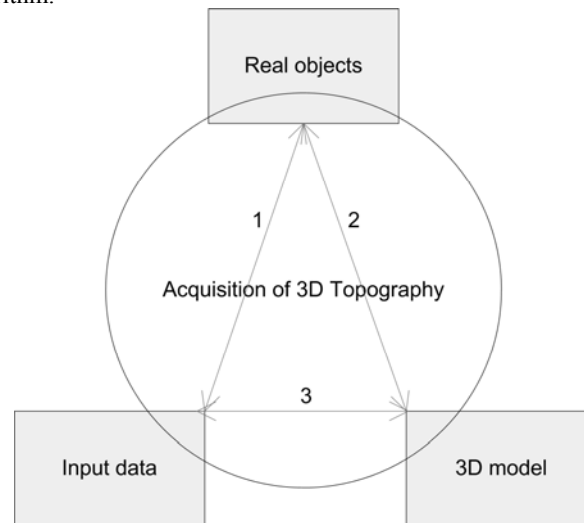


Figure 1-2 Placement of research field connecting three terms.

The acquisition of 3D topography therefore consists of connecting these three fields. Connection lines are numbered in Figure 1-2. Our research task includes understanding:

1. how objects (reality) appear in the data,
2. how objects should be described in a 3D model, and
3. how the input data should be processed to get 3D topographic models.

The figure also explains that our reconstruction strategy is built upon this triangular pattern. For example, when processing data into 3D models (indicated with line 3), we use the knowledge about how the real objects appear in the data.

1.2 Scope and limitations

Often, objects are denoted as three dimensional if the objects have three dimensions. For some applications assigning a height value to an object or location is enough to be labeled as 3D topography. In a strict definition, this is called 2.5D as there is only space for one height value per location. In our interpretation, 3D topography also includes multiple heights or even multiple objects on top of each other at a certain location.

We limit our scope of research to reconstructing objects that are visible from an airborne point of view. This means detailed structures on building facades, indoor environments and underground objects do not fall inside our scope, although these objects are of high interest for other kinds of 3D applications. The dissertation of Pu (2010) handles the reconstruction of façade elements for urban planning and safety.

The research tasks focus on two specific objects: roads and buildings. These objects are of high importance in 3D city models as they are two major topographic classes in urban environment. Another important topographic class is vegetation, including trees; the reconstruction of these objects is a research field at itself and does not fall inside our project.

We aim at the geometric reconstruction of objects. Automated texturing of these objects is an enormous, time-consuming challenge and is not incorporated in this research.

Unless stated otherwise, all processes in this thesis are automated processes. This means that there is no human measurement involved to determine 3D coordinates of an object. We assume that the human activities are selecting laser and map datasets covering the same area, interpretation of (intermediate) results, and possibly changing default parameters in order to influence these (intermediate) results.

1.3 Input data

The central task in our research is to develop a method that describes how to process data to get 3D topographic models as automated as possible. One of the points of departure of our algorithm is that we can use both 2D topographic information and airborne laser scanner data to get 3D topographic information. It is expected that both datasets are defined on the same planimetric coordinate system. Fusing these two geometric dataset is based on planimetric coordinates.

2D topographic map data delivers 2D semantics and 2D neighbourhood relations of topographic objects. We assume these objects are stored as closed polygons. Laser data provides 3D coordinates of arbitrary points on the surface. One of the most valuable processing steps is segmenting laser data into partitions or patches, in our research field called laser segments. These segments contain groups of laser points that geometrically are located in a smooth or planar surface. In general, laser data is stored as a list of 3D points, which are labelled by segment number after segmentation.

Theoretically, fusing both datasets gives 3D geometric information to the topographic map, and enriches the laser data with topographic/semantic information.

1.4 Research problems

Problems can be grouped into general data fusion problems and object specific modelling problems. In this introductory chapter the problems are briefly described and introduced in order to emphasize the need for this research. In the chapters that describe the actual reconstruction methods, the problems will be more deeply analysed in order to motivate the details of the approach.

Data fusion

Attention needs to be given to the correct assignment of (3D) laser points to (2D) map polygons. Do they represent the same object, and what is the best way to transfer height information to the map? To give an example to the first question, buildings in a map do not have to represent what is visible in laser data. Often, building outlines in maps are defined by the location of the building walls, whereas in airborne laser data mainly the roofs are visible.

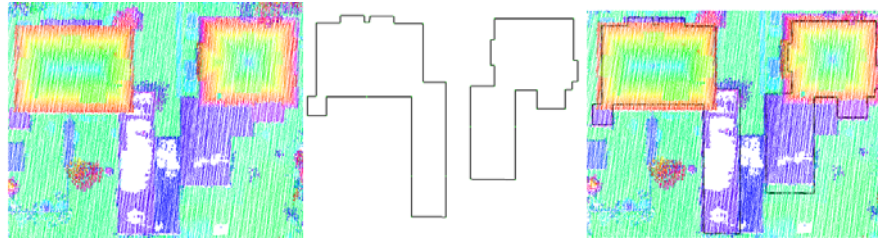


Figure 1-3 (Left) Laser points colored by height, (middle) buildings in topographic map and (right) overlay of both datasets.

Figure 1-3 shows laser data and map of two buildings. Laser points are characterised by their irregular point spacing, depending on the acquisition configuration and surface reflectivity. Data gaps can occur, in this case caused by absorption of laser pulses by water on flat building parts. Note that overlaying laser points on map data shows the complementary aspects of both datasets. The map represents the wall location, and laser data represents the height structure of the roof.

Roads

The representation of roads differs from that of buildings. When examining 3D road objects, we can expect that multiple road objects cross at a certain location. This crossing can be a simple crossover, but can also be a complex interchange with multiple roads at different height levels. Next to the general data fusion problems, the problem is that there are areas that are occluded by upper roads. This causes that some lower areas do not have laser data coverage. Locally our algorithm has to deal with less or no laser points for that road part, at that specific height level. In addition, laser pulses do not reflect optimal on (dark) asphalt surfaces, so some of the returns of laser pulses on roads did not get recorded.

Buildings

Reconstructing buildings in 3D has been a challenging research topic for at least ten years, and will be in future as long as acquisition systems are improving and model requirements are increasing. Despite the fact that many researchers presented approaches to automatically reconstruct 3D buildings, there are still a significant number of problems to be solved. Problems in automatic building reconstruction lie in the grey area between assumptions and reality. Not every object in the data appears as the algorithm expects. So, an additional task is to detect areas that cannot be reconstructed automatically, to be able to continue with the remaining parts.

Using map and laser data we can easily detect which laser points are inside the map polygon, but this does not give the shape of the roofs. This is essentially different from road objects, where we can assume that the roads' shape can be represented by a planar surface to the other side of the road. Next to that, laser points on overhanging parts are not included if one selects points with a 'points-in-polygon' algorithm, as the polygon does not include overhanging parts. These overhanging parts should be included to reconstruct the shape of the roofs.

Data gaps can be caused by various reasons. Occlusions can be found next to high objects, trees or near vegetated areas. In addition, data gaps are caused by absorption of laser pulses, as we have seen in Figure 1-3. This doesn't make it straightforward to handle gaps in laser data.

Laser data does not directly give the outline of roof faces. The outline has to be regularised as a function of laser data, map outline and roof type. The main research problem is that our algorithm should handle the combination of the variety of building shapes with the variety of the appearance of these objects in the data.

1.5 Goal and objectives

The goal is to present an automated reconstruction approach that upgrades a topographic object from two to three dimensions. Reconstructed models can be used properly if and only if quality is known. So, an additional goal is to deliver quality measures with the reconstruction model.

These general goals are narrowed into the following objectives:

- To design and implement an algorithm that reconstructs road objects with multiple height levels at the same location. The algorithm should be capable of dealing with the fact that data on each height level might be incomplete.
- To design and implement an algorithm that reconstructs buildings with differentiated roof structures. The algorithm should be capable of deciding which parts can be reconstructed with a certain strategy, and which parts can not.

- The message of the thesis is to show how complementary features of map, laser data and object knowledge can be used for an accurate 3D object reconstruction.

1.6 Importance

In near future national height models are built up with high point density laser data. Combining this data set with existing topographic maps will be done by many (new) users. This thesis will give insights in the possibilities, requirements, pitfalls and solutions for reconstructing 3D objects. Important is the connection between object knowledge and data during the reconstruction process. Information from data can show many details, but it can also be missing or misleading at some parts of the object. Object knowledge is limited to a certain level of general properties of the object, but can be very helpful when reconstructing specific parts of the building where data is locally missing. Even when there is data, the object knowledge can give constraints to the model.

Both map data and laser data are results of a chain of stochastic measurements. It is important to acknowledge the fact that data has a stochastic character, by taking these uncertainties into the processing steps from data to model. In this thesis, we explicitly describe the relation between data quality and the processing parameters that ensure a certain quality of the output model.

1.7 Thesis outline

This thesis consists of four parts, of which the middle two contain the main scientific contribution.

Part I describes the research background and introduction to the field of 3D Topography in **Chapter 1** and the how 3D Topography is used in practice, now and in the future, in **Chapter 2**.

Part II handles the research activities on 3D roads. The reconstruction steps from the national databases AHN and TOP10NL to 3D road models are described in **Chapter 3**. Assigning laser data to the correct topographic map polygon is a challenging task, as 3D road objects contain many small polygons, at different height levels, with no or a few laser points. Therefore an algorithm is presented that starts outside the actual 3D situation, following each of the roads to be able to combine road polygons and laser data that belongs to a certain road at a certain height level. After assigning the correct laser data to the polygons, the reconstruction itself consists of a combination of plane fitting and handling geometric and topologic constraints between neighbouring polygons. Examples are shown for highway interchanges including their surroundings. The geometric quality of these reconstructed roads is both calculated as a function of the quality of the input and checked on reference data, and described in **Chapter 4**.

Part III covers the acquisition of 3D buildings. **Chapter 5** deals with research problems on building reconstruction and the possibility to detect roof shapes in our data. High point density laser data is used to be able to detect roof faces and roof details such as dormers. Detailed topographic map data (map scale 1:1000) gives the opportunity to

select laser segments per building and to reconstruct the building walls, which might show a planimetric difference with the roof edge. Main part of our approach is the target based graph matching algorithm that relates data features with model information (targets). Data features represent roof faces and their intersections, whereas the targets contain knowledge on the most common combinations of roofs and ridges. Data features are matched according their correspondences with the targets, in order to detect roof shapes in the data. The actual reconstruction of roof shapes is described in **Chapter 6**. We use the relation between data and targets to decide how to reconstruct the individual roof faces and how to combine them. Map data is integrated in this part of the process to give hints on the location of ridges, step edges and to reconstruct walls. In **Chapter 7** the results are shown and evaluated.

Finally, in **Part IV**, which consists of chapter 8, the main conclusions and recommendations for future research and directions are described.

2 Use of 3D topography¹

¹ This chapter contains content from:
Oude Elberink, S. (2008) Re - using laser scanner data in applications for 3D topography. In: Advances in 3D geoinformation systems / ed. by ed. by P. van Oosterom, S. Zlatanova, F. Penninga and E. Fendel. Berlin : Springer, 2008. (Lecture Notes in Geoinformation and Cartography) ISBN 978-3-540-72134-5 pp. 87-99.

This chapter shows the use of 3D topography within different kinds of organizations, in different kinds of applications. The goal of the use cases is to describe 3D topographic information from a user's point of view. The intention of describing the user's point of view is to relate the practical use of 3D topographic information to the scientific activities described in part II and III. The user's point of view has been recorded at the start of this PhD trajectory and can be seen as a motivation to perform research on the acquisition of 3D topographic models. In 2.1 we shortly introduce four use cases, followed by the user requirements in 2.2. Section 2.3 discusses the observation that organisations are re-using 3D models, often to supply information for new applications. This has an impact on the user requirements on the 3D models. In 2.4 the relation between the use cases and our research activities is highlighted, followed by a list of recent developments and conclusions in 2.5 and 2.6.

2.1 Introduction

Several years ago, local and national geo-information departments started building up their experiences with laser scanner data, to better and faster acquire DTMs or to support updating topographic maps, as shown in (Vosselman et al., 2005). Laser data and its derived products like 3D city models are relatively new data sources for other departments in many organizations.

The use cases have been accomplished by information analysis at four major geo-information organizations in The Netherlands. These organisations already gained some experience with the acquisition, storage and analyses of laser scanner data and its derived 3D products. In interview sessions and a subsequent workshop we collected and discussed user experiences concerning the quality requirements, applications, acquisition and storage of 3D topographic data.

Interview sessions were organised between researchers of ITC and TU Delft at one hand and owners and users of 3D geo-information at the other hand. The four organizations are:

- Municipality of Den Bosch;
- Survey department of Rijkswaterstaat (RWS);
- Water board "Hoogheemraadschap de Stichtsche Rijnlanden" (HDSR);
- Topographic Service of the Dutch Cadastre.

For each of these organisations we discussed several applications that represent (a part of) their users use of 3D topographic objects.

During the interviews we collected information on the necessity to use 3D data instead of the existing 2D data. Limitations of analysing 2D data are important to justify the need for 3D data. Major limitations of 2D topographic information are the lack of insight of multi-layered surfaces and the inability to calculate volumes. We asked to list the most important applications that actually need 3D data, or at least 2.5D data. The overview of this part of the study can be seen in Figure 2-1.

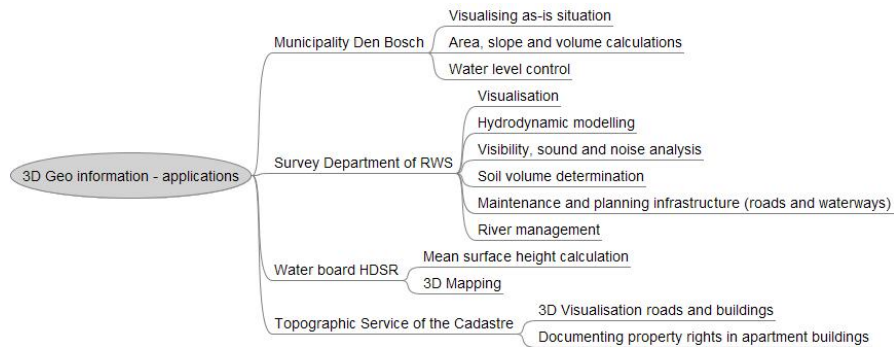


Figure 2-1 Initial list of 3D applications.

The figure shows an initial list of applications that are based on 2.5D or 3D data. In all of the applications height information is essential to correctly perform the task.

2.2 User requirements

The major purpose of the interviews was to specify user requirements for 3D topography. User requirements should cover topics like specific wishes on data quality, distribution and analyses.

2.2.1 Municipality of Den Bosch

Den Bosch aims for the production of a large scale 3D geo-database. Their main motive for acquiring 3D data is to perform height-related tasks like volume determination and water management tasks, but also for visualising the “as-is” situation. Visualising models close to reality is an important tool to communicate with their citizens. Their list with 3D model requirements starts with the modelling of shapes of buildings, followed by the possibility to store and analyse multiple objects on top of each other. These requirements are added to the existing requirements for DTM production or determination of height profiles, formerly measured by GPS.

2.2.2 Survey Department of Rijkswaterstaat

The Survey Department is responsible for acquiring and maintaining geo-information of national infrastructures (stored in Digital Topographic Database DTB) and a nation wide height model (AHN).

The Digital Topographic Database (DTB) is a topographic database with map scale 1:1.000, containing detailed information about all national infrastructural objects, like highways and national water ways.

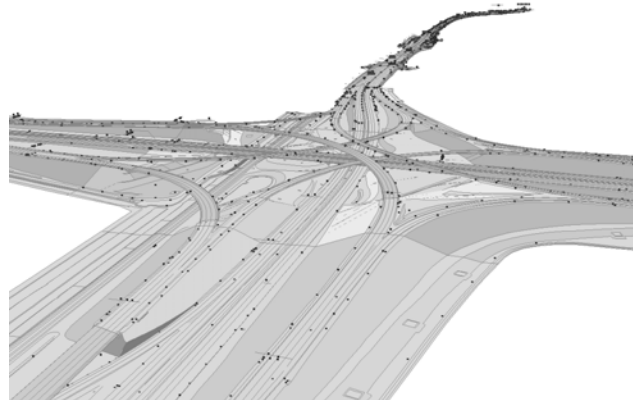


Figure 2-2 Points, lines and surfaces in interchange of DTB.

Acquisition has been done in 3D, by measuring in stereo imagery added with terrestrial measurements at interchanges and tunnels. Points, lines and polygons have been classified manually and stored in the database. Quality requirements depend on the idealisation precision of the object, e.g. paint strips can be measured with a higher accuracy than a border between two meadow fields. Besides this, user requirements are strongly related to the acquisition method. Demands for terrestrial measurements are higher than photogrammetric demands. In the near future terrestrial and airborne laser scanner data might be introduced as a new data source for fast and automated acquisition of the objects.

The Actual Height model of the Netherlands (AHN) is a national DTM, initiated by three governmental organizations: Rijkswaterstaat, the provinces and the union of water boards. User requirements of the AHN changed over time due to the growing number of applications. Most important change is the need for higher point density. In 1996, at the beginning of the project, 1 point per 16 m² was supposed to be dense enough to fulfil all user requirements. When users started to detect features, or fused the laser data with other detailed datasets, the demand grew for a higher point density laser data set. In 2004, the growing technical possibilities of laser scanners strengthened the idea that the next version of AHN should have at least 1 point per 9 m². In 2006 it was proposed that if increasing the point density even more, many new applications could be performed. To give an example, the state of coastal objects, like dikes, can be monitored by analysing high point density laser data. In 2007, a pilot project started to acquire new AHN² (denoted as AHN-2) data with a point density of 10 points per m². As this pilot turned out to be successful, it has been decided that in the period 2008-2012 AHN-2 will be acquired nationwide.

² In this thesis, the term AHN is meant for the first version of the national height model with point densities of 1 point per 9-16 m²; AHN-2 stands for the second version of AHN which for the greater part still has to be acquired.

2.2.3 Water board “Hoogheemraadschap de Stichtse Rijnlanden”

For inspection and maintenance of regional dikes, bridges and waterways, the water board needs up-to-date and reliable geo-information. Requirements for a 3D model are that breaklines and objects on top and at the bottom of a dike are measured with high precision, typically in the order 2-3 cm height accuracy. Existing AHN data is not dense enough for detailed mapping purposes. Breaklines are important features for the condition (shape and strength) of dikes. In the past, parallel profiles were measured with GPS. Water board HDSR decided to acquire a helicopter based laser data set with point density of more than 10 points per m², together with high resolution images. Important objects like bridges, dikes, water pipes have been measured manually using the laser point cloud for geometric information, and images for detection and thematic information. By using laser data, the water board is able to calculate strength analysis locally instead of globally. This is important for analysing the behaviour of its dikes. Now that a detailed 3D model of the dike and its neighbouring objects has been captured, analysing strengths accurately in time and space will be possible when acquiring the next data set.

2.2.4 Topographic Service of the Dutch Cadastre

The Topographic Service of the Dutch Cadastre produces national 2D topographic databases from scale 1:10.000 to 1:250.000. Implicit height information has been integrated at specific parts in the 2D topographic maps by:

- Shadowing, visualising local height differences;
- Symbols, representing a high obstacle like churches, wind mills, etc;
- Building classifications, discriminating between high and low buildings;
- Level code, indicating on which level an object is, when looking from above.

More explicit and absolute height information has been given by:

- Contour lines, representing a virtual line at a specific height;
- Height numbers, representing the local height at a certain location.

Whereas in the past the height information mentioned above is introduced mainly for cartographic purposes, the Topographic Service would like to extend the possibilities and acquire and store objects in 3D. When building up a 3D topographic database the customers of the products of the Topographic Service will be able to perform traffic analysis, volume calculations and 3D visualizations. User requirements can be summarised by the wish to acquire and store rough 3D building models and to add height values to road polygons. Figure 2-3 lists a summary of user requirements of all four organizations.

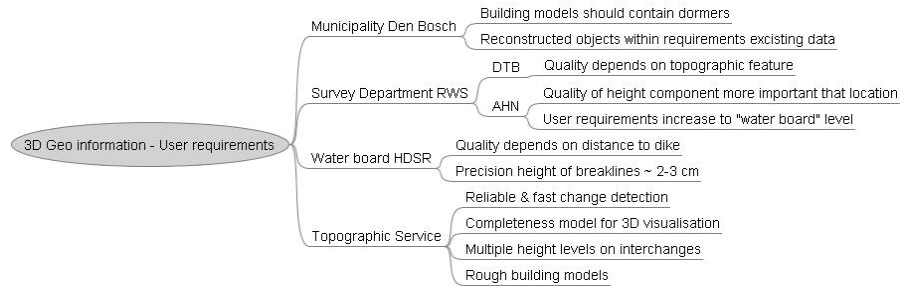


Figure 2-3 User requirements based on interviews.

Note that requirements were mentioned in terms of global use, a kind of wish list. The potential 3D product should be able to perform a certain task. Users did not give detailed product specifications, let alone specific quality parameters.

2.3 Re-using 3D models

During the interviews, users mentioned the increasing number of applications, using laser scanner data or its derived products.

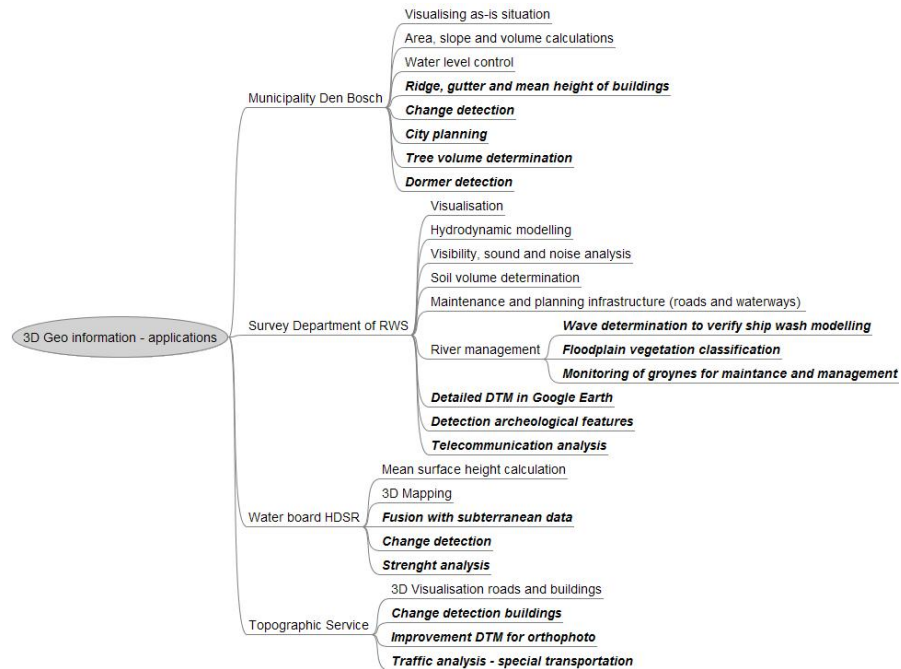


Figure 2-4. Extended list of 3D applications.

All four organizations re-used their laser data and its derived products, more than expected. Figure 2-4 shows the extended list of 3D topography applications. Applications shown in bold and italic represent ‘new’ applications: they were initiated after the organizations captured their data for the originally applications. Total number of applications mentioned in the interviews is 29, whereas the originally planned number was 12.

Users mentioned the data-driven character of the new applications. These applications are in explorative phase, what implies that the users first look at what can be done with the 3D data they have. This can be seen by the fact that the user requirements are characterised by the specifications of the available data. With the maturation of these applications, the requirements will become more demand-driven, resulting in a more detailed description of what the specifications of 3D data should be. Figure 2-5 shows the iterative circle on how 3D models and their requirements are refined by using the models in different kind of applications.

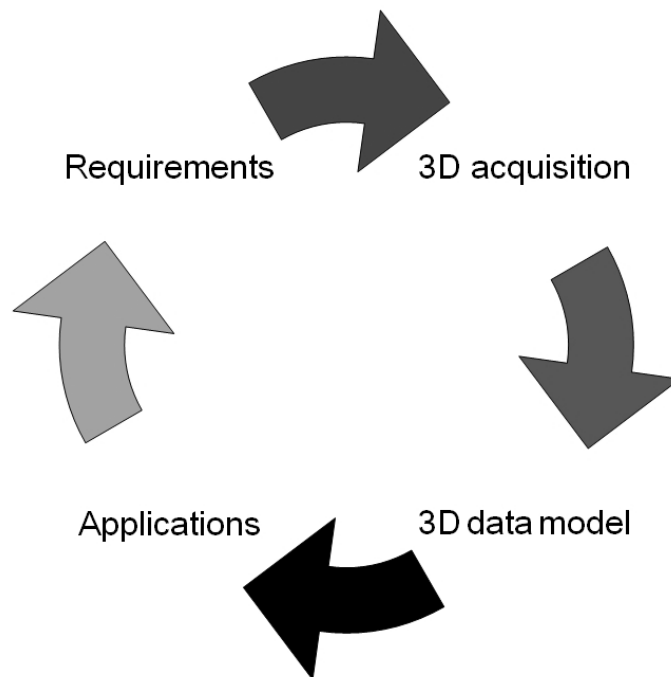


Figure 2-5. Iterative circle connecting data and applications.

In this section we want to look in further detail to the growing numbers of applications re-using laser data at these four organizations.

2.3.1 Municipality of Den Bosch

The engineering department re-used the parts of laser data classified as 'hard' terrain. They fused it with their existing topographic map and road database to better analyze the drainage of rainwater. The tax department initiated a project to detect dormers more quickly and more accurately, using laser data and imagery. Municipalities are looking for quantitative and fast methods to determine urban tree volumes for various reasons. Therefore, research has been done to detect individual trees and calculate urban tree crown volume in the city of Den Bosch, using their existing laser data. Figure 2-6 shows two applications that are useful for municipalities, namely detection of dormers and change detection. Although the examples are from the area of Enschede, it shows the potential for Den Bosch and any other municipality to quickly detect changes and dormers.

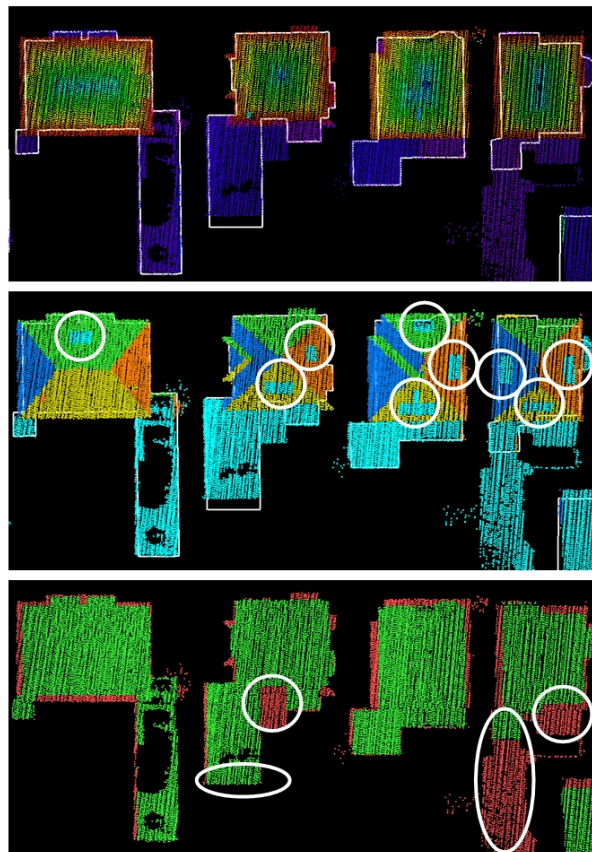


Figure 2-6 Map and laser data (top), detected dormers (middle) and change detection (bottom). Examples shown with data in area of Enschede.

2.3.2 Survey Department of Rijkswaterstaat

Rijkswaterstaat can perform various river management applications with one high point density dataset. Some of the time consuming terrestrial measurements, visual inspections and mapping from imagery, can be replaced by laser altimetry. In case of extreme low-water levels, laser altimetry enables RWS to acquire detailed morphologic information of the groyne fields, which usually cannot be measured. In combination with multi beam echo-sounder data, acquired at high-water level, behaviour of the riverbed and groyne fields can be analysed simultaneously.

AHN data has intensively been used by archaeologists. Large scale morphological structures, possibly indicating historical objects or activities, which cannot be seen from the ground, may clearly be visible in the DTM. Besides this, slopes can indicate the locations where to look, using the knowledge that historical objects tend to slide to lower parts in the terrain.

2.3.3 Water board “Hoogheemraadschap de Stichtsche Rijnlanden”

Information of the topography can be combined with subsurface information, to better analyze the strength of a dike. The use of laser scanner data is essential to correctly fuse topographic features with the (also 3D) subterranean information. Change detection is a hot topic in the maintenance of dikes. Already existing data sets are as important as future laser data sets when looking at differences between them.

2.3.4 Topographic Service of the Dutch Cadastre

The Topographic Service seeks methods for fast and reliable change detection. Laser data can be used to automatically detect changes in the 2D map. However, changes between laser data and map data should be handled with care. Changes can be caused by misinterpretations of the aerial photographs, laser data, or by differences in generalization of the map.

In the interviews, users mentioned various factors that have had a positive influence on the re-use of the laser data.

2.3.5 Availability and distribution

GIS based intranet applications make it possible to show geo-data to the organization. Google Earth already showed the success of simple visualising, navigating and zooming of 2D geo data. When visualising the as-is situation in 3D, it generates an alternative perspective for new user groups, including tax departments and citizens who want to walk through their streets in the model. Eye opening is the first and most important step in using a new kind of data for existing or even new applications.

2.3.6 Data fusion

Combining data sources not only delivers information on the similarities and differences between the two datasets, it can use the complementary aspects to create new or better

products. Examples can be found in fusion of map and laser data, where map data delivers thematic and topologic information and laser data adds geometric information.

2.3.7 Generalization and filtering

Although several authors use both terms Generalization and Filtering as being the same activity, we distinguish between generalising 3D data, focusing on the representation of the output (reducing derived 3D data), and filtering laser scanner data, focusing on data reduction of the input (reducing raw data). Generalization allows organizations to use 3D geo data multiple times at multiple scales, thus reducing the costs of acquiring 3D data. For water boards a special kind of generalization is important, because objects close to dikes have to be represented in more detail than objects located further away. Although high point density laser data is useful for a reliable classification of buildings, vegetation and other objects, and for extraction of breaklines in the terrain, it is clear that for large parts in the terrain the point density is too high to allow efficient processing of a DTM. Filter algorithms help the user to reduce laser data in an early stage of the process, making the huge datasets much more flexible for their application.

2.3.8 3D Represents as-is situation

The reason of the increasing number of users, when using 3D data instead of 2D data, is that 3D better represents the as-is situation. From this situation, many users perform their activities. For example, city planners can add features to the as-is situation, civil engineers are able to calculate volumes and strengths at given situations, etc. Whereas the 3D information started at the geo information departments, as being a faster way to detect 2D objects automatically and as added value to the existing 2D information, it is for many other departments the first contact to geo information. Note that for a number of applications representing in 2D is still the most convenient way to reach their goal. Examples can be found in route descriptions and assessing parcel information. Although airborne laser data is a good method to quickly acquire detailed information, it cannot replace all terrestrial measurements for purposes like measuring and monitoring point objects.

User requirements of 3D objects and databases are still under development. One of the reasons is that the number of applications and users is still growing. On the other hand, the technical possibilities of airborne imagery and laser altimetry are increasing in terms of geometric and radiometric resolution. With the growing offer of detailed information, the user requirements get more specific and the demand for more detailed information grows. Science projects in data acquisition, data fusion and storage are essential for users to show the re-usability of their data.

2.4 Role of use cases in research project

As mentioned in the first paragraph of this chapter the use cases describe the user's point of view, from which we take elements to propose research activities. Three major elements are listed here.

- Input data: map and laser data. Users handle 3D topographic objects as upgraded versions of their 2D objects. It is expected that acquiring and maintaining 2D maps will remain for the next decades. Therefore, our

approach takes 2D maps as reliable and up-to-date input source. As we believe laser scanner data has the largest potential to add the third dimension to those 2D maps in a highly automated manner, our intention is to use map and airborne laser scanner data as input data sources.

- 3D objects: roads and buildings. Roads and buildings are man-made objects which are mostly mapped in 2D. However to gain insight in multi-layered surfaces, urban situations in general and to be able to calculate volumes it is of interest to analyse the ability to generate 3D representations out of these 2D objects.
- Target group: using national databases. The aim of our project is to develop methods for acquiring, storing and querying 3D topographic data, as a feasibility study for a future national 3D topographic database. For 3D road reconstruction, use is therefore made of the current national 2D topographic database TOP10NL and the national elevation model AHN. Research activities on 3D building reconstruction are based on building outlines from the national cadastral database GBKN and airborne laser scanner data with point density of 10 pts/ m² (AHN-2) or more. Our target group of potential users is therefore those who use these national databases.

2.5 Recent developments in using 3D topography

So far, we presented the use of 3D topographic information, as recorded in 2005 and 2006. To emphasize the growing demand for 3D information, we discuss in this section a number of recent developments (2008- 2009) showing the need for fast and accurate 3D reconstruction techniques. The upcoming AHN-2 dataset, which will be acquired from 2008-2012, is an important input data source to generate 3D information. It is expected that AHN-2 gives a boost to applications using detailed 3D geo-information. Processing AHN-2 data into usable 3D products is therefore an interesting activity. We will list a number of “requests for cooperation” we received in the spring 2009 that highlight the current need for 3D geo information. Next to that it shows that processing laser data into geo-information is still a technique towards maturation.

- 3D Building models for a large municipality

The municipality is looking for 3D models that at the one hand fit to actual laser data, but at floor level the 3D model should fit to the cadastral map.

- Actualising 3D city models

What would be the optimal workflow for municipalities to build up and to maintain 3D city models? Can we use laser data to build up and aerial images to maintain the 3D models?

- Modelling of 3D cities for visualisations of real estate

A request by an animation house that creates visualisations for real estate agencies is to acquire 3D building models.

- Roof face inclination and orientation for roof covering

One of the UN millennium goals³ is to ensure environmental sustainability. One of the implementations of this goal is to integrate durable elements in country policies and programmes. Durable roof covering is becoming such an important element when looking at energy saving and building a durable environment. The inclination and orientation of individual roof faces are important parameters to determine the optimal roof covering.

- Roof face size, inclination and orientation for solar energy collectors

Another task relating to durability is to select suitable locations for the placement of solar energy collectors. Although there has been research on this topic (Jochem et al., 2009) and (Voegtle et al., 2005), the step from research to implementation still has to be made.

2.6 Conclusions

In our study, we analysed user requirements on 3D geo information in four major organizations. The user requirements were based on originally expected applications. 3D Topography is in the early stage towards a mature usage in practice. Acquisition systems, such as laser scanning systems or imagery based systems, are constantly developing, and resulting in denser or more accurate data. While organizations are showing and using 3D models, the number of new applications using those models increases. These new applications can be found in the traditional geo information departments, but also for other information based activities, such as those in environmental and tax departments.

User requirements were mentioned in terms of global use, instead of detailed geometric product specifications.

We recognised the flexibility of organizations to explore what can be done with the data that they have. Therefore, the most important insight was the large potential for re-using existing 3D geo information. Once a 3D data set had been acquired, many 'new' users recognised the benefit of 3D data for their application.

With the growing of number of users, the user requirements also evolve. A good example is the desired point density of the national height model AHN, increasing from 1 point per 16 m² in 1996 to 10 points per m² in 2006.

Even information analyses can be re-used for different purposes. The actual purpose of analysing the interview information was to specify user requirements, whereas the re-used version was to show advantages of re-using the geo-information and the data driven character of many user requirements.

Not only the use of 3D Topography is under development, also the processing from data to 3D topographic information is still maturing. The remaining of this PhD research aims to fasten the maturing phase by proposing automated methods to reconstruct 3D models from existing 2D topographic information and airborne laser scanner data.

³ <http://www.un.org/millenniumgoals/>

Acknowledgement

The author would like to thank Bram Verbruggen of the municipality of Den Bosch for providing additional information on the re-use of data, and the other persons who cooperated in this part of the research: Friso Penninga, Edward Verbree, Nico Bakker, Garnt Zuidema, Paul van Asperen, Job Nijman, Nico Bakker and Stefan Flos.

Part II: 3D Roads

Part II contains two chapters:

3 3D reconstruction of roads

4 Quality analysis on 3D roads

3 3D Reconstruction of roads¹

¹ This chapter is mainly based on content from the following papers:

Oude Elberink, S. and Vosselman, G., 2006a. 3D Modelling of Topographic Objects by Fusing 2D Maps and Lidar Data. *International Archives of Photogrammetry, Remote Sensing and Spatial Information Sciences*, 36 (part 4): (on CD-ROM).

Oude Elberink, S. and Vosselman, G., 2006b. Adding the Third Dimension to a Topographic Database Using Airborne Laser Scanner Data. *International Archives of Photogrammetry, Remote Sensing and Spatial Information Sciences*, 36 (part 3): 92-97.

Oude Elberink, S.J. and Vosselman, G., 2009. 3D information extraction from laser point clouds covering complex road junctions. *The Photogrammetric Record*, 24(125): 23-36.

3.1 Introduction

In this chapter, we describe the steps to acquire complex 3D topographic road objects, such as interchanges and road junctions.

Modelling interchanges and flyovers is of great importance for visualisation purposes for infrastructural objects. Besides this, realistic traffic noise and pollution models need accurate road models. Modern car navigation systems tend to shift from oblique views on 2D roads to showing actual 3D road models. Many navigation systems claim to have 3D models. However, they show 2.5D road models and building block models. Figure 3-1 shows a junction of two highways that needs up to four height levels at one location. In 3D topographic databases, it should be possible to store multiple topographic features on different height levels at the same 2D location.



Figure 3-1 Complex 3D infrastructural object “Prins Clausplein”, The Hague.
Source: Beeldbank VenW.nl

Three-dimensional reconstruction of complex interchanges can be done by airborne measurements and terrestrial measurements. As terrestrial measurements might imply closing parts of the highway it is of interest to analyse remote acquisition techniques.

3.2 Related work

3.2.1 Road reconstruction from aerial images

Most of the research papers on road reconstruction from images deal with the automation of mapping (2D) road outlines or centrelines. Mayer et al. (2006) describes a test where a couple of road extraction approaches have been analysed and compared. They conclude that automatic extraction of centrelines from aerial images can only be done for scenes with limited complexity. There are a few attempts that use stereo configuration of aerial images to assign height information to roads. Zhang (2003) describes a 3D reconstruction model of roads by an edge matching technique in aerial images. He uses a set of image processing tools to extract various cues about the existence of road objects in stereo-images. Road hypotheses have been created to narrow the search space, and to reconstruct road parts which are missing because of occlusions. Results have been shown in (Zhang, 2003) for 2½D situations, showing only one height at a certain location.

The complexity of the appearance of roads makes it difficult to automate the road extraction in images. The property that roads are generally flat, or at least smooth, allows us to investigate road extraction methods from lidar data, which use height information of the scene.

3.2.2 2D Road mapping from laser data

2D mapping of roads is a necessary step in 3D road reconstruction if one can not use existing 2D road information. Literature in this section deals with the ability to map roads in 2D using laser scanner data. This group has been divided into two parts, where the first part deals with finding road networks and the second with detecting and reconstructing the road outlines.

Road network detection

Network detection is based on the continuity and connectivity of planar patches on or just above the DTM. In (Abo Akel et al., 2005) points on roads have been classified after segmentation of the point cloud. The classification is based on decision rules: road segments are large and the area-to-boundary ratio is small. Centrelines of these segments are extracted to get a road network. Hu et al. (2004) describe the combination of lidar and aerial imagery to detect road networks in dense urban areas. The complexity of the finding road networks has been reduced by combining the spectral information from the images, with the height information from the lidar data.

Road outline extraction

In general, extraction of road outlines requires more prior knowledge about the expected roads to analyse the laser data than road network detection. Hatger and Brenner (2003) and Hatger (2005) start with an initialization by importing the centrelines from an existing database. This centreline is projected on the DSM; perpendicular to this centreline samples are drawn. At each sample laser data has been analysed to find height or slope discontinuities. This will indicate border points of the road. Next, outlines have been extracted parallel to the centreline through these border points by

(median) filtering. Their methods can deal with small parts of missing data, for example when buildings or trees occlude the streets. Clode et al (2004) show the use of laser pulse intensity information to extract outlines between roads and other terrain objects. Classification is based on intensity information of laser points near the terrain surface. Their method may fail at bridges and at trees covering the streets.

In urban environments humans should guide the road measurement process, to get a high quality road extraction. Complex situations are hard or impossible to automatically interpret by algorithms. Bridges, trees and parking lots are the main examples where algorithms typically will fail. Operators have to guide the classification and mapping process, by selecting some road segments and outlines visually.

3.2.3 3D Reconstruction from laser data

If 2D road information is already available in existing topographic maps, the 3D road reconstruction consists of upgrading from two to three dimensions. Vosselman (2003) describes several algorithms and procedures developed for the 3D reconstruction of streets and trees from airborne laser altimetry data in combination with a cadastral map. Using the boundaries of cadastral objects and knowledge about smoothness of streets, the laser data is processed into realistic street models. The method works for 2.5D situations. Results have been shown for an urban area containing a single layered road network. Simonse et al. (2000) describe how to convert a road crossing from a 2D map to two layers in a 3D triangular irregular network (TIN). However, this approach is limited to simple crossings for reconstructing at most two layers.

Airborne laser data has the potential to speed up the reconstruction process due to the higher degree of automation in processing. Height from laser data can be transferred to 2D information from map data as shown in (Vosselman, 2003). In literature no methods have been found for reconstructing multi-layered interchanges as shown in Figure 3-1.

3.3 Proposed approach

We aim at reconstructing the road surface, without objects such as cars and traffic lights. As we already have the planimetric location of the road edges from the 2D map, the task is to transfer height information from the laser data to the road edges and surfaces. This means we have to discard laser points on cars and other road furniture from the dataset, and make use of the remaining points to determine the height of the road objects. Quality parameters are calculated by error propagation and checking of reference data.

In Figure 3-2 an overview is given on the input data and its processing steps.

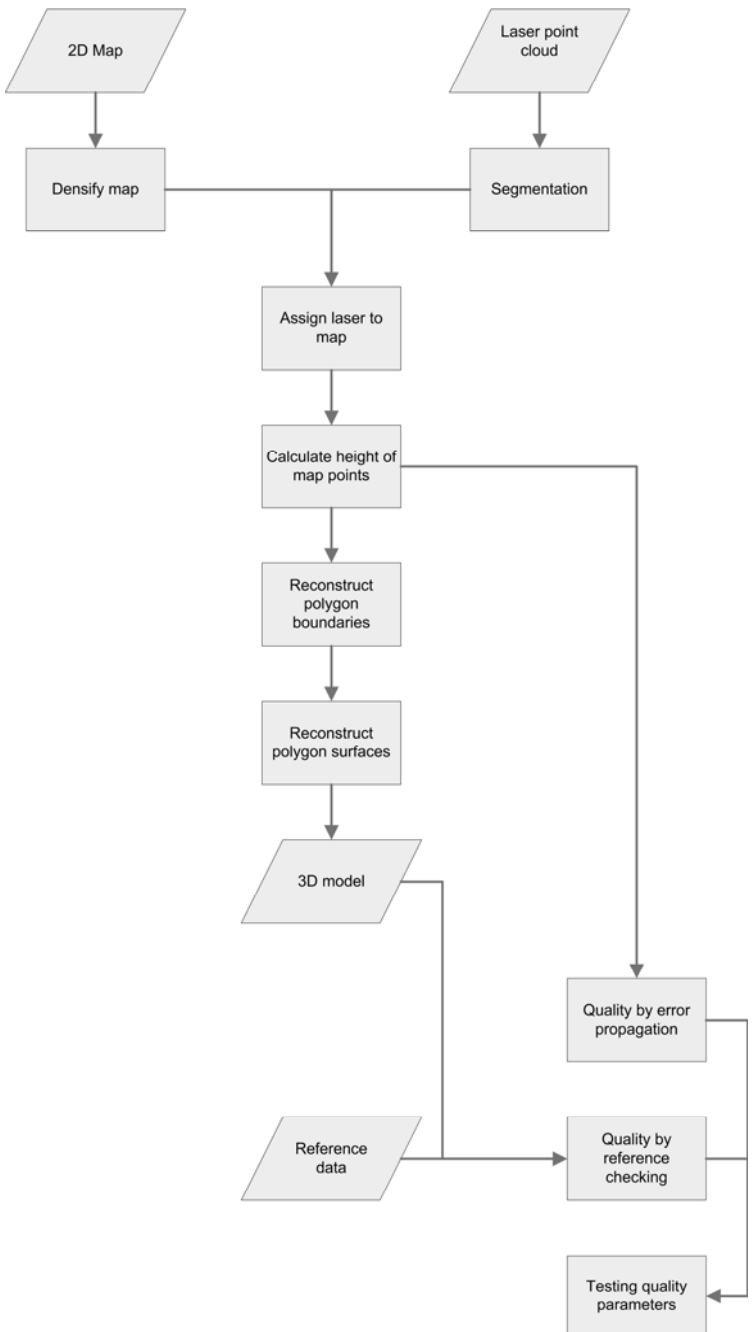


Figure 3-2 Workflow from input data to 3D road models.

3.4 Data sources

We use the current national 2D topographic database TOP10NL and the national elevation model AHN, see Figure 3-3.

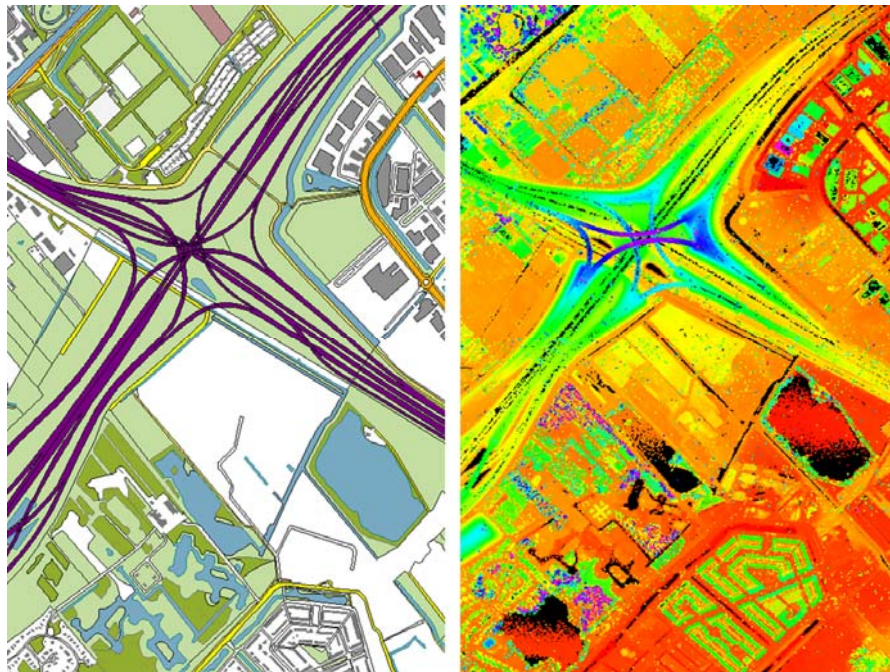


Figure 3-3 Topographic map TOP10NL (left) and AHN laser data (right) of Prins Clausplein.

The working of the algorithms will be presented using these two data sources. However, the algorithms are designed to be flexible, thus enabling the use of other datasets. The most important input requirements for using the algorithms are:

- (1) topographic map consists of closed polygons;
- (2) polygons have been classified into topographic classes;
- (3) laser data has been registered in the same coordinate system as the map;
- (4) laser data is delivered as point cloud, preferably unfiltered.

This makes the strategy to a certain extent independent of the input data source. In particular, semantic information was not used other than the class information from the topographic map TOP10NL, because it would narrow down the possibilities of using other topographic map data. The algorithm has been designed for upgrading a 2D map to a 3D map. Map updating is not included in the process; therefore, the 2D map and laser data were assumed to be up to date. For every map polygon, laser data inside the polygon is assigned to the class of that polygon. Laser data is further processed according to properties of the class of the polygon.

3.4.1 Airborne laser scanner data

The national height model of the Netherlands (AHN) has been acquired by airborne laser scanner data with average point density of at least one point per 16 m² and a height precision of about 15 cm standard deviation per point. As can be seen in Figure 3-3, there are some black parts in the area, meaning that there were no reflected pulses from the surface. This happens for water surfaces and over large parts of some highways. This type of asphalt greatly absorbs the laser pulse. The modelling strategy should deal with varying laser point density. Knowledge on the shape of roads should be added if laser points are missing. To reduce the influence of outliers and objects such as cars and road furniture, laser data has to be pre-processed before fusion with map data.

3.4.2 Pre-processing laser data

We assume that the topographic objects can all be described by smooth surface patches. The purpose of the point cloud segmentation is therefore to find piece-wise continuous surfaces that can be used to infer the heights of the topographic objects. Traditional filter algorithms that are used to produce digital elevation models often completely or partially remove objects like bridges and road crossings (Sithole and Vosselman, 2004). By segmenting a scene into piece-wise continuous patches and further classifying the segments this problem can be avoided (Sithole and Vosselman, 2005); (Tóvári and Pfeifer, 2005).

For the segmentation of the point cloud a surface growing algorithm is used with some modifications that allow a fast processing of large datasets (Vosselman et al., 2004). The surface growing method consists of a seed surface detection followed by the actual growing of the seed surface. For the detection of seed surfaces we employ the 3D Hough transform. This transform is applied to the k nearest points of some arbitrary point. If the Hough transform reveals that a minimum number of points in this set is located in a plane, the parameters of this plane are improved by a least squares fit and the points in this plane constitute the seed surface. To speed up the seed detection, we do not search for the optimal seed (with most points in a plane and the lowest residual RMS of the plane fit), but start with the growing once an acceptable seed surface is found.

In the growing phase we add a point to the surface if the distance of the point to a locally estimated plane is below some threshold. This threshold is set such that some amount of noise is accepted. At the same time it also serves to allow for a small curvature in the surface. For a faster processing, the normal vectors of points are not computed and checked. The distance of a point to the local plane is the only criterion. If a point is accepted as an expansion of the surface, a local plane needs to be assigned to this point. In case the distance computed for this point was very small, no new local plane is estimated, but the plane parameters of the neighbouring surface point is copied to the new point. This strategy again serves a faster processing of the point cloud. Once no more points can be added to a surface, the seed detection is repeated. This process continues until no more seed surfaces are found.

In our case, we do not perform a classification of the segments, but just use the segmentation results to eliminate laser points on small objects like cars, light poles, traffic signs, and trees. By requiring a minimum segment size, all these points will be left without a segment number after the segmentation step and can be easily removed.

Figure 3-4 shows the result of removing small segments from the point cloud. Many small features like cars and bushes are being removed in this step.

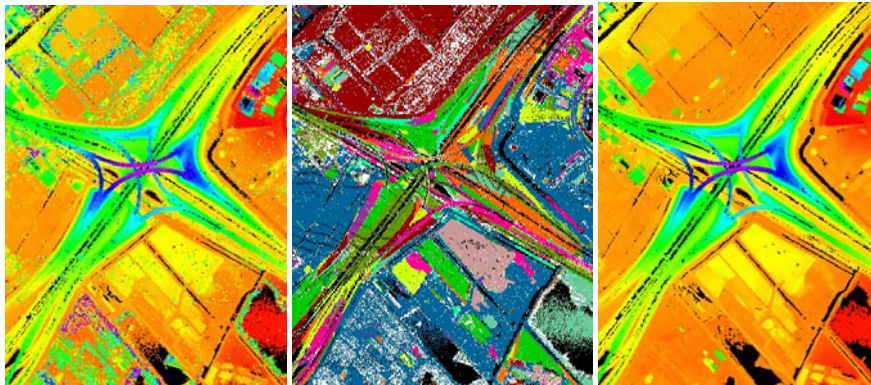


Figure 3-4 Laser scanner data height colour coded (left), segmented laser data (middle) and after the removal of small segments (right). Black areas contain no laser points.

3.4.3 2D Topographic map data

TOP10NL is a digital 2D topographic database intended for use at a map scale of 1:10.000. It has been built up in a fully coded object structure. The database has been acquired from photographs at a scale of 1:18.000 and has an planimetric accuracy of 1 to 2 m.

3.4.4 Pre-processing 2D map

Topographic segments are represented by closed polygons. Its geometry has been defined by the coordinates of map points (vertices) and the topology. Figure 3-5b clarifies that adding height to 2D vertices is not enough to get a 3D model. As shown in Figure 3-5b, edges that are straight in the 2D map do not need to be straight in the 3D model. At a certain point the terrain will connect the upper road with the lower road; part of the edges between terrain and road, which were connected in 2D do not connect to each other in 3D. To correctly capture the shape of the infrastructural objects, the edges therefore need to be described by more vertices. For this purpose, vertices were inserted into the edges of the polygons at every 10 m. For all these points and the original map points the height needs to be determined from the laser data.

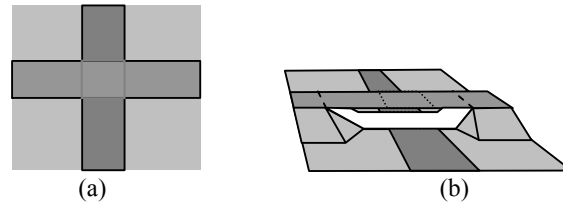


Figure 3-5 Straight edges in 2D (a) do not need to be straight in 3D (b).

3.5 Fusion of map and laser data

The underlying principle for the 3D reconstruction is to use the laser points inside each polygon. This can be done with a points-in-polygon algorithm, which can be seen as a simple data fusion process. However, in complex multi-level situations the fusion process has to be refined to handle problems with too few or incorrect points in a polygon. This section explains that for complex situations some more knowledge has to be added to the process.

3.5.1 Research problems on fusing map and laser data

When looking at a complex infrastructural object, the following characteristic problems may occur (Figure 3-6):

- **Map displacement (P1).** Road features at the top level show large horizontal distortions in the map. Roads are usually mapped from orthophotos. In a complex situation like this, the DEM used for orthophoto production neglects the height of the higher features, resulting in a horizontal displacement. These displacements can easily rise up to 5 meter. This means that not all corresponding laser data will be found by performing a points-in-polygon operation. Knowledge has to be added to correctly fuse laser data with the topographic polygon representing the object.
- **Points on overlapping surfaces (P2).** Laser points may be reflected on all road levels. Due to the large across track scanning angle it is possible to acquire height data at different levels at the same horizontal location. Although in the segmentation step these points will not be grouped into the same segment, large segments can be found each at different height levels. The problem here is to select the correct laser points for the height level to be reconstructed.
- **Lack of points (P3).** Problems arise when handling polygons with only a few points. These problems are caused by the small size of the polygon, by the surface material of the object feature resulting in bad reflectance or by the fact that this road part is occluded. The problem with airborne techniques is that occlusions occur underneath the upper object parts, resulting in gaps in the input data. As the goal is to assign heights to polygons, the problem is to assign the height if the polygon contains no or just a few laser points.

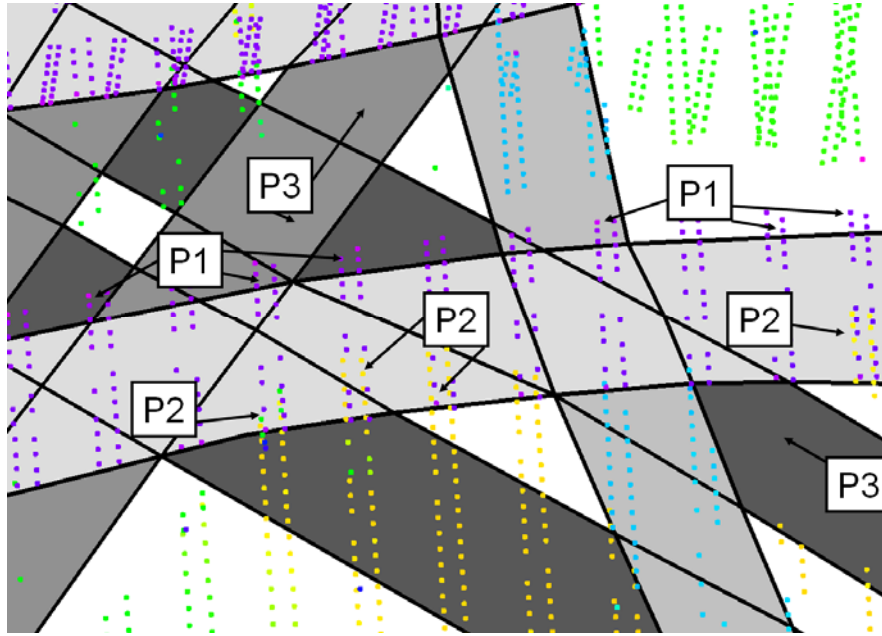


Figure 3-6 Three sorts of problems mentioned above (P1, P2, P3) when fusing laser and map data.

When combining laser and map data of interchanges and road crossings it is likely that all abovementioned problems will occur.

3.5.2 Proposed fusion algorithm

Problems with polygons containing no or just a few laser points are solved by integrating object shape knowledge into the 3D road reconstruction. In this case, shape information is the assumption that every road polygon in the map is part of a larger road network and that neighbouring individual road polygons should connect to each other. This assumption is important for polygons with no laser data or if the object has multiple height levels. In these cases it is necessary to obtain height information from the neighbouring polygons, in order to include and exclude laser points for height calculation of that polygon.

In the next section we will describe our implementation of the correct assignment of laser points to map data that solves the research problems mentioned in 3.5.1. Special focus is on complex 3D situations where a single map polygon can occur on multiple levels, and laser data can represent heights on one or more levels.

3.5.2.1 Merging small road parts

To handle these problems we do not want to reconstruct small road parts individually. We choose to first connect the small road parts to each other if they belong to the same road. Then corresponding laser points are selected that belong to the road. By

performing this step, we are able to connect road parts without laser points to other road parts which have laser points. But even more important is the removal of laser points that belong to a crossing road at another height. In the following, the map-growing algorithm will be explained in more detail.

The map-growing algorithm is based on the assumption that neighbouring road polygons can be merged together if they represent parts of the same road. In our algorithm we take large polygons (more than 100 m in length) as seed polygons, in Figure 3-7a indicated with the letter S; laser points are shown in black. The assumption is that large road parts have enough length to initiate a direction to search for. Neighbouring polygons are candidates for merging with the seed polygon. To see if the candidate polygon can be merged, we check if the candidate lies in the growing direction of the seed. The direction of a road has been estimated by analysing angles between consecutive polygon vertices. Only vertices have been selected that are within a radius of 50 meter of the common edge with the candidate polygon. The direction of the polygon vertices (red dots in Figure 3-7) will be taken as input for Hough transformation. The best score in Hough space will fit to nodes with similar direction, in Figure 3-7b shown in red. This will give the local direction of the road. This direction is displayed by the red arrow. If the line through the middle point of the neighbouring polygon intersects with the common boundary (shown in blue), then this polygon will be merged with the seed polygon. The process repeats until there is no more potential polygon to merge with, or when the growing polygon has merged with another seed polygon, see Figure 3-7c and d.

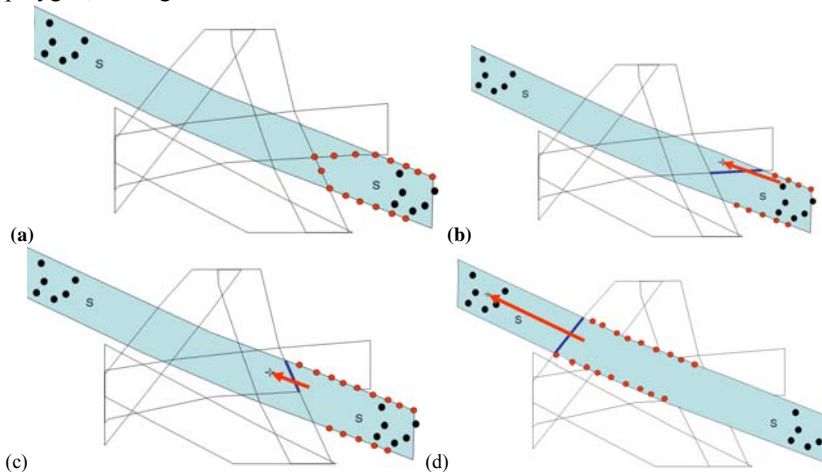


Figure 3-7 Map-growing algorithm, see text for explanation.

The reason why we use a relatively complicated Hough transformation for direction estimation is that we now are able to merge curved polygons as long as the direction is changing gradually, on a length within 50 meters. Normally, this is the case in situations on highways. However, if roads curve more frequently this threshold of 50 meters should be decreased.

3.5.2.2 Assigning laser points to merged road parts

In every iteration step of the map-merging algorithm as described in the previous section, laser points will be added to the road polygon. Laser points in the growing polygon are added to the laser point set if they have the same segment number as available in the growing laser point set or if they are near the plane fitted through the nearest large laser segment in the polygon. To visualise the working of this step, we will introduce the next figures. Laser points are shown superimposed on a 3D model of the road. This model is the final result of our reconstruction method (see next section). Here we only use the model to visualise the assigning of laser points to the growing map polygons. In Figure 3-8a, a seed polygon is chosen automatically to grow and merge with neighbouring road polygons. This is the same polygon as shown in Figure 3-7a. Laser points in adjacent polygons are added if they are in the same segment as the largest nearest laser segment in the seed polygon, shown in large green dots in b. Laser points are also added if they are within a certain distance (1.5 meter) from a fitted plane through the largest laser segment, (c). This step is important because it selects only laser points that belong to the growing road. Doing so, we can grow underneath several other highways, merging all small road polygons without laser points, and connect to the other side of the interchange where we have enough laser points on the road. This process continues as long as the map-polygon-growing algorithm is active (d). The map-polygon-growing algorithm stops when all seed polygons have been processed. Note that in this approach we will avoid assigning laser points from other height levels than the one from the growing polygon.

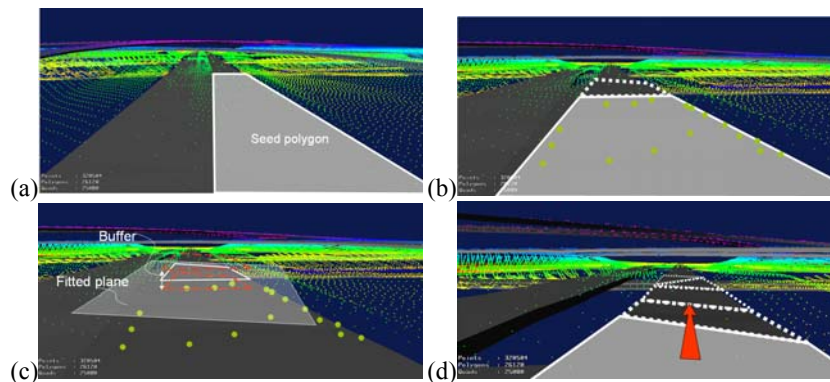


Figure 3-8 Laser growing algorithm, see text for explanation.

Figure 3-9 shows the results of this assignment algorithm. Laser points on a secondary road underneath the highway are correctly assigned, although the original segmentation consisted of four separate segments. Height determination of this road is now based only on laser points from the correct height level.

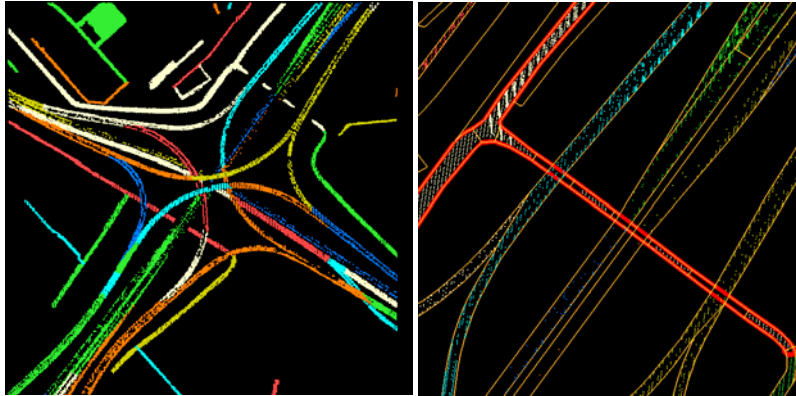


Figure 3-9 Laser points coloured by merged map polygons. (Right) Red boundary indicates a secondary road, containing only laser points of correct height level.

3.6 3D Reconstruction of polygons

Now that laser points have been assigned to map polygons, the actual reconstruction consists of adding height values to the polygons.

3.6.1 Polygon boundaries

Road segments are represented by closed polygons. Its geometry has been defined by the coordinates of vertices and the topology.

Every map point belongs to two or more polygons. In each of the neighbouring polygons laser data is selected to calculate the height at the map point, see Figure 3-10. By calculating multiple heights at every map point, height discontinuities can be detected and modelled.

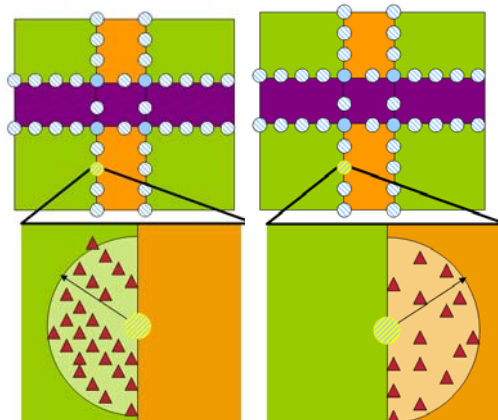


Figure 3-10 Selection of laser points (triangular symbols) near a map point, from grass land (left) and road object (right).

The height is calculated by taking the height value of a plane at the map point location.

$$z = f(x, y) = -xp_1 - yp_2 + p_3 \quad (3.1)$$

Where p_1 and p_2 are two slope parameters and p_3 a distance parameter of the plane. This plane is calculated by least squares adjustment through the selected laser points. To reduce influences of single laser points, only points from the largest segment within in the selection have been used. If the number of points does not exceed a certain minimum threshold (default: 8 points), the search radius is automatically increased until the minimum of points has been found. We can write the plane calculation in a system of linear equations:

$$E\{y\} = Ax. \quad (3.2)$$

In equation (3.2), y contains observations (z -values of laser points), x is a vector of the three unknown plane parameters and matrix A contains information about the configuration of laser points. Each row consists of the horizontal location of a single laser point $(-x, -y, 1)$.

$$E \begin{Bmatrix} z_1 \\ z_2 \\ z_3 \\ \dots \\ z_n \end{Bmatrix} = \begin{pmatrix} -x_1 & -y_1 & 1 \\ -x_2 & -y_2 & 1 \\ -x_3 & -y_3 & 1 \\ \dots & \dots & \dots \\ -x_n & -y_n & 1 \end{pmatrix} \begin{pmatrix} p_1 \\ p_2 \\ p_3 \end{pmatrix}. \quad (3.3)$$

To solve these equations in a least squares adjustment, observations are given a weight, and plane parameters are estimated by:

$$\hat{x} = (A^* Q_y^{-1} A)^{-1} A^* Q_y^{-1} y; Q_{\hat{x}} = (A^* Q_y^{-1} A)^{-1}. \quad (3.4)$$

The height of the plane with these parameters at the location of the map point is taken as map point height, using the formula of (3.1). The reason why we listed equations 3.2-3.4 here is that these describe the *functional* model of our reconstruction algorithm. The functional model defines the mathematical description of the map height determination. We will need this for understanding the *stochastic* model, which describes the uncertainty of the height determination. The stochastic model will be described in chapter 4.

3.6.2 Additional polygons

Earlier in Figure 3-5 we have seen that additional vertices were needed to correctly capture the 3D shape of crossings. Figure 3-11b clarifies that adding height to 2D vertices is not enough to get a 3D model. At a certain point the terrain will connect the upper road with the lower road; part of the edges between terrain and road, which were connected in 2D do not connect to each other in 3D. This means that, next to additional vertices, also additional 3D edges have to be created for overlapping objects. After the map polygon growing step other gaps remain at both sides of the ‘invisible’ polygons,

as can be seen in Figure 3-11c. This means that, next to additional vertices and edges, also additional polygons are necessary. The gaps can be filled by creating new polygons, which have the 2D shape (and topology) of the road polygons lying above them. The heights of the new nodes are determined by searching for map points at neighbouring polygons that lie on the ground surface. Doing so, these new polygons are connected to lower neighbouring polygons, like in Figure 3-11d. New polygons are coloured grey.

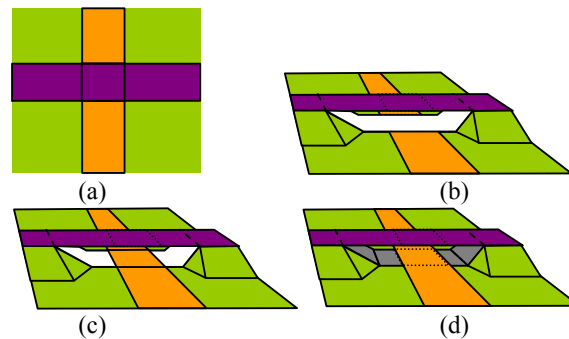


Figure 3-11 Creating new objects: crossing in 2D (a); additional edges are necessary to reconstruct height of 2D features (b); connecting lower road parts still leaves gaps at the sides in the terrain (c); added occluded surfaces (d).

Detection of situations as shown in Figure 3-11 is based on comparing height values at map point locations that have been determined by fitting planes through the neighbouring polygons.

3.6.3 Assumptions on boundaries

Each map point has at least two 2D neighbouring polygons. Map point heights have been calculated from each neighbouring polygon, using laser points assigned to that polygon. The actual height determination at map point locations from laser data depends on the topographic class of the polygon:

- (A) Map points of water polygons are restricted to have the same height, in this case the minimum height of laser points of the most frequent segment number inside the water polygon. The result is that the boundary of polygon has equal height, so the water surface is horizontal.
- (B) In this part of research, 3D buildings are simplified as flat roof buildings. Map points of building polygons are set to the maximum height of laser points of the most frequent segment number inside the building polygon. The result is that the boundary of polygon has equal height, which corresponds to reconstructing buildings in LOD-1 according to the definitions of CityGML (Kolbe et al., 2005).
- (C) For each of the map points on boundaries of other topographic classes, a plane is fitted through nearby laser points and the height of this plane at the location of the map point is taken as the boundary height.

At this point, rules have been introduced to decide whether the multiple calculated heights should be merged into one height, or not. Knowledge about topographic features has been introduced about the behaviour and (dis-)continuity of the boundary, originally proposed by (Koch, 2004). The following connection rules have been applied:

- (1) Water – terrain (e.g. meadow): Minimum height of the laser points in the water polygon is kept for all map points along the water boundary. Heights calculated from adjacent terrain polygons are set to the water height.
- (2) Water – road: Both heights are kept, resulting in a step edge between road and water polygons.
- (3) Road – terrain: If height differences are below a certain threshold (1.5 meter) terrain heights are set to the road height. Otherwise it is assumed that the polygons lie on different height levels. The program then creates new 3D map points at two height levels.
- (4) Road – road: If height differences are below a certain threshold (1.5 meter) two road heights are set to the average height. Otherwise it is assumed that the polygons lie on different height levels.
- (5) Terrain – terrain: A TIN surface is created using laser data from both terrain polygons. Height of map points between two terrain polygons has been interpolated from the TIN. Note that, in this case, the earlier calculated height by plane fitting will be replaced by a TIN interpolated height.

3.6.4 Surfaces

After height calculation of the map points, 3D boundaries are triangulated to get a solid surface description of the object. Most of the terrain objects show some relief at its surface. Laser points lying on the terrain are used as nodes in the surface TIN model. Morphological filtering has been applied to prevent unwanted spikes near edges between roads and meadow. These spikes are caused by misregistrations between the laser and map data, e.g. when laser points are located within meadow polygons but actually lie on upper roads of the interchange. These mistakes did not influence the height determination of the map points, because a plane was fitted through a dominant segment of laser points. However, when adding individual laser points to the surface these errors show up as steep triangles in the TIN, and have to be removed. This filtering is performed for each object separately.

To get a smooth surface at road, building and water objects, map points at those boundaries have been used to generate a constrained TIN model for each polygon, without adding laser points lying inside that polygon. Note that for buildings and water polygons this means reconstructing horizontal surfaces due to the equal height of the map points on those boundaries. Figure 3-12 shows an example of our surface description. TIN edges and faces are shown for road and water polygons, TIN faces are shown for terrain polygons. To enhance the appearance of our reconstructed roads and water bodies we automatically generate a thickness by adding a sidewall of 1 meter height underneath the reconstructed roads and water bodies. Most of the sidewalls for water bodies are underneath the surface and therefore not visible. However, when water bodies are next to each other, or next to road surfaces, the 3D boundaries have different heights. In those cases the sidewall closes the gap between the two objects. As we build

one TIN for each reconstructed polygon we can generate multi-layered TIN models as shown in Figure 3-12.

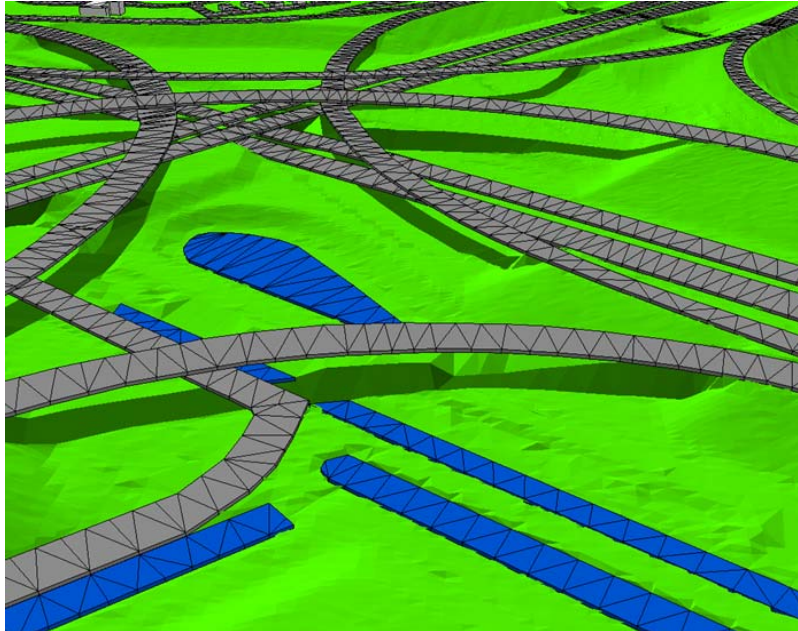


Figure 3-12 3D Surface representation on roads, water and terrain polygons.

3.7 Results

Two interchanges in the Netherlands have been reconstructed and visualised here, each with their own difficulty. “Prins Clausplein” is a four level interchange near The Hague with many small map polygons and obstructed parts. In the data of “Waterberg” near Arnhem laser data has been filtered out at locations of interchanges, so the challenge is to reconstruct the interchange at all levels without having laser data at those locations. In this chapter results are shown and discussed. Details on the geometric quality description of these roads are handled in chapter 4.

3.7.1 Interchange “Prins Clausplein”

Interchange “Prins Clausplein” is a challenging infrastructural object to reconstruct. The presence of four height levels of highways causes many occluded views. This results in several gaps in the laser data. Additionally, due to the weak reflectance of some (low) parts of highways (asphalt absorbs laser pulses) point density decreases to 1 point per 100 m², and in extreme cases 1 point per 400 m². Beside the low density in the laser data, the multiple crossing roads cause many small road polygons in the map. These are the main reasons why this interchange is a challenging object.

In the following we show examples of the 3D reconstructed models. The models have been reconstructed automatically, without manual intervention or editing. In Figure 3-13 four levels of highways are shown. Horizontal bends in road polygons are inherited from the 2D map.



Figure 3-13 Four levels of highways have been reconstructed automatically.

At every location in our datasets where height information was unavailable (60 polygons) our method was able to reconstruct 3D roads by connecting them to neighbouring polygons. Hidden polygons that are reconstructed underneath elevated 3D roads are classified as special land cover class. However, we implemented an optional version such that these polygons can take over the most prominent classification of the neighbouring polygons. Examples are shown in Figure 3-14 where two hidden polygons have taken over the classification 'water' from their neighbours.

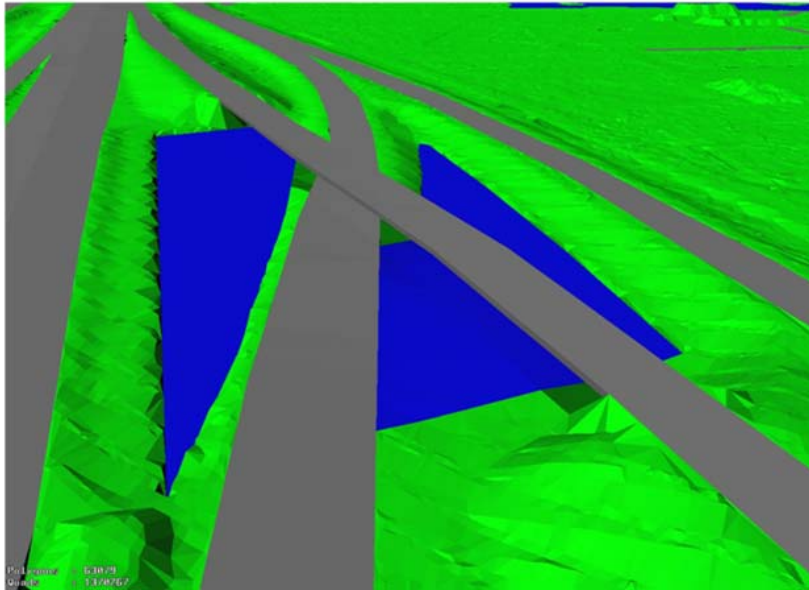


Figure 3-14 Simple highway crossing with water and terrain. Hidden polygons have taken the classification from their neighbouring polygons. Water bodies are reconstructed as horizontal surfaces and height relief can be seen inside terrain polygons.

3.7.2 Interchange “Waterberg”

Remarkable in the laser data of interchange Waterberg is the lack of laser points at interchanges. These were filtered out by the contracted company that acquired the laser dataset. This removal was done on behalf of the Survey Department, who used the laser data for production of DTM. Several polygons contain no laser points inside their boundary, see Figure 3-15.

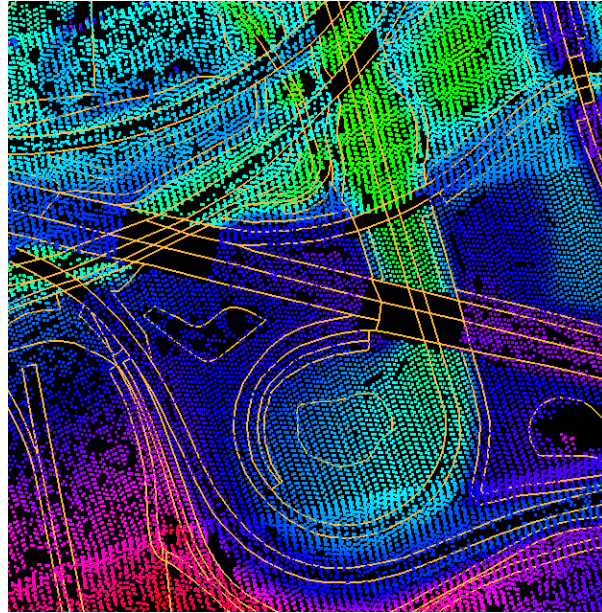


Figure 3-15 Laser data and map boundary data.

As our map growing algorithm connects single map polygons if they belong to the same road, we were able to 'bridge' the gap of laser points.

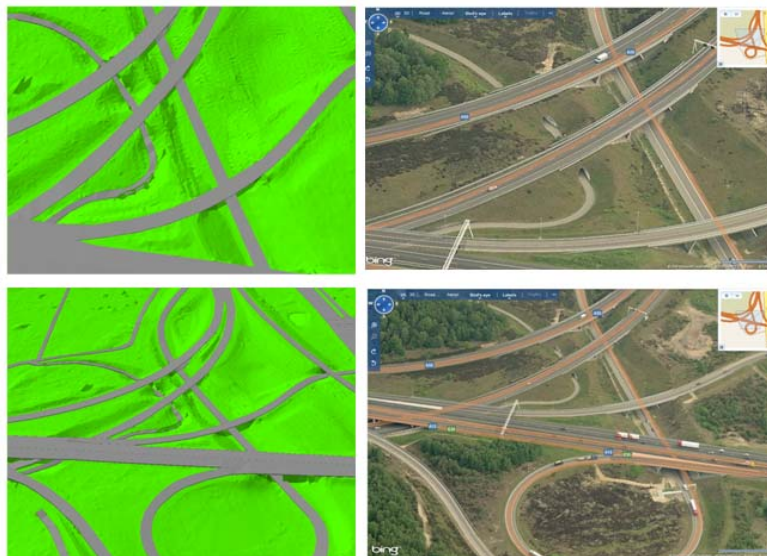


Figure 3-16 Reconstructed model (left) and oblique images (right, ©Bing Maps).

3.8 Discussion

In this section we discuss the parameter settings and topological correctness of the reconstructed model. The geometrical accuracy is discussed in the next chapter 4.

3.8.1 Parameter settings

The results of our approach depend on a number of parameter settings. These settings define threshold values that relate to processing of the input data and relate to defining the level of detail of the output. The advantage of using national databases as input source is that the specifications of the input are more or less fixed to certain standards. These standards can be helpful to propose relative stable threshold values in our 3D reconstruction algorithm. However, appearances of data and objects can change from scene to scene. Table 3-1 gives an overview on the parameters and default parameter values. Some of the default values are adapted automatically if that value does not give satisfactory intermediate results, the others can be changed by the user when necessary.

Table 3-1 Processing parameters and default values.

	Default value	Automatically adapted in following situation
Pre-processing stage		
Map point densification	10 meter	
Minimum segment size	10 laser points	
Fusing map and laser data stage		
Minimum size seed polygon	100 meter	50 meter if no seed polygons are found
Maximum vertical distance between plane and laser points to be added to growing map polygon	1.5 meter	
3D Reconstruction stage		
Minimum number of laser points inside selection	8 points	
Radius for selecting nearby laser points	15 meter	Doubled automatically if too few laser points are found
Maximum height difference at map point location to decide if neighbouring polygons connect to each other in 3D.	1.5 meter	

For scenes that do not fit to standard highway situations, the operator might want to tune parameters, e.g. concerning the size of small objects to be filtered or the size of the seed growing polygon. The laser data used in our examples were part of the relative coarse AHN dataset. The new national height dataset, AHN-2, will be acquired with a

higher point density. When using higher density laser scanner data, some parameter values can be changed in order to improve the 3D model. Increasing point density results in better detection (and removal) of small unwanted objects. In Table 3-2 an example is given what could be done if the point density would be doubled.

Table 3-2 Adapting parameter values when using higher point density laser data.

	When using higher (double) point density laser data. Relative to default value.	Example values adapted parameter settings.	Motivation
Pre-processing stage			
Map point densification	Decrease distance	5 meter	More details can be found, so more details can be modelled
Minimum segment size	Increase segment size	20 points	Size of unwanted objects increase in terms of number of points
Fusing map and laser data stage			
Minimum size seed polygon	No change	100 meter	Input map data remained unchanged
Maximum vertical distance between plane and laser points to be added to growing map polygon	No change	1.5 meter	Modelling issue, less dependent from input data.
3D Reconstruction stage			
Minimum number of laser points inside selection	No change	8 points	Minimum number is to ensure a reliable plane fitting.
Radius for selecting nearby laser points	Decrease radius	7.5 meter	Radius can be decreased as there are more points near the map point
Maximum height difference at map point location to decide if neighbouring polygons connect to each other in 3D.	No change	1.5 meter	Modelling issue, less dependent from input data.

3.8.2 Topological correctness

At this moment, our reconstructed model is not completely watertight. Examples are found at locations where terrain and road do connect in 2D but not in 3D, as shown in Figure 3-17. If the height difference of these two neighbouring objects is smaller than 1.5 meter at the boundary, the polygon of the terrain will take over the height of the road. However, in some situations the difference is higher than this threshold value; at those locations (indicated with grey arrows in Figure 3-17) the 3D model is not watertight. Due to the selection of points on a small hill that act as noise barrier next to the road a plane through the selected points crosses at more than 1.5 meter above the road height at that edge location. Increasing this threshold value would be a solution in this example but will cause distortions at other locations where we would like to detect and keep multi layer situations. The assumption that terrain polygons always are on the lowest level would also be a solution for this case but does not hold for 'ecoducts', tunnel situations and some crossings where terrain polygons are located at the higher level of the crossing. Using higher density laser data would be the optimal solution to these problems, as this means that the search radius can be reduced and only laser points close to the boundary will be chosen.

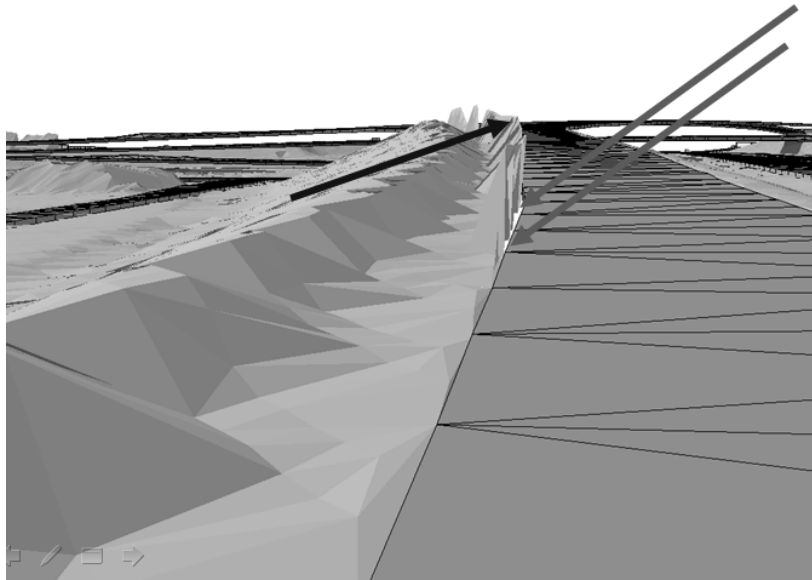


Figure 3-17 Plane fitted through points on small hill. The direction of the plane is approximated by a black arrow. Terrain polygon has not been snapped to with road polygon, causing leaks in the 3D model (grey arrows).

4 Quality analysis on 3D roads¹

¹ This chapter is mainly based on content from the following papers:

Oude Elberink, S. and Vosselman, G., 2007. Quality analysis of 3D road reconstruction. *International Archives of Photogrammetry, Remote Sensing and Spatial Information Sciences*, 36 (part 3/W52): 305-310.

Oude Elberink, S. and Vosselman, G., 2008. Quality analysis of 3D road reconstruction. *The Photogrammetric Journal of Finland*, Vol. 21 (No. 1): 51-60.

In this chapter we analyse the geometric quality of the reconstructed 3D roads, as described in chapter 3. In 4.1, quality is described as a function of the quality of the input data. This is done by using error propagation formulas, giving us the opportunity to predict the uncertainty of the calculated 3D roads at any location in the model. Next to that, reference data has been used for the Prins Clausplein to give an independent check on our model, described in 4.2. These two quality parameters can be used to see if the height difference between reference data and 3D model (as calculated in 4.2) can be explained by the uncertainty in the model (calculated in 4.1). This process, which is known as ‘testing’ in geodetic and photogrammetric practice, is described in 4.3.

4.1 Error propagation

By using formulas from network design analysis, we can predict the quality of our reconstructed model (Teunissen, 1991). Although this can be done before the actual reconstruction, we present this together with checking on reference data. For researchers quality prediction is useful for optimising parameters used in their algorithms, in geodetic terminology known as “designing the network”. For users, predicting quality is important because it answers the question whether the input data and the processing steps can fulfil the user requirements on the desired 3D model.

We distinguish three components in the precision of the map points calculated with our algorithm:

$$\sigma_{map_pnt}^2 = \sigma_{plane}^2 + \sigma_{laser_block}^2 + \sigma_{plane_model}^2 \quad (4.1)$$

σ_{plane}^2 is the uncertainty caused by variations in the plane parameters, which are influenced by laser point noise. $\sigma_{laser_block}^2$ represents a precision value for the whole laser dataset, and $\sigma_{plane_model}^2$ stands for discrepancies between the fitted plane and the actual shape of the road.

4.1.1 Quality of plane at map point location

To predict uncertainty in the plane parameters, which have been calculated according formulas 3-2 to 3-4, we need information about the quality and configuration of the input data. (Crombaghs et al., 2002) present a practical method to describe quality of laser data sets as a function of four error sources (error 1 to 4, denoted as E1 to E4). These error sources are point noise (E1), GPS (E2) and INS noise (E3) and strip adjustment noise (E4). Influence of each of these error sources depend on the size of the area of interest. Within the radius for selecting laser data, it can be expected that all laser points are influenced by the same E2, E3 and E4. When using least squares adjustment, these three error sources act as systematic errors, not stochastically influencing the quality of the plane equation. These error sources will be added later to the precision of the map point (see eq. 4.1). When only assuming influence of point noise in equation (3.4), Q_y turns into σ^2I and (3.1) can then be written in the form:

$$\hat{x} = (A^* A)^{-1} A^* y. \quad (4.2)$$

Equation (4.2) shows that a diagonal matrix Q_y does not have an effect on the estimation of plane parameters. However, it does affect the quality of the plane parameters.

$$Q_{\hat{x}} = (A^* Q_y^{-1} A)^{-1} = \left(\frac{1}{\sigma_z^2} \begin{pmatrix} \sum_{i=1}^n x_i^2 & \sum_{i=1}^n x_i y_i & \sum_{i=1}^n -x_i \\ \sum_{i=1}^n x_i y_i & \sum_{i=1}^n y_i^2 & \sum_{i=1}^n -y_i \\ \sum_{i=1}^n -x_i & \sum_{i=1}^n -y_i & n \end{pmatrix} \right)^{-1} \quad (4.3)$$

In order to avoid singularity when inverting the 3x3 normal matrix, columns of A^*A have to be linearly independent. This can be achieved by selecting at least three laser points that do not lie in a straight line. For a stable calculation we proceeded with local coordinates by subtracting the mean location of the laser points. Once the quality of plane parameters is known, we can calculate the height precision of the plane at the location of the map point.

$$\sigma_{plane}^2 = x^2 \sigma_{p_1}^2 + y^2 \sigma_{p_2}^2 + \sigma_{p_3}^2. \quad (4.4)$$

4.1.2 Quality of laser block

Remember that equation (4.1) consisted of multiple components: plane uncertainty, systematic errors in laser data and model uncertainty. Laser point noise was taken into account in the plane uncertainty; other errors in laser data (E2, E3, and E4 as mentioned in section 4.1.1) did not reflect the plane equations. However, they influence the precision of the map point height, as they influence the height of the total group of laser points selected for calculation of the map point height. Each of these three uncertainties is present in every selection of laser points, and can be summed quadratic as we may assume them to occur independently for this selection (Crombaghs et al., 2002). We can group these errors by:

$$\sigma_{laser_block}^2 = \sigma_{E_2}^2 + \sigma_{E_3}^2 + \sigma_{E_4}^2 \quad (4.5)$$

4.1.3 Quality of plane model

Plane model quality covers the discrepancy at the map point between the actual shape of the road and the modelled plane. If the horizontal distance between map point and laser points is small it can be expected that a plane through these laser points accurately represents the road height at the map point. Model uncertainty becomes of interest when we need to extrapolate over a certain distance, in case we are short of laser points. We can quantify the differences between a local plane and the actual shape, by analysing the

curvature of roads. This quantification is a function of horizontal distance between plane origin and map point. To estimate the idealisation precision, we have to use height differences between plane and reality instead of curvatures. For distances smaller than a few hundred meters, we can approximate the difference between the road and a plane by a quadratic term.



Figure 4-1 Extrapolation error caused by model uncertainty.

Figure 4-1 can be translated into a stochastic measure for model uncertainty by calculating the standard deviation of extrapolation errors as a function of the distance. We have approximated this value by dividing maximum extrapolation error, calculated by integrating curvatures, by three.

Figure 4-2 shows predicted standard deviations of map point heights. The figure shows the position of map points, coloured by predicted standard deviation of the map point height. For visibility reasons the standard deviation has been classified into three categories: standard deviations larger than 50 cm (shown in red), larger than 20 cm (yellow), and below 20 cm (green). To better understand the cause of large variations at some locations, the blue box in Figure 4-2 shows the laser points used for 3D road reconstruction. The relation between lack of laser data and large height variations can easily be seen for locations in black ellipses. Point densities in these black ellipses drop to 1 point per 100 m², with extremes to 1 point per 400 m². At map point locations in those areas, map point heights show standard deviations of more than 50 cm. Two factors play an important role here. First, the plane has been determined by just a few laser points; standard deviations of laser points will have a great influence because they are not averaged out. Secondly, the search radius for finding enough laser points increases up to 50 or even 100 meter. This results in extrapolation errors rising up to 50 cm or more.

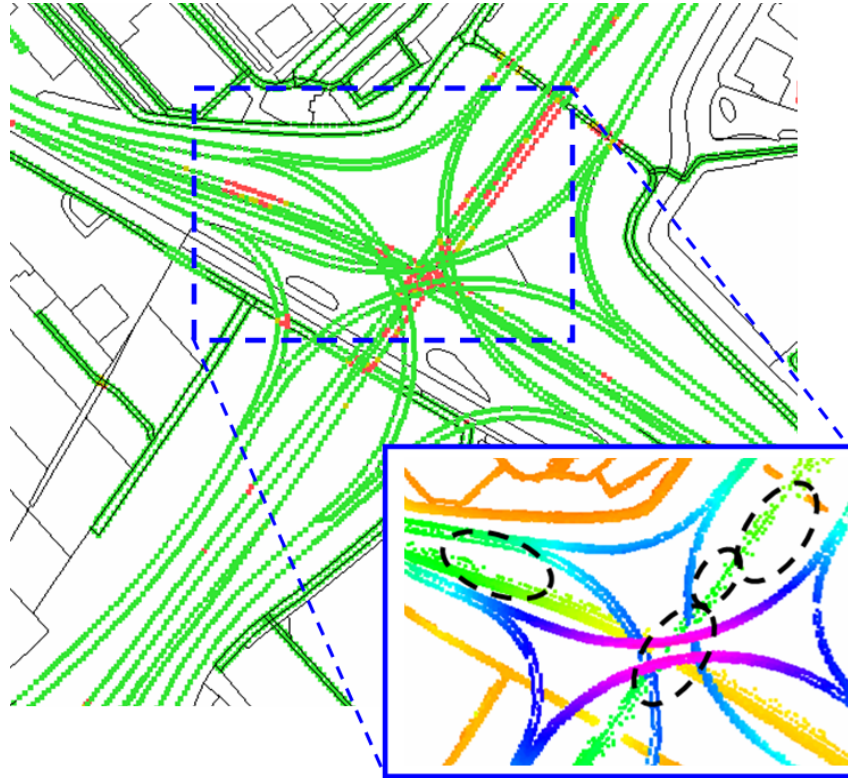


Figure 4-2 Standard deviations of map point heights. Compare with available laser points (lower right corner).

Poor configuration of the laser points leads to large standard deviations. Figure 4-3 shows a situation where the majority of laser points lie on a straight line, in this case clearly measured in just one or two scan lines. Fitted planes are badly determined in the direction perpendicular to this scan line. Blue circles have a radius of 15 meter.

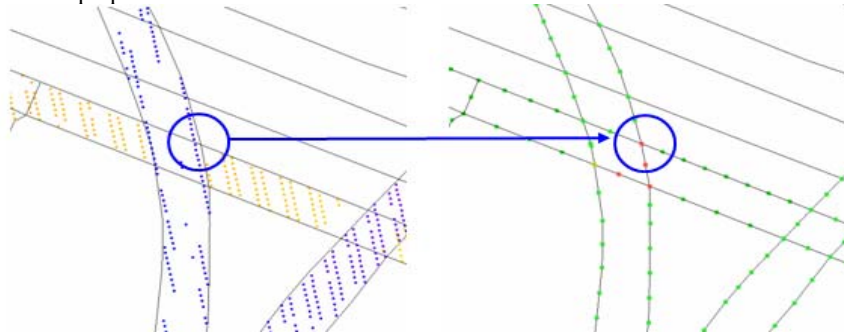


Figure 4-3 Poor configuration of laser points (left) leads to large predicted standard deviations (right).

In Figure 4-4 precision values of map point heights are visualised at 3D map point locations and superimposed on the reconstructed model. The standard deviation has been visualised with coloured dots at map point locations. Obviously, absence of laser points on the lower parts of the interchange cause larger a priori standard deviations.

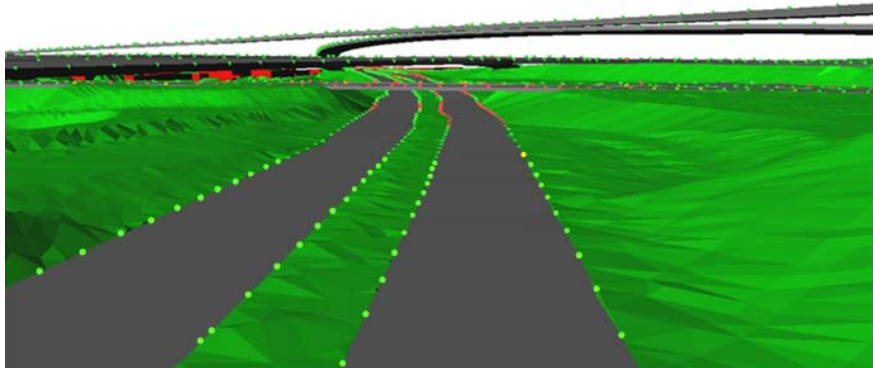


Figure 4-4 Precision of map point heights visualised in 3D model.

In the previous sections we have described our 3D road reconstruction method and its stochastic model. To be able to test our –functional and stochastic– model, heights on reconstructed roads have been compared with independent reference data.

4.2 Reference data

Accurate geometric information of highways in the Netherlands is stored in a photogrammetrically derived topographic database, called DTB. Terrestrial measurements have been added to complete road information underneath interchanges and in tunnels. The DTB contains 3D geometric and semantic information of points, boundaries, centrelines and surface features of national roads, at a map scale of 1:1000. This also includes information on road details like locations of paint strips, traffic lights, road signs and other detailed infrastructural objects. DTM information (2.5D) has been integrated into the DTB by photogrammetric measurements on breaklines in the terrain. An example of DTB data is given in Figure 4-5, showing the complex interchange Prins Clausplein near The Hague.

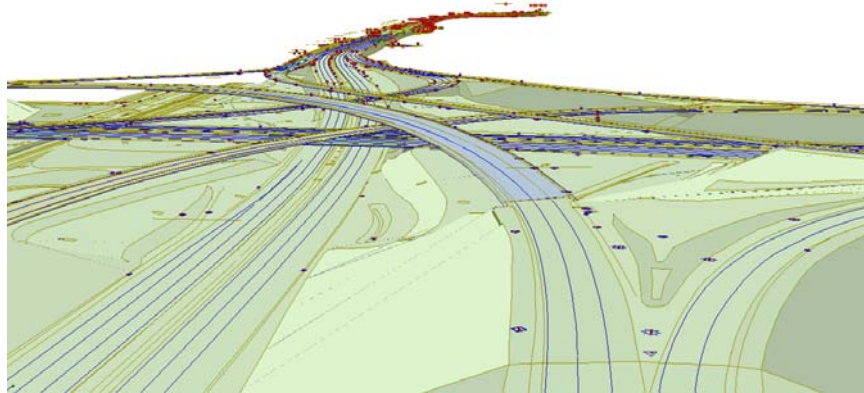


Figure 4-5 DTB data is used for reference information. Paint strips, shown as blue lines, have been selected to test reconstructed roads.

Paint strips have been measured by manual photogrammetric or tachymetric measurements. Paint strips belong to the so-called ‘hard topography’ category, what means that this object can be identified and measured with high precision. The standard deviation of heights of these points is required to be 9 cm or better.

4.2.1 Height differences between reference data and 3D model

Overlaying reference data of paint strips on our 3D model gives the first impression whether the two datasets can be compared. In Figure 4-6 reference data is shown in blue, overlaid on the gray reconstructed roads.

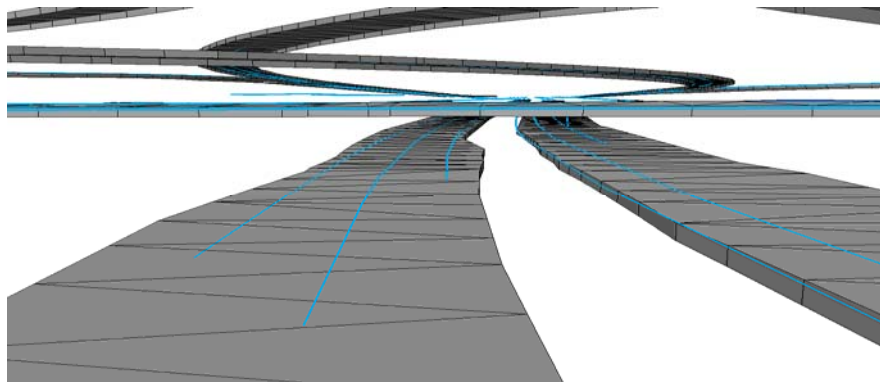


Figure 4-6 Visual inspection of 3D roads by superimposing reference data (blue lines represent paint strip locations).

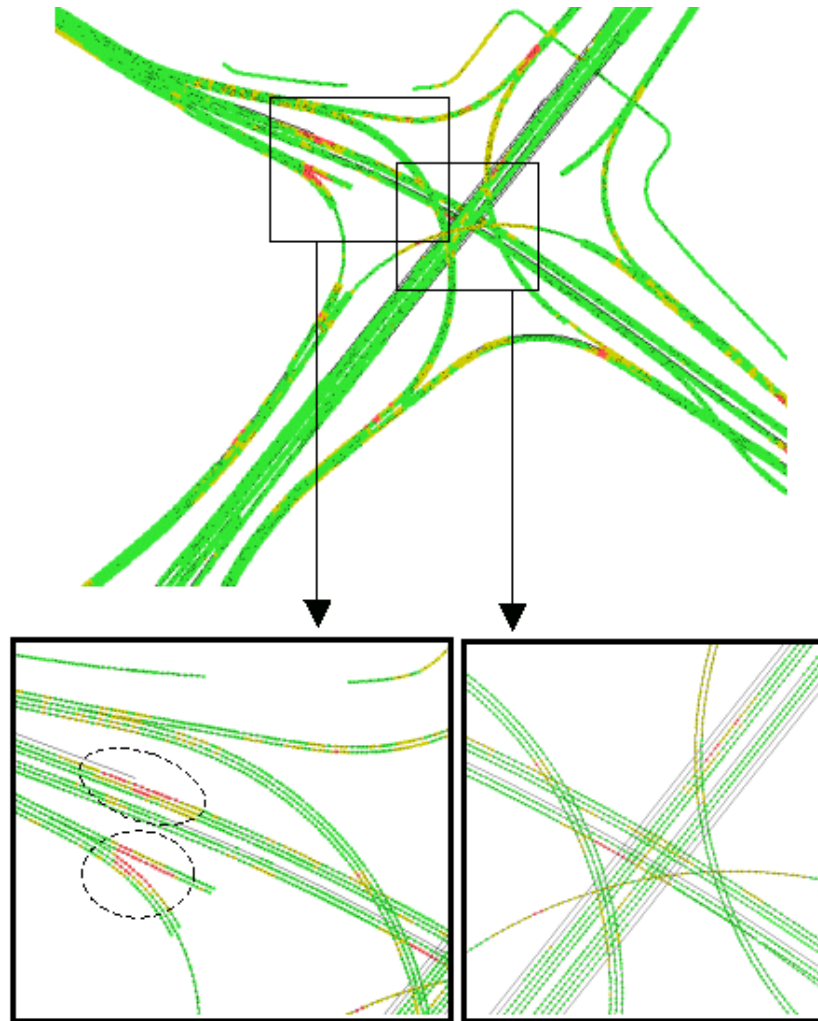


Figure 4-7 Paint strip locations coloured by height difference with 3D model. differences are coloured as red (larger than 50 cm), yellow (larger than 20 cm) and green (below 20 cm).

Results of calculated differences at paint strip locations can be seen in Figure 4-7. Note that reference data is not completely covering the interchange. Some parts of flyovers have not been measured in the reference data, test results are therefore locally missing. Still we calculated over 10.000 height differences for this area of 1.2 x 1.2 km. A further look at Figure 4-7 learns that in the centre of the interchange (highlighted in the lower right corner box), where laser points were scarce at all height levels, the calculated differences are remarkably small. A few differences are more than 50 cm, some between 20 and 50 cm and many below 20 cm (green). In the lower left corner

box, two situations are highlighted which show large height differences with a systematic character. In the higher ellipse height differences could be expected, due to the lack of laser points, see Figure 4-2. The reason for differences in the lower circle is that the search radius selects laser points from both road parts, which happen to curve strongly at those locations. Therefore, fitting a plane through the selected points will differ from reality.

Number of reference points inside test area	10922
Mean difference	0.5 cm
Standard deviation of vector of differences	15.4 cm
Maximum absolute difference	121 cm

Table 1. Statistical results of comparing heights of 3D roads.

Table 1 summarizes most important statistic information of height differences between reference data and 3D reconstructed model. The mean difference includes systematic errors between reference data and our reconstructed model. Normally, it is expected to be in the order of 0-5 cm, due to systematic errors in laser data (Crombaghs et al., 2002). In this case, the mean difference happens to be very small (0.5 cm). Looking at the standard deviation of the differences of 15.4 cm, and knowing that it includes uncertainty in the reference data ($\sigma_{\text{ref}} = 9$ cm), we can calculate the uncertainty of our reconstructed model:

$$\sigma_{\text{mod}} = \sqrt{(15.4^2 - 9^2)} = 12.5\text{cm} \quad (4.6)$$

It should be noted that this value is biased by some systematic errors in the reconstructed model.

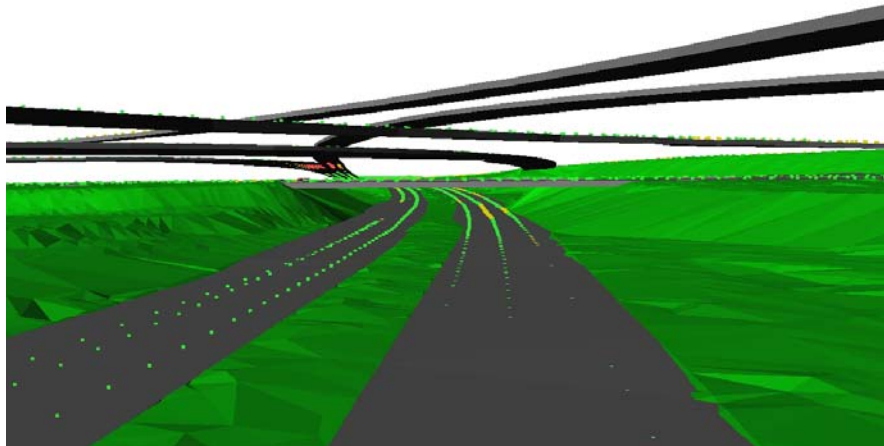


Figure 4-8 Height differences between reconstructed model and reference data, shown as dots at paint strip locations.

Results of measuring the vertical distance between reference data and the 3D model are superimposed onto the 3D model and shown in Figure 4-8. At the lower parts of the interchange, at places where no laser data was available at a length of 100 meters,

differences are between 20 and 50 cm (yellow). Note that the estimated precision value in that area (Figure 4-2) is larger than the actual height difference.

4.3 Testing of predicted quality

Now that the actual difference is known, we divide each difference with the expected standard deviation of the difference. In this section we will describe our testing configuration by comparing reference data with our reconstructed model. As we have seen in section 3.6 roads are represented as a TIN surface, using 3D map points on the boundary as TIN nodes. Figure 4-9 explains the set-up of our height testing procedure. The bullets represent three map points that form one TIN triangle. The plus marks represent 3D positions on paint strips, which are measured with high accuracy in the reference dataset. At these plus marks height differences and its precision have been calculated.

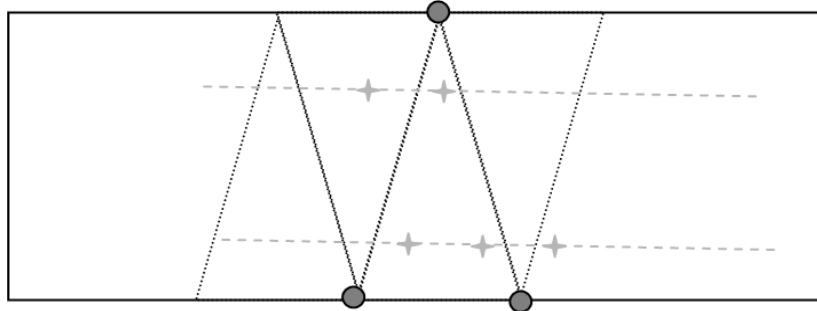


Figure 4-9 Configuration of height testing: TIN patches and points on paint strips.

Our expectation is that the height difference between reference data and our 3D model should vary around zero. Deviations should be explainable by uncertainty in the 3D model and in the reference data.

$$\begin{aligned} \Delta h_i &= h_{\text{mod}_i} - h_{\text{ref}_i} \sim N(0, \sigma_{\Delta h_i}) \\ \sigma_{\Delta h_i}^2 &= \sigma_{h_{\text{mod}_i}}^2 + \sigma_{h_{\text{ref}_i}}^2 \end{aligned} \quad (4.7)$$

The term $\sigma_{h_{\text{mod}_i}}^2$ contains the height variance of the model, at the location of the reference point. We therefore have to propagate precisions of the map points, calculated as described in section 4.1, to the location of the reference point. Looking again at Figure 4-9, we see that the precision of three map points influence the precision at reference point location.

First, the location of the reference point within the TIN mesh is important to describe the influence of each of the map points. If the reference point is close to one of the three map points, the precision of the TIN height is highly influenced by the precision of the height of this single map point.

Then we investigate the influence of covariance between the three map points. Extreme cases here are no covariance and full covariance. If the three map point heights have been calculated by three different groups of laser points, we can assume that the correlation equals zero. This occurs when using a small radius to select laser points. If the three map point heights have been calculated by the same group of laser points, the correlation equals one.

$$\sigma_{\text{mod}} = \frac{TIN(\sigma_{\text{map_points}})}{\alpha} \quad (4.8)$$

Equation (4.8) shows the calculation of the precision of the reconstructed model, at locations of reference points, by TIN interpolation of 3 precision values of three map points, divided by a correlation term α ($1 < \alpha < \sqrt{3}$).

In section 4.1 we have calculated the precision of map point heights by using error propagation techniques and properties of least squares plane fitting, followed by an actual quality check using reference data in 4.2. To test the stochastic model we check if the actual differences can be explained by the predicted accuracy. With the outcomes of equation (4.7), we test if the difference is significant by using a modified version of the w-test statistics or local error detection as described by (Baarda, 1968) and (Teunissen, 1991). In their approaches, the w-test calculates normalised residuals of geodetic observations. If the test exceeds a critical value, this observation will be recognised as a possible outlier. In an iterative procedure the observation with the highest w-test value has been removed from the adjustment.

$$w_i = \frac{\Delta h_i}{\sigma_{\Delta h_i}} \sim N(0,1) \quad (4.9)$$

A closer look at the w_i learns that it indicates how well one can predict the actual quality. This is an informative measure to show if the predicted quality represents the actual quality. If the stochastic model is correct, the total of all w-test values should have a standard normal distribution. To rely on predicted quality is important for future users who want to predict the quality of 3D reconstructed roads, without checking on highly detailed reference data. Beside this, reference data might not be available at some locations.

Large w-test values indicate that the actual quality is worse than predicted. In our approach it is of interest to find reasons for large w-test values, because the functional or stochastic model might not be correct at those locations.

In Figure 4-10 large w-test values have been coloured yellow (larger than 3) and red (larger than 4). At these points the actual height difference was three or four times larger than expected, meaning that either the standard deviation was too small or the calculated height was significantly wrong. Note that the former case deals with the stochastic model, and the latter case with the functional model. Due to the systematic

character of large w -test values, we assume a functional error causes the problems at those locations, mostly where one road splits into two roads, see Figure 4-11. The distribution of all w -tests is close to the standard normal distribution, as 68% of the w -test values are less than 1 and 92% are less than 2. If we remove outliers, standard deviation is 1.06 (with outliers 1.22). This means that the predicted stochastic model is a bit too optimistic, but still realistic.

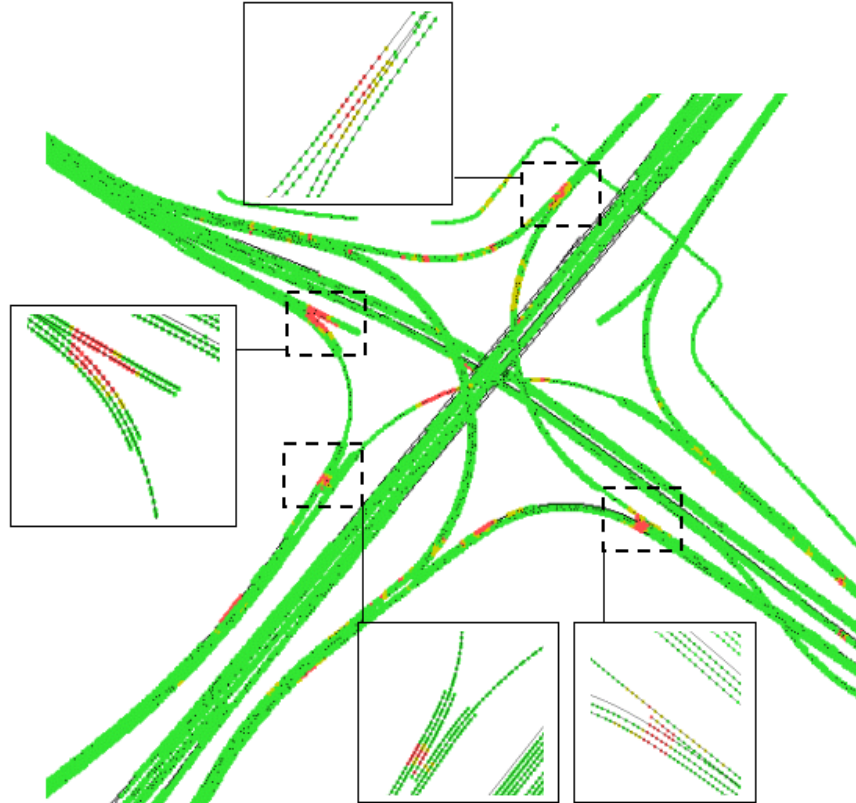


Figure 4-10 W-test values at reference point locations.

4.4 Discussion

Although the distribution of w -test values was close to the standard normal distribution, some systematic patterns could be seen at locations where the road has split into two road parts. In Figure 4-11 a situation is highlighted which show large height differences with a systematic character. The reason for differences is that the search radius selects laser points from both road parts, which happen to curve strongly at those locations. Therefore, fitting a plane through the selected points will result in a lower height value than the real height. In addition to this, the predicted standard deviation is low, because of the large number of laser points found in this radius. That is why the w -test values are likely to be large at these locations.

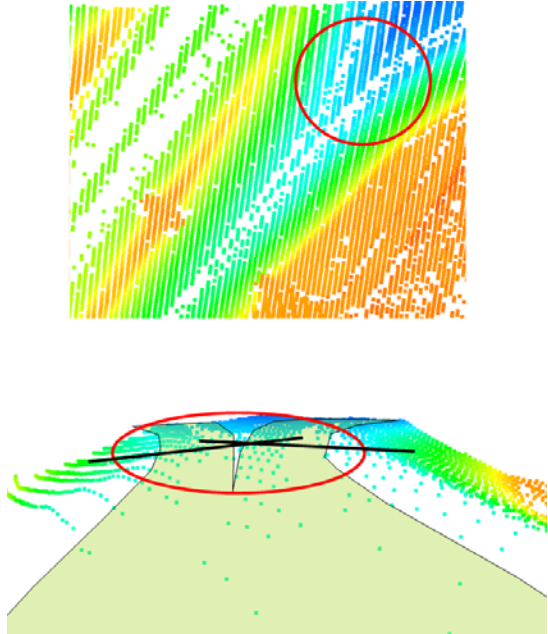


Figure 4-11 Road splits into two roads. Selected points do not represent a planar surface.

Part III: 3D Buildings

This part consists of three chapters:

- 5 Building shape detection
- 6 3D Building reconstruction
- 7 Results and evaluation

5 Building shape detection¹

¹ This chapter contains content from:

- Oude Elberink, S., 2008. Problems in Automated Building Reconstruction based on Dense Airborne Laser Scanning Data. In: *International Archives of Photogrammetry, Remote Sensing and Spatial Information Sciences*, XXXVII, part 3A: pp. 93-98.
- Oude Elberink, S., 2009. Target Graph Matching for Building Reconstruction. In: *International Archives of Photogrammetry, Remote Sensing and Spatial Information Sciences*, XXXVIII, 3/W8: pp. 49-54.
- Oude Elberink, S. and Vosselman, G., 2009. Building Reconstruction by Target Based Graph Matching on Incomplete Laser Data: Analysis and Limitations. *Sensors*, 9(8): 6101-6118.

5.1 Introduction

In the introductory chapter we already stated that upgrading 2D maps to 3D models on a national scale is a task that preferably is done as automatic as possible. In Denmark and in The Netherlands, national mapping agencies recently started to build up national DTMs with 0.5 to 10 points per square meter respectively. When such detailed height products become standard for whole countries it is of high interest to develop automated methods that can effectively use these national datasets. As we have seen in the list of recent developments (chapter 2.9), 3D building models are requested as input source for a variety of urban applications. Despite the progress that has been made in the past, when handling more detailed input and output data other research problems arise and new solutions are needed.

As we have sketched in chapter 1 a reconstruction algorithm should be able to establish a link between the features found in the data and the desired output. In this chapter, the output is a virtual representation of the topographic object “buildings”. The generalization level should be in balance with the data density and what is required by the applications having in mind. As our intention is to reconstruct buildings with general shapes, we aim at storing polyhedral model descriptions. This means our reconstructed building consists of a combination of roof faces. These roof faces are bounded by roof edges, representing ridges, eaves and gutters. Each of these edges is defined as straight line between two points. From the data side we can expect to find laser segments representing roof faces and map polygons representing building outlines. In Figure 5-1 the general research field is shown for our 3D building reconstruction algorithm. Basic assumptions and specifications are given, although they are subject to user requirements and local conditions which are explained in more detail later in this chapter.

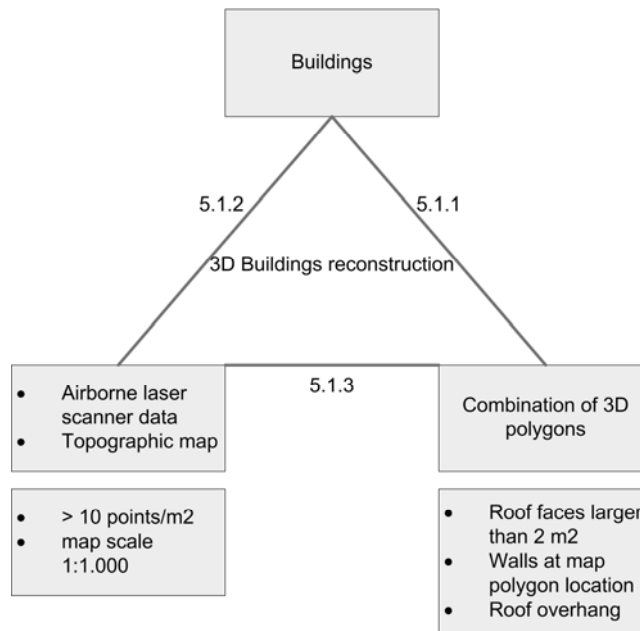


Figure 5-1 Placing 3D Building reconstruction in relation to real buildings, input data and 3D model specifications. Relations between two fields are shown by lines and further described in accompanying section number.

5.1.1 Real buildings vs 3D model representation

Describing the urban scene, in particular roof faces, becomes more complex when looking at a higher level of detail. For the moment, assume we aim at reconstructing roof faces of at least 2 m² area size. Looking at built-up areas with this level of detail, one can see a great amount of variety of small objects such as chimneys, air conditioning boxes and small dormers, Figure 5-2. These objects' sizes are near the level of detail and therefore on the edge of being reconstructed or discarded.

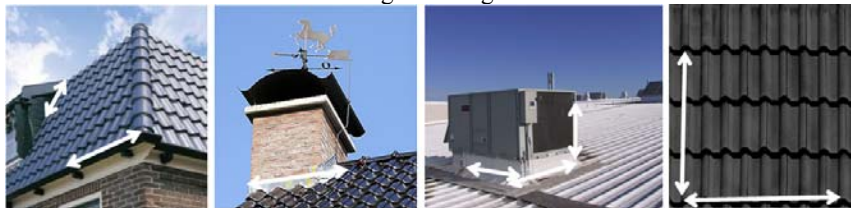


Figure 5-2 The size of one meter in object space. White arrows approximately measure one meter.

At the right of Figure 5-2 roof tiles are shown for an area of about 1 m². Individual roof tiles are considered to be too small to detect², however it is important to realise that the

² On average, about 16 roof tiles per square meter are used for standard gable shaped buildings, in the Netherlands.

roof surface is not exactly flat. When representing roof faces by planar faces, we discard the height texture/structure at the objects' surface. The majority of the roof tiles as shown in Figure 5-2 show a height difference at the tiles' surface of about between 3 and 5 cm. When examining the deviations to a plane for the whole roof, we see that systematic changes can occur. The roof itself is not exactly planar, due to construction inaccuracy or in case of horizontal roofs to drain the precipitation. Another example is enforcing the roof gutters to be horizontal. This assumption definitively harms the reality, as gutters are made to drain the water. However, this is inherent to modelling buildings when simplifying the real world objects.

5.1.2 Real buildings vs appearance in input data

Buildings are measured in laser data by recording 3D coordinates of arbitrary points on the buildings' surface. Points are reflected on e.g. walls, doors, windows, gutters and roofs. Probably, some of the laser pulses have hit nearby objects such as cars, trees and garden furniture. In laser data, urban complexity expresses itself by difficulties in judging whether groups of points belong to a certain building part or to other objects. Besides the deviations between the real objects and the generalization, the data acquisition of the objects also contains uncertainties. Systematic and stochastic errors occur in the acquisition systems. Errors and uncertainties in GPS, IMU and laser scanner systems influence the location of individual laser points and groups of laser points. If the data is corrected for systematic errors, e.g. boresight misalignment of the IMU, as proposed by (Vosselman, 2008), the planimetric accuracy can be expected to be clearly below decimeter level. Vertical accuracy of single laser scanner points depends a.o. on the flying height (Crombaghs et al., 2002) and the terrain roughness (Pfeifer et al., 2004), but is expected to be better than the planimetric accuracy (Vosselman and Maas, 2001).

In 2D topographic maps buildings appear as closed polygons, representing the 2D footprint of building walls³. The level of detail in this polygon is based on the generalization of the 2D map.

5.1.3 Appearance in input data vs 3D model representation

The third relation describes the transition between how buildings appear in the data, and how they are modelled in 3D. Laser points on each roof face need to be modelled as closed planar polygons. Therefore two main processing steps are needed:

1. A planar face has to be created by fitting planes to a group of laser points;
2. The planar face has to be closed by a sequence of straight edges.

³ We assume the topographic map has been acquired such that the building outline represents the wall location. If the map has been acquired by stereo photogrammetric measurements, it is assumed that the building outline has been corrected for roof overhang. The assumption that the map represents the wall holds for the large scale topographic maps in the Netherlands.

The relation between the 2D topographic map and the 3D representation is that the map directly delivers the location of vertical walls. The height of the walls depends on the height on DTM level and the roof face height.

The main strength and weakness of data driven approaches relate to the strong dependency on the data. The strength is the flexibility to reconstruct what is in the data. With the increasing point density and geometric quality of laser scan data, the level of detail and the quality of the 3D models also increase. At the other hand, the weakness of data driven approaches is that missing data or misleading information from the data has direct consequences for the 3D model. Missing data will result in incomplete 3D models, whereas misleading information will produce incorrect reconstructed buildings. Examples of missing data are to be found at wet, steep or dark roof faces. The term misleading information covers the total of undetected situations where assumptions of the algorithm do not fit to the features found in the data.

The challenge is threefold: the first one is to detect if points belong buildings, and, if this is the case, to which building part they belong. The third challenge is to decide what the shape (boundary) is of each of the roof faces.

In this chapter the research problem and proposed solution are presented. The main part of the solution is a target graph based matching algorithm which relates data and model information. This relation results in the roof shape detections of buildings. Based on these matching results we propose an algorithm to actually reconstruct buildings. This reconstruction algorithm will be described in chapter 6.

5.2 Related work

From the late nineties till now several researchers contributed to the research field of 3D building reconstruction. In this section we give an overview of the most important approaches.

Laser data provides valuable information about the orientation of roof faces, and possible partitions of the roof into smaller roof patches, whereas in aerial images the information extraction mostly is on the outlines of the building (Kaartinen et al., 2005). Not only does laser data provide information about the absolute 3D shape of buildings, it also provides relative height information, which can be used to separate terrain from (elevated) objects.

5.2.1 2D Mapping of building outlines

Several papers first calculate the 2D area or outline of buildings, before determining the 3D shape. Most classification methods based on laser data use the information that:

1. buildings are elevated from the terrain;
2. buildings show regular geometric patterns (planar patches, rectangular shapes etc).

Rottensteiner and Briese (2002), Oude Elberink and Maas (2000), Alharty and Bethel (2002) and Matikainen et al. (2003) present approaches that classify building regions on gridded laser scan data. Building regions are extracted by thresholding and texture

analysis or multiple pass filtering (Bretar et al., 2004). Hofmann et al. (2002) additionally use map data to classify the segments that were generated by a clustering procedure.

The contours of the building regions can be used to reconstruct the outline of the building (Elaksher and Bethel, 2002; Morgan and Habib, 2002; Sampath and Shan, 2004; Vosselman, 1999; Wang et al., 2006). The building regions can be taken from the detection step mentioned above. A common procedure is to take the convex hull of the building segment and fit straight lines through this polygon. The main orientation of the building can help to constrain the fitted lines to directions either parallel or perpendicular to this orientation, (Alharthy and Bethel, 2002; Vosselman, 1999). Once the lines have been fitted, a geometrically regular polygon has been derived. For some applications, like 2D mapping, these 2D polygons can be seen as a final result of laser data analysis.

5.2.2 3D Reconstruction of buildings

However, for many other applications, like 3D city modelling, these polygons are used as input source for the reconstruction of 3D building models. Rottensteiner and Briese (2002, 2003) discuss problems related to (step) edge detection and how to constrain and group data driven features. They present an approach by analysing the roof segments, looking for an intersection, a step edge, or both an intersection and a step edge. Also, geometric constraints on the consistence of buildings are proposed by performing an overall adjustment including available sensor information, parameters of the planes and vertices. Geometric constraints can be applied on lines, planes or combinations of them. More improvements can be found in (Rottensteiner et al., 2005) where step edges and outlines are reconstructed more reliable and building hypotheses are tested and parameters estimated. Rottensteiner (2006) proposes an adjustment approach that can handle data observations, geometric constraint observations and approximate values for the unknown parameters as input. So, within this adjustment data and model driven information can be taken as input. Each observation group is given its own weight in the adjustment procedure. The topology of the model is assumed to be known, as being a result of hypotheses tests as described in (Rottensteiner et al., 2005)

In (Vosselman, 1999) an approach is presented which is based on the detection and outlining of planar faces in dense height data. Planar faces have been detected by Hough-based plane extraction. These faces are split up in a connected components algorithm in order to let each component represent a roof face. Next, assumptions are made that there is a main building orientation and that step edges are either parallel or perpendicular to this main direction. Maas and Vosselman (1999) describe two methods for building reconstruction from high point density data. The first works on invariant moments; closed solutions can be formulated for the parameters of simple building models. The second works on intersection of planar faces, which were fitted on the point cloud. The authors propose to add shape constraints like symmetry and collinearity to this data-driven approach. Vosselman and Dijkman (2001) propose to divide ground plans by extending polygon segments at concave corner points. Within each subdivided part the ground plan is further being split at height jump locations and intersection lines.

Haala and Brenner (1997) propose a method to reconstruct buildings from a skeleton derived from building ground plan. Inside the regions of the skeleton, roof patches from a digital surface model are analysed and accepted or rejected according to a hypothesis-and-test algorithm. Brenner (2000) describes the use of segment regions instead of the skeleton regions, and tries to form logical sequences of segment patches. Although this approach is data-driven, the reconstruction possibilities are limited to the acceptance criteria. One of these criteria is the region labelling, where segments are accepted looking at the sequence of regions along the map outline. Complex roof structures where roofs change across the map outlines (e.g. mansard roofs) cannot be labelled correctly. Brenner (2004) describes in a theoretical manner, a combination of model- and data-driven approach, by using weak primitives. These weak primitives have the ability to vary constraints without losing topological information. This approach is of interest if the topological information is known.

In (Dorninger and Pfeifer, 2008) the authors present a data driven approach that regularizes borders of planar segments to determine building outlines. These borders are approximated by α -shapes, and are regularised by enforcing border lines to be parallel or orthogonal to a calculated main direction if they fall within a certain threshold.

The French combination of MATIS (IGN) and INFRA has got a thorough research history in reconstruction 3D buildings from aerial images and DEMs (Taillandier and Deriche, 2004) and (Durupt and Taillandier, 2006). Rectangular footprints are fitted to the DSM and at corners of building blocks a solution is proposed for overlapping or nearby rectangles. Building roof shapes are limited to contain two sloped roofs. For their purpose of robust and practical 3D city modelling the method works, but it does not work sufficiently for more detailed roof structures and complex building shapes.

Similar limitations hold for the building reconstruction approach presented by Kada and McKinley (2009), although they can handle more parameterised building shapes. Their approach is to generalise and partition the 2D footprint such that they can fit a parameterised model on each partition. For building up 3D models for visualisation purposes this approach works well, as they show examples of Berlin and Cologne. One has to keep in mind that the generalisation step disturbs the structure of walls in order to automate the reconstruction of roofs. Note that roof overhangs can not be reconstructed by this algorithm.

5.3 Research problems

Reconstructing buildings automatically is assumed to be timesaving in relation to manual or semi automatic reconstruction. However, the condition should be fulfilled that the assumptions for automated processing are correct for the area to be processed. Problems in automatic building reconstruction lie in the grey area between assumptions and reality. Not every object in the data appears as the algorithm expects. Causes can be found in variations in both the data and the real object. Laser data on unwanted objects like trees or cars will have a negative influence on the reconstruction results. In addition, laser data might be missing due to occlusions or lack of returned pulses from non-reflecting surfaces. Automated reconstruction methods should therefore detect and

select those areas where assumptions work fine, and at the same time detect areas that need extra attention.

5.3.1 Problems on roof shape detection

Detecting buildings and their outlines is interesting for 2D applications, e.g. for mapping purposes, as well as for intermediate steps in 3D reconstruction algorithms, e.g. to select the laser points on this particular building. The use of ground plans for this purpose has been described in many papers. Most of the ground plans contain information about the outlines of buildings. Additional motivations to use them vary from detection of regions of interest (Hofmann et al., 2002), giving hints about the roof structure (Brenner, 2000) to using them as outline of the 3D building (Haala et al., 1998), (Hofmann, 2004) and (Vosselman and Dijkman, 2001). About as many authors reject the idea of using ground plans because of the limiting factors like unavailability of precise GIS data (Maas and Vosselman, 1999; Rottensteiner et al., 2005; Vosselman, 1999). Their approaches are solely based on their primary data source. Each of the two groups has got their motivation whether or not to use the ground plan. In this section we first show problems when using ground plans, followed by a list of problems when not having them.

Most of the topographic maps are acquired by stereo photogrammetry, at some points assisted by additional terrestrial measurements. Normally the outlines of buildings are corrected for roof overhangs, so they represent the walls of buildings. This can also be seen in Figure 5-3 where laser points and map data are visualised together. Laser points on roofs seem to cover a bigger area than the outline of map data. Another interesting issue is the shape difference between the map outline and roof outline. The map outline represents the walls including bay windows at the front and other extrusions at the backside of the building, where the roof outline approximately is a rectangle without extrusions. However, on top of the roof there are dormers and chimneys, for which no hint was given from the map.

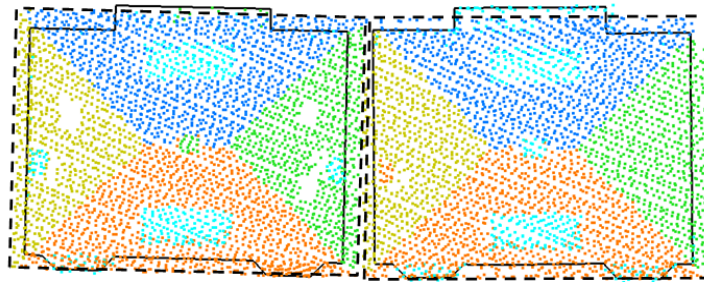


Figure 5-3 Segmented laser data, 2D map outline (solid) and roof outline (dashed).

Interpretation of differences between outline of laser data and map data is difficult because it can have multiple causes:

- time difference
- measuring walls instead of roof outlines
- missing laser data or map data

- uncertainty in both datasets

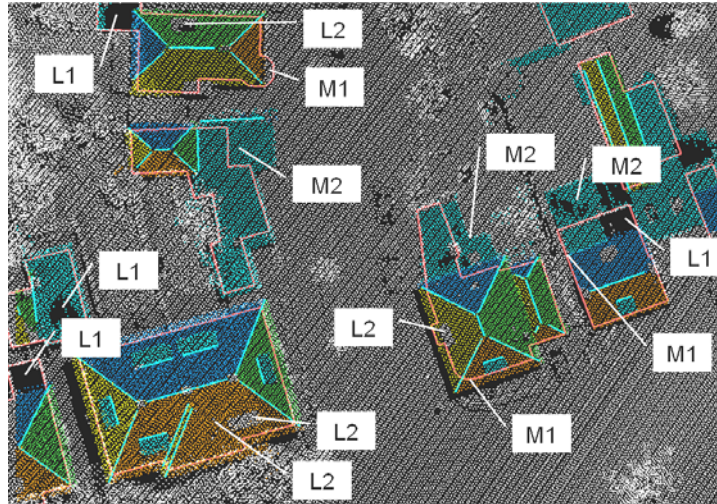


Figure 5-4 Missing laser data (L1), missing segments (L2), shape of map outline does not follow roof shape (M1), map outline does not cover roof area (M2).

In Figure 5-4 the strong and weak sides of using map data has been shown. In cases of missing laser data (L1) or not segmented laser points (L2) map data might be helpful to at least propose a simple building hypothesis later on in the reconstruction. However, in cases where the map outline does not give clear hints about the roof shape (M1) and where map data might be outdated or imprecise (M2) fusion might not be the best option.

Most of the problems described in the literature on approaches that do not use ground plans can be found in the detection part of the reconstruction. Although using multi-pulse information and full wave form analysis might improve the classification between vegetation and buildings, objects like vehicles and containers will cause several false classifications. Figure 5-5 shows a relative simple scene, but missing laser data (D1) and objects that geometrically appear as building parts (D2), will cause problems in automatic building detection without using ground plans.

Outlining of buildings from point clouds still remains a difficult problem, despite the many papers describing solutions to this task. Solutions have been described to outline non rectangular buildings (Dorninger and Pfeifer, 2008; Rottensteiner and Briese, 2002) and solutions by combining laser and image data (Rottensteiner et al., 2004; Sohn and Dowman, 2003). The largest remaining problem is to outline building parts that does not contain laser points, for example buildings indicated with D1 in Figure 5-5 or the lower parts of gambrel roofs as shown in Figure 5-6. Second type of problem relates to the complexity of the scene, definition of building outline and how this is represented in the laser data. For example, sun awnings and other temporary extrusions might have the

same geometric properties as sheds, carports or garages and therefore are hard to automatically eliminate from the building outline.

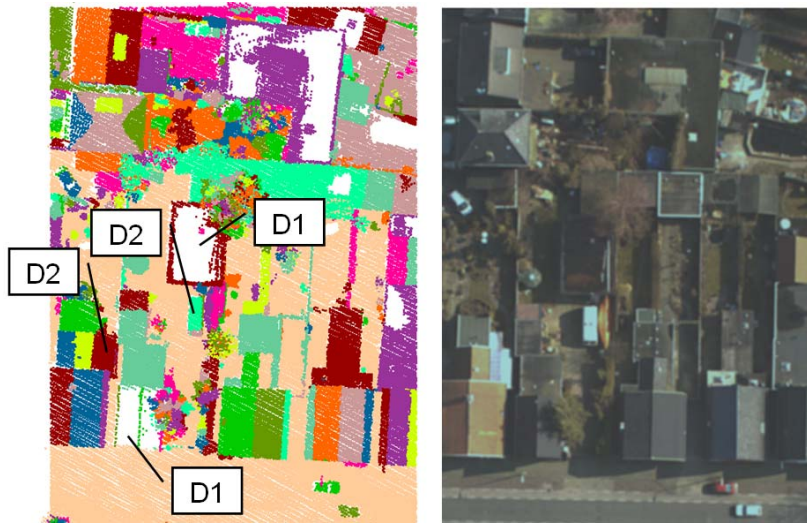


Figure 5-5 Four problem areas in a simple scene.



Figure 5-6 Gambrel roof types (top) are often modelled as gable roofs (middle), caused by missing laser segments at the lower roof faces of the gambrel roof (bottom) because of occlusion by the higher roofs.

5.3.2 Problems on scene complexity

In the previous section examples were shown for relatively simple urban scenery. When only looking at those problems, one can argue that using a model driven approach will be the solution to most of the problems. After all, using a model as starting point will solve some of the problems with missing data. Another advantage is that starting with a predefined model, its topology implicitly describes the building hypothesis. In this section we focus on problems with finding the right building model automatically.

Model driven approaches are proven robust and popular in rough 3D city modelling. The appearance of these 3D models often look structured and because of the absence of strange shaped reconstructed buildings, one can understand its popularity for visualisation purposes. However, as many authors of data driven approaches mention in their first section, model driven techniques are too generalised to be able to reconstruct complex building shapes, as shown in Figure 5-7. For interpretability reasons, images are shown instead of point clouds of complex scenes which might be hard to interpret on paper.

Even if approaches can handle combinations of primitives, it cannot be expected that characteristic buildings, like city halls, domes and churches, can be described by an automatically detected combination of primitives. In Figure 5-7 six situations are shown with unusual topological building parts. Normally, a library of predefined buildings will not contain possibilities to reconstruct scenes as shown in the figure.



Figure 5-7 Complex building shapes in urban scene.

5.4 Proposed approach

Based on the research problems as described in 5.3 we describe our proposed reconstruction approach. Major elements that should be included are:

1. the selection of laser points that belong to a building,
2. detecting the roof structure, and
3. proposing solutions for the outer boundaries of the roof faces.

If we group laser segments belonging to a map polygon and intersect neighbouring segments we are able to get intersection lines, representing roof edges that lie in the inside of the roof structure.

The next step towards proposing a 3D roof shape is to detect logical combinations in extracted features. We define these logical combinations in a list of targets of common roof types. Detection of these combinations is done in a target based graph matching algorithm (Bengoetxea, 2003). Target based matching for building reconstruction has earlier been described by Verma et al. (2006). After grouping the detected logical combinations we establish the link between features found in the data and what we have defined as common roof information.

From photogrammetric applications we know the goal of target matching: detecting and locating target templates in an image. Often the task is locating and measuring

predefined targets (Mikhail et al., 2001), such as fiducial marks. The exact measuring of those targets can be done using area based matching or feature based matching approach. The basis idea is that the shape and orientation of a target is fixed if the correlation between target and image exceeds a certain threshold value. The shape and orientation parameters are often calculated in a least squares adjustment procedure.

For our research we first focus on the detection part, describing which of the common logical combination can be found in the data. The target based graph matching algorithm is the crucial part which relates specific information (data features) with global/general information (database of common roof types). To deal with the large variety of how each building type can appear in reality and in the data we have to find robust elements that are common/invariant for a large variety of appearances for each building type. That is the reason why we propose to establish a link based on *topological relations between roof faces*. These topological relations are invariant to size or orientation.

The inner boundary of roof faces is mostly defined by intersections between two segments. Proposing solutions for the outer boundary of roof faces is based on the results of the matching algorithm. From the targets information is transferred to each of the segments. This information contains hints and constraints to reconstruct the outer boundary of the segment. This reconstruction step is further described in chapter 6. Also, this chapter includes a more model driven approach by reconstructing the matched targets according to the same match results. In Figure 5-8 the workflow from data to 3D models is presented. Chapter 7 contains the results and evaluates our building reconstruction methods.

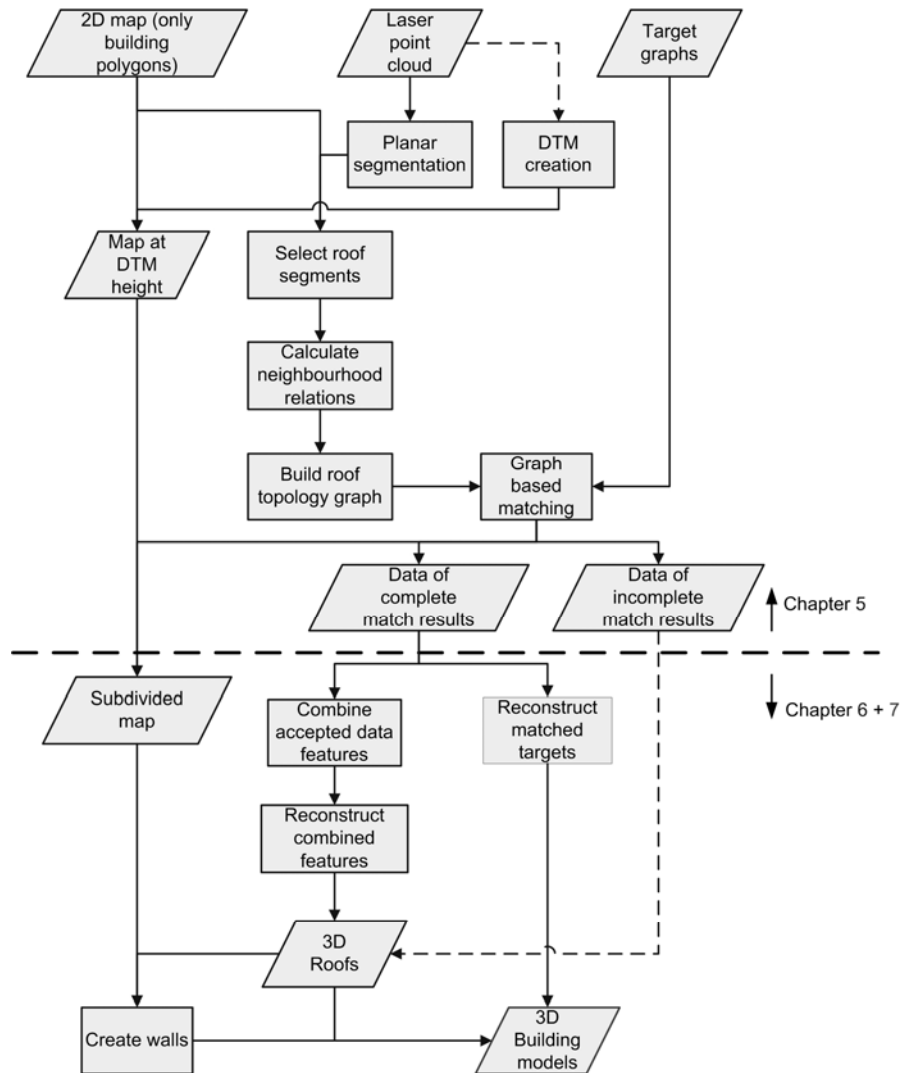


Figure 5-8 Workflow from source data to 3D buildings. Dotted lines represent semi-automatic processing steps, and are not considered to be part of our scientific contribution.

5.5 Information from map data

Using existing 2D map data in the reconstruction process has been described as helpful, (Brenner, 2000; Vosselman and Dijkman, 2001). As our point of departure is that we could use both 2D map data and laser data to reconstruct 3D buildings, we describe the value of 2D map data. An important assumption is that 2D map data of buildings detect

areas of interest, and helps detecting roof faces in laser scanner data. Map polygons represent planimetric information of walls, instead of outer edges of the roof. This knowledge is used in the detection and the reconstruction phase:

- Our detection method is based on a segment-in-polygon algorithm. If a planar segment (partly) falls inside the polygon, all laser points of that segment are taken as potential building roof points.
- The location of the map does not represent the outline of the 3D model exactly for all objects. We can use the map outline as an approximation, which we have to adjust to the roof outline if we can determine the roof outline better by other data sources. Exceptions are made for horizontal segments touching the map outline. We propose to take the map outline as location of that roof part, as the reliability of outer boundaries of flat segments is rather poor. This is further explained in section 6.5.1 of the next chapter, where we will present the reconstruction of roof faces.

5.6 Features from laser data

5.6.1 Segmentation of laser scanner data

An important step in the processing chain from laser data towards building models is segmenting the laser data. As our goal is to build models consisting of planar faces, we segment the data into planar patches. Automatic approaches strongly depend on the success of this segmentation step. Our segmentation algorithm is based on the surface growing algorithm as described in (Vosselman et al., 2004). Several parameters have to be set to define assumptions how to optimally segment the data. These assumptions are made on spatial appearance of objects in the laser data, such as minimum size and smoothness of expected objects, and how well laser points can record these objects. If locally these segmentation parameters do not fit the actual situation, over- and under-segmentation can occur. Although our aim is to segment the data as good as possible, we have to accept that these "errors" can be present.

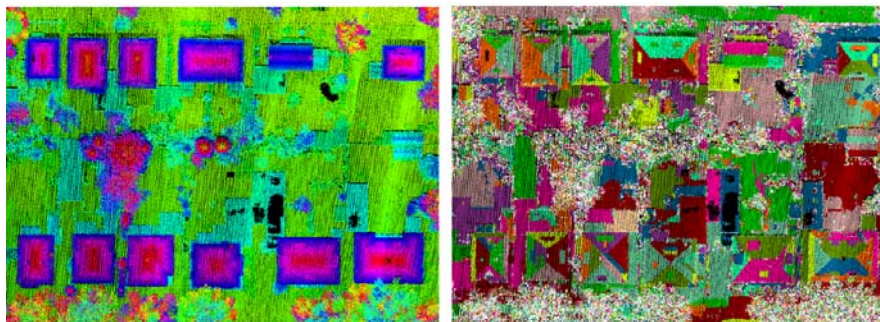


Figure 5-9 Color coded laser data (left) and segmented laser data (right). Small segments (< 10 points) are white.

It is in this stage, that we assign a ground level height to the map polygon. The minimum height of laser points within 2 meters near the polygon is taken as ground level height for the whole polygon. This height is stored as attribute value, which can be

invoked at the final stage of reconstruction when placing the walls between roofs and DTM.

Segments that are located for more than 50 % inside a map polygon are assigned to that polygon. For each polygon we continue with the corresponding laser segments.

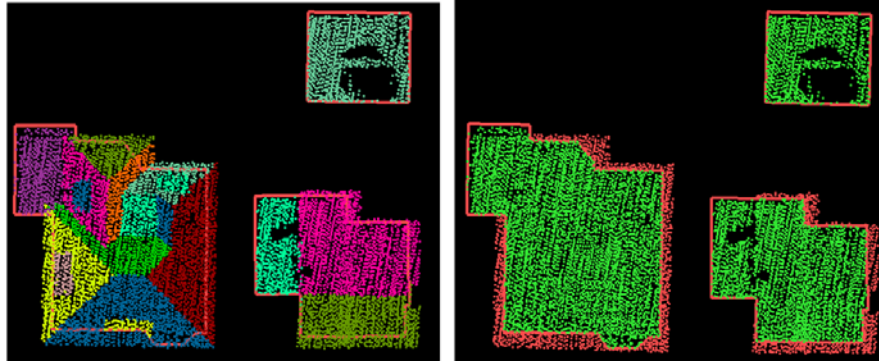


Figure 5-10 Segment-in-polygon selection: segments are assigned to a polygon if more than 50% is inside. Right: as a result, laser points that are on overhanging roof parts (coloured red) are included for further processing.

5.6.2 Intersection lines

Intersection lines are determined by calculating the intersection line between planes through two segments. Mathematically, the intersection of any two planes gives an infinite line in 3D space, unless two planes are parallel to each other. As we try to describe a roof edge (with a finite length) between two roof faces we have to limit the number of possible intersections and we have to limit the length of the intersection line. We use the location of laser points of both segments to determine (1) *if* two segments share an intersection line and (2) what the end points are.

- 1) Lines have been determined if two segments have laser points within a specified distance. Setting the distance parameter is not done for the whole data set, but for each intersection line individually. The distance is a function of the median point spacing of those two segments: twice the median point spacing of the less dense segment of the two segments.
- 2) Laser points of both segments that are within the above mentioned distance are selected for determining the length of the line. The end points of the line have been determined by projecting nearby points of both segments to the intersection line. From each of the segments we keep the two outer projected locations. This results in four points on the line, where, if the two projected parts overlap, the middle two have been taken as end point location for the intersection line. The minimum length of intersection lines has been made dependent on the density of the data. Again we take twice the median point spacing. Higher density data can better represent short ridge lines than coarse segments. Setting parameter values by analysing data locally is an important

aspect in automated processing. It reduces the highly arbitrarily influence of an object being acquired in a single, double or triple coverage. Shorter lines are removed in this step.

Intersection lines and step edges are important features in our approach. Not only do they give an approximate location for boundaries of roof faces, they also indicate neighbourhood relations between two segments. These relations are labelled according to the way how two segments spatially intersect, as indicated in Table 5-1. In section 5.6.4 we describe how we can use the topological relation between two segments.

Table 5-1 Labelling of intersection lines and step edges.

Label	Description	Situations
1	Intersection line between segments with opposite planimetric normals ⁴	Gable, middle of hip/gambrel roof types
2	Intersection line between segments with same planimetric normals	Gambrel
3	One horizontal, one tilted segment	Mansard
4	One segment inside other segment, horizontal intersection plus height jump edge(s)	Dormers
5	Tilted, convex	Hip roof types, pyramid shapes
6	Tilted, concave	L-shapes, sub objects on gable roof
7	Step edges	Height jumps

5.6.3 Step edges

If two segments do not share an intersection line, we check if they might connect through a step edge. Rottensteiner and Briese (2003) detect and reconstruct step edges by looking at height differences between two neighbouring segments, and regularising the direction of the step edge. In this step we only detect step edges. The geometric reconstruction of step edges is considered in a later stage. We detect step edges by analysing 2D and 3D relations between two segments. Our implementation is such that we create a point set of any combination of two segments. This point set is triangulated and saved in a TIN structure. We analyse the points that share TIN edges between points with different segment number. If a minimum number of points (N_{\min}) from two segments are within a certain planimetric distance d_{\max} , but are separated in 3D (height difference at edge location is more than threshold ΔH_{\min}) we keep the topological information that these two segments connect through a step edge, see Figure 5-11. The minimum length of the step edge is implicitly defined by the minimum number of points (N_{\min}).

⁴ With planimetric normals we mean the direction of the normal vector, projected on a horizontal plane.

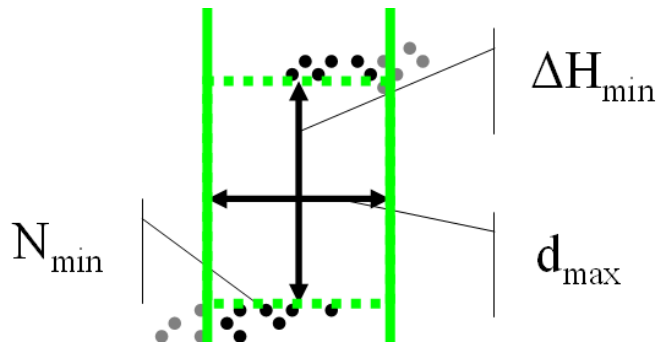


Figure 5-11 Three parameters used for detecting step edges.

Note that step edges can appear in several configurations, as shown in Figure 5-12.

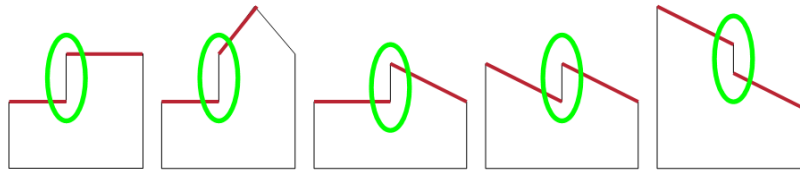


Figure 5-12 Various configurations of step edges.

Although the configurations might vary, the detection of step edges is the same for all appearances. All step edges are labelled equally, independent of the configurations how they appear. In Figure 5-13 both step edges and intersection lines are shown, labelled by their geometric intersection. Step edges are visualised by an orange line with default length of 1 m. The actual reconstruction of the step edge depends on the reconstruction of the two neighbouring faces.

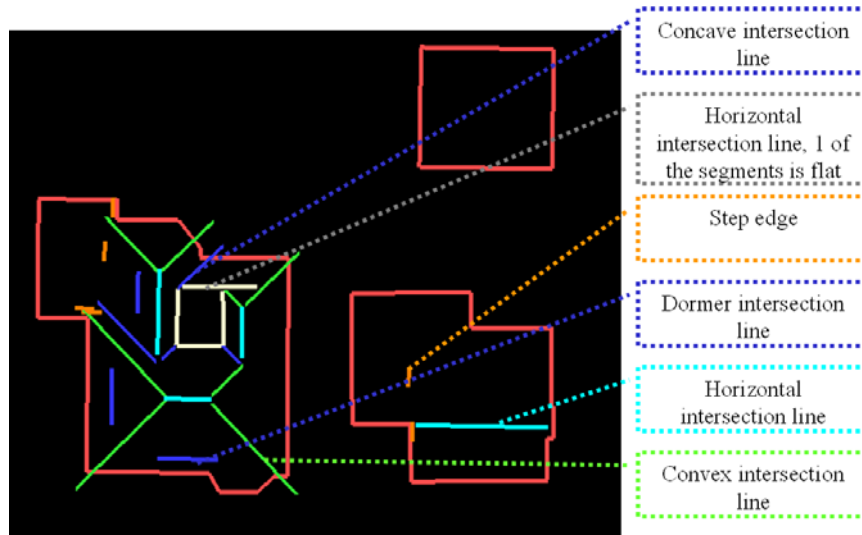


Figure 5-13 Labeled intersection lines and map outlines.

Figure 5-14 gives an impression on the total of our data feature types: on the left roof segments and the map outlines, in the middle intersection lines and step edges together with the map outlines.

5.6.4 Roof topology graph

Based on the intersection lines and height jumps, a roof topology graph is constructed. Each node in the graph represents a laser segment. Graph edges represent the topological relation between two segments. Each graph edge inherits the label value of its corresponding intersection line or step edge.



Figure 5-14 Roof segments (left), intersection lines and step edges (middle) and roof topology graph (right).





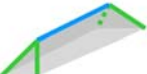

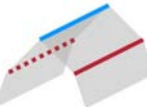





As can be seen in the left building in Figure 5-14 taking the topological relations instead of geometrical relations avoids potential problems with disconnected intersection lines.









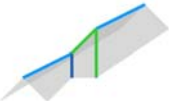





To improve the reliability of the individual data features we will analyse if this feature makes sense as being part of a building roof. To decide if a feature makes sense we check if this feature and its neighbouring features are present in a database of common roof structures.

5.7 Target graphs

In our database we describe a limited number of roof shapes, which we call targets. Similarly to data features, targets can be described in terms of topological relations. These relations are labelled according to the same definitions as the data (Table 5-1) and stored in target graphs, see Table 5-2. Most of the buildings can be described as an aggregation of simple roof structures (Suveg and Vosselman, 2004). The basic idea of the target graphs is that each of them represent a (part of the) building structure. The advantage of using the graph representation is that the detection of structures is based on the topology of the roof structure, instead of the geometry. The topology is more robust as it is flexible for shape variations within a building type. For example, a gable roof does not have to be symmetric in size of shape to be labelled as gable roof. The targets are kept simple shaped structures which can be combined later in order to represent complex structures. The structures in Table 5-2 are therefore representing the most common roof shapes, and covering the majority of the structures that can be found in reality and in the data.

Table 5-2 Target representations

Roof name	Schematic representation	Graph representation
Gable		
Half hip roof		
Hip roof		
Gambrel roof		
Simple dormer		
Mansard roof type (tilted in single direction)		

Pyramid shape		
L-shape building		
Step edge		
Mansard corner (tilted in double directions)		
Gable extension at (half) hipped roof type		
Gable shaped dormer		
Flat building		-
Shed building		-

5.8 Target based graph matching

Target based graph matching relates the roof segments topology to topological relations between roof faces from a database. Matching between data and model takes place on these roof topology graphs and target graphs. As the label of the edges is taken into account, this is called a labelled graph matching algorithm. Figure 5-15 explains that the matching takes place on the graph representations of data and target information.

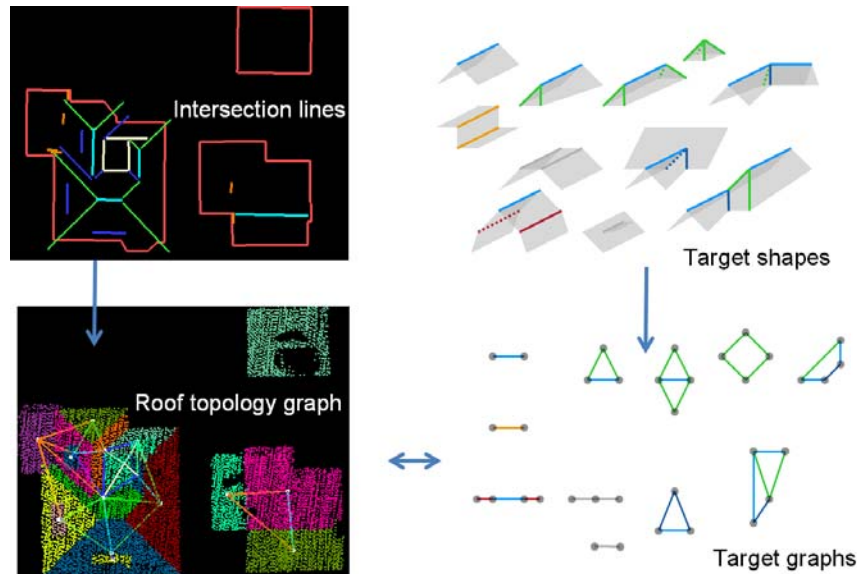


Figure 5-15 Sketch of matching algorithm: data features (left) are matched with data target features, based on the labelled graph representation.

For each edge in the roof topology graph we find corresponding edges in the target graph that contain the same label. Targets with corresponding edges are stored in a list of initial target graphs. This is the starting point for searching more similarities between roof topology graph and target graph. In a graph searching algorithm the neighbouring labelled edges and the nodes of the target graphs are compared with the neighbouring edges and nodes of the roof topology graph. If the edge label corresponds, the matching algorithm records the link between segment and target face. This procedure continues until all edges in the initial target graphs have been checked. Next to the correspondences between data features and target features the matching algorithm stores the completeness of the matching to each of the targets.

If we would use various labels on the nodes of the graphs, it would be called an attributed graph matching algorithm. In our implementation we use a uniform label for the nodes in the graph. This means we do not label the nodes on orientation, size or shape of the segments. The reason is that the appearances of these attributes are highly variable in laser scanner data. This would make the labelling of those attributes a weak factor of the matching algorithm. Note that the orientation and shape of the segments is implicitly taken into account in the label of the edges between two segments. As this edge label is based on the stronger geometry of intersection of two planes, it is expected to be more reliable than labels such as size on individual segments. Looking at our target graphs, we see that for some of the targets the graph searching stops after one labelled edge correspondence is found, e.g. for gable roofs, simple dormers and step edges. The risk of adding an uncommon roof structure to the database is that it, by mistake, matches with erroneous data features.

5.9 Complete matching results

A matching result is the assignment of a target graph to corresponding segments and intersection lines. For each target, multiple match results can be stored per building if that shape appears more than once. Logically, each segment and intersection line can be part of more than one target graph. Results after matching can be input for both model and data driven approaches. Match results are stored, as follows:

- Match result nr
- Building nr
- Target nr
- Target face 1,..., n – segment nr 1,..., n
- Target edge 1,..., e. – line nr 1,..., e

The reason why the building number is stored is that we easily can combine all match results per building. This will be discussed in chapter 6. Implicitly, the total number of laser points that match with a target is stored as the segment number holds information about the size of that segment. This information can be used in a generalization phase, when for example only the main shape of the building is stored. Examples are shown later in section 0.

A complete matching results stands for a full relation between all nodes and edges of a target with segments and intersection lines in the data. In case of the building in Figure 5-16, the summary of complete matching results is: three gable roofs, two half hip roofs, two L-shaped roofs and seven dormers. Note that there is redundancy as segments and intersection lines might have matched on multiple targets. Verma et al. (2006) avoids redundant information by starting with the most complex target and stops when a full match is found.

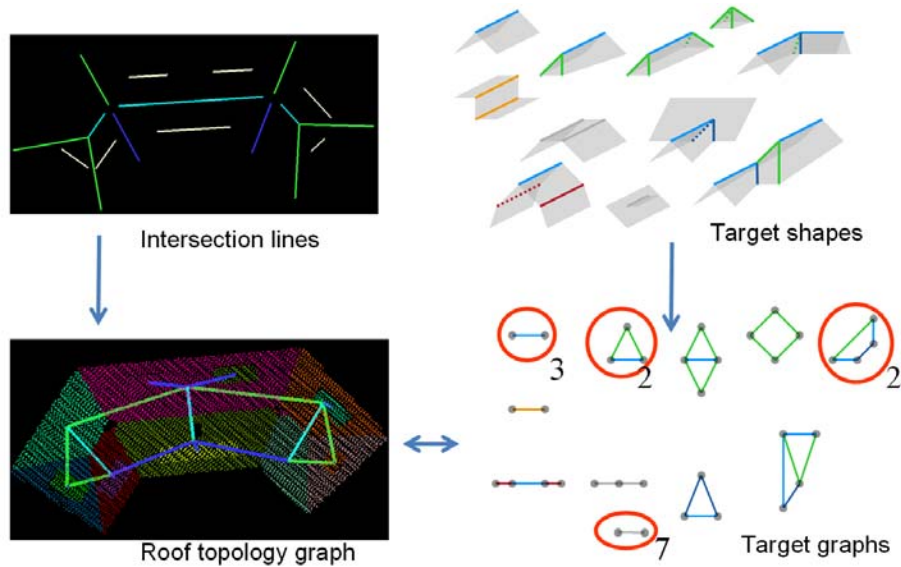


Figure 5-16 Matching result for one building: 3 gable targets, 2 half hip roofs, 2 L-shaped buildings and 7 dormers.

For complete match results, it is not needed to explicitly store the assignments between target edges and intersection lines, as the full assignment of the faces and segments already define the relation between target and data. Segments and lines are denoted as accepted if they are part of a complete match between data and target. This means that the structure from (a part of) the roof topology graph exactly corresponds to the target graph.

5.10 Incomplete matching results

Our approach also records incomplete matching results. This means that if segments and/or intersection lines are missing, we still may record a partly match. Note that this implies that multiple match results will be stored. To give an example, half hip roofs will also partly match on the hip roof target. To avoid unnecessary information storage, we only keep incomplete match results for segments that are not part of any complete match result. Figure 5-17 shows an example of two segments that are only part of incomplete matching results. These segments are matched partly on a gable-shaped dormer, because the other side of the dormer was missing. Building models in this section are results of our automated reconstruction approach which is presented in chapter 6. Here, the models are shown to visualise the context by superimposing incomplete match results.

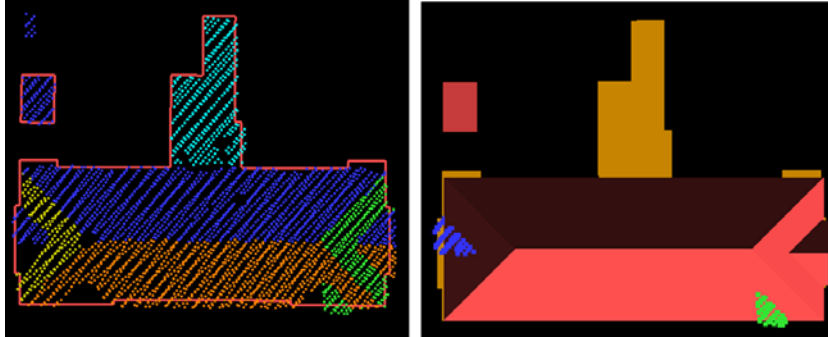


Figure 5-17 Segmented laser data and map data (left), segments on incomplete matches superimposed on a 3D model (right).

In 7.3.2 a deeper analysis is given on the incomplete match results.

In 5.4 we have described our building reconstruction task in three main parts:

1. to select laser points belonging to building roofs,
2. to detect the roof structure of that building, and
3. to reconstruct the outlines of the roof.

So far, our target based graph matching algorithm supported the first two goals. The segments that were selected in the segment-in-polygon algorithm were selected as initial roof segments. The matching algorithm performed a filtering task: data features that topologically correspond with common roof structures are considered to be part of the roof structure of that building. These data features will be transferred to our automated building reconstruction, where the outlines of the roof faces have to be reconstructed. This reconstruction algorithm covers the third main part of our building reconstruction task and is described in chapters 6 and 7.

6 3D Building Reconstruction¹

¹ This chapter contains content from:

Oude Elberink, S., 2009. Target Graph Matching for Building Reconstruction. In: *International Archives of Photogrammetry, Remote Sensing and Spatial Information Sciences*, XXXVIII, 3/W8: pp. 49-54.

Oude Elberink, S. and Vosselman, G., 2009. Building Reconstruction by Target Based Graph Matching on Incomplete Laser Data: Analysis and Limitations. *Sensors*, 9(8): 6101-6118.

6.1 Introduction

In the previous chapter we established a relation between data features and building shapes from a database. The target based graph matching algorithm actually performed two important tasks:

- Detection: the target shapes that can be detected in the data
- Filtering: the data features that do not fit on the targets

Establishing a relation between model and data information, is important in the reconstruction phase, as it provides hints to reconstruct the outer boundary of the roof faces. It can still be decided if the reconstruction itself is more data driven or more model driven. In the target database we can find reconstruction rules for the each of the targets. For example, conditions to force the model to constraints can be stored per target. When reconstructing the buildings we can choose which information should be taken for the given application. To give an example we present a simple gable roof building. This building will have complete match results on a gable target.

- Match result 1
- Building number 1
- Target “gable”
- Face 1 – segment 20
- Face 2 – segment 21

In a more data driven approach we get the main information from the segments 20 and 21, added with some constraints from the target “gable”. We fit a plane through each of the segments to determine the inclination and orientation of each roof face, whereas in a more model driven approach we take a basic “gable” model, and use additional information from (part of) the data to reshape and resize that model, see Figure 6-1.

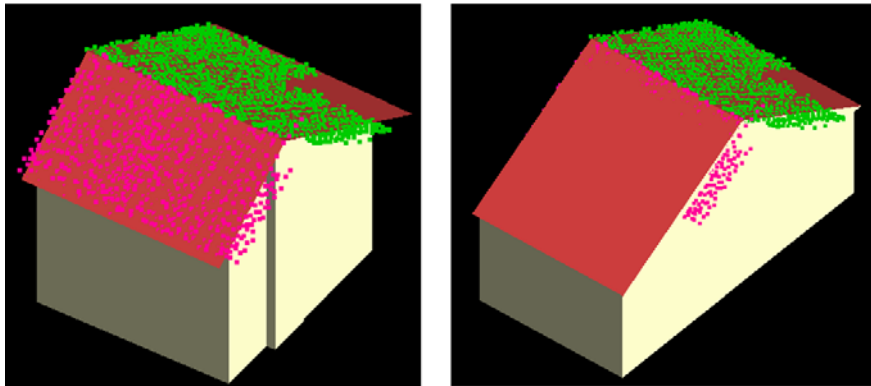


Figure 6-1 Two laser segments visualised on a more data driven model (left) and on a more model driven model (right).

In this chapter we describe how this information can be incorporated when reconstructing the roof faces. We present two approaches that can adapt the amount of

information what will be used from the targets. The first approach is more data oriented, whereas the second is model oriented. The first approach is based on combining all data features that were part of a complete matching result. These data features describe the orientation of roof faces (by the segments) and the interior boundary edges of the roof faces. The challenge is to reconstruct the outer boundary of the faces as realistic as possible. The task is to find a balance between assumptions on the building and information that you find in the data. The first approach is described in sections 6.3 to 6.7. Using the same match results as the first approach, the second approach starts by reconstructing parameterised target models. In that sense it can be seen as more model driven than the first approach. However, we show that we can adapt the more general models by adding more data information. The user can specify for which target models and for which criteria the reconstructed models are refined. The second approach is described in section 6.8. For both approaches our assumption is that we need to cope with the more complex buildings that consist of a combination of target shapes.

6.2 Components of a roof boundary

First, an overview is given of the components of a roof boundary. Some of the terms used in this chapter, might be interpretable in multiple ways. Figure 6-2 visualizes the components in order to avoid potential misunderstanding. Here, the terms are presented, whereas later in sections 6.4, 6.5 and 6.6 the geometric reconstruction of those components is explained.

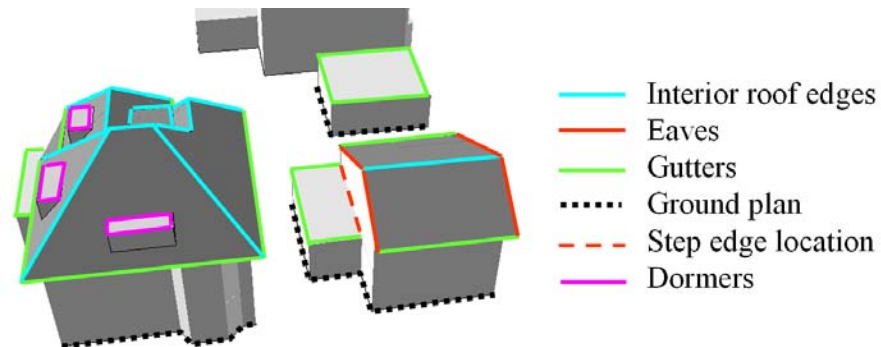


Figure 6-2 Components of roof faces labelled by our definitions.

Interior roof edges are edges at intersections of two roof faces. They include horizontal ridges at gable roofs and hip roofs, but also the tilted intersections, e.g. on hip roofs, L-shapes and pyramid structures.

Eaves are located at the outer boundaries of roof faces. They connect the higher edge of the roof face (ridge) with the lower edge (mostly gutters). Note that at for some roof types (e.g. hip roofs, left building in Figure 6-2) there is no eave according to our definition.

Gutters are located at the lower part of the outer boundaries of roof faces. They are nearly horizontal and are made to drain the rain water from the roof face. As can be seen

at the left building in Figure 6-2 gutters do not have to have the same shape as the underlying ground plan.

In chapter 1 the detection of step edges was explained. In this chapter we will discuss how to place the location of step edges. In Figure 6-2 we see that the upper part of this particular step edge is on the gable roof type and represented by eave edges. As we constrain the step edge to be exactly vertical the planimetric location of the upper and lower step edge is the same. The location is set by first reconstructing the upper roof face, and taking the planimetry of the corresponding edge location as step edge location. In this example, the lower part is at the flat roof face. For the flat roof part the step edge location is giving the fourth side of the rectangular shape, where the other three are gutters. Exceptions are at places where the upper face is flat, and the lower face is part of a gable roof type: we assume that edges of a gable roof type can be reconstructed more reliable than one from a flat roof type. The reason is that tilted roofs have a planimetric normal direction that gives a preferred edge direction. Furthermore, flat surfaces may contain water that disturbs the outer boundary of flat segments. In that case the lower (tilted) face of the step edge is giving the planimetric location.

Here, dormers represent an object with a single roof face and three vertical faces connecting the roof face with the supporting roof face. One side of the dormer roof face is the intersection between dormer roof and the supporting roof. The other three dormer roof edges are constructed as described later in 6.6.1. More complex dormer types are considered as -and reconstructed as- any other roof type. Their edges are handled as interior roof edges. The reason why simple dormers are reconstructed separately is that the only intersection line does not need to be connected to other intersection lines of the interior edges. Therefore the reconstruction of these dormers can be done independently.

6.3 Approach 1: Combine features from complete match results

The first approach presented here, actually works from a bottom-up perspective: we accept intersection lines and segments from complete match results. Together with the topology of accepted lines and segments, we can connect end points of intersection lines with each other. For each segment, all accepted intersection lines are connected. Important element in the target based graph matching is that the intersection lines are extended to corner points. This is done by extending intersection lines to object points that are intersected by more than two planes. Note that the shape of each roof can be more complex than the target shapes. For object points that are intersected by three planes, extension of three intersection lines is unambiguous as they intersect in one point. Directions and position of accepted intersection lines are supposed to represent directions and positions of ridges. Object points connected by two or more intersection lines are fixed. Figure 6-3 shows the extension of intersection lines according to the accepted topologic relations. Corner points where three planes intersect are considered to be reliably determined in 3D. Intersection lines through these fixed corner points form the skeleton, or the interior boundary of the roof faces. Cyan arrows indicate that the exact end position on these intersection lines still has to be determined. The geometric accuracy of these original end points along the line direction is at best in the order of median point spacing of the two concerned laser segments.

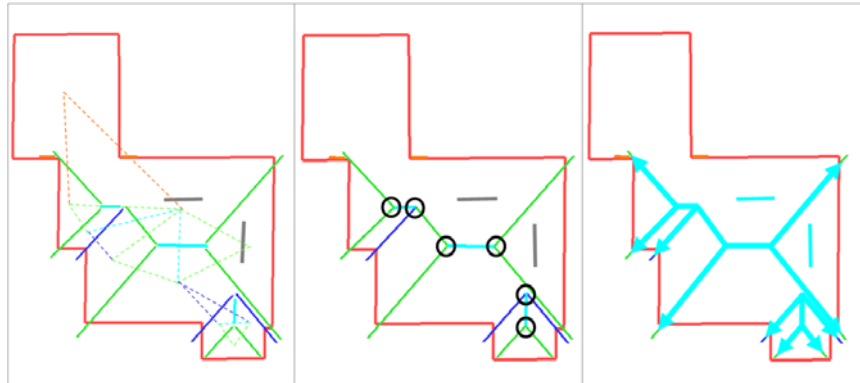


Figure 6-3. *Left:* Accepted intersection lines (solid) and topological relations (dashed). *Middle:* Lines extended according to accepted topology. Fixed corner points are indicated by black circles. *Right:* Skeleton of interior roof boundary.

If four intersection lines should intersect in one point, as is the case for pyramid structures and L-shape building parts, we have to force one plane to intersect the other three in the same point. Our implementation is such that planes through the three largest segments define the intersection point, and the four intersection lines are forced to intersect in that point.

Figure 6-4 shows the working of the combining accepted intersection lines for our example buildings. Lines are only extended (or shortened) if three or more roof faces intersect in one point, e.g. the ridge line at the lower right building did not change.

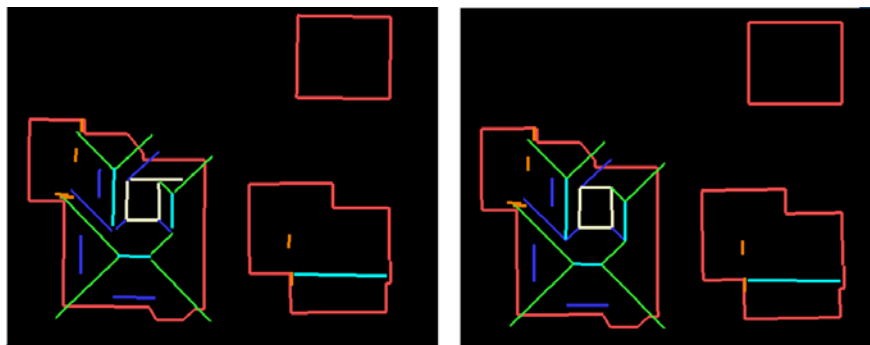


Figure 6-4 Result of combining accepted features: (*left*) intersection lines, (*right*) extended and shortened lines according to accepted topology.

Before adding eaves and/or gutters to the roof faces, we focus on the skeleton of the interior roof boundary, especially the outer points of the skeleton. As we have seen in Figure 6-3 the cyan arrows indicate that the tilted intersection lines might be extended

towards the gutter. Figure 6-5 shows the outer points of the skeleton. These points are connected to either a horizontal or a tilted intersection line.

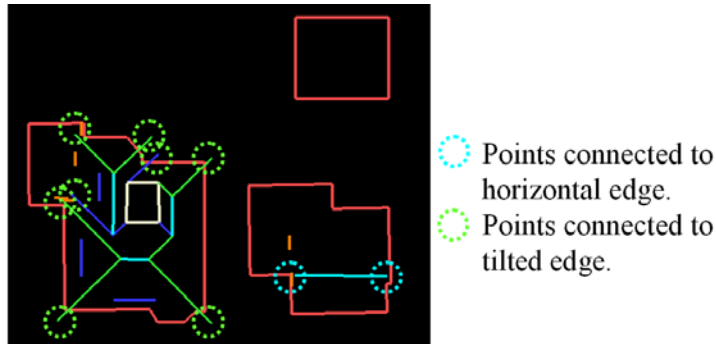


Figure 6-5 Outer points (in dashed circles) of skeleton of interior roof edges.

Extending horizontal lines is based on extension to a certain planimetric location (further explained in 6.4), whereas extending tilted lines is based on extending to a certain (gutter) height (see section 6.5.3).

6.4 Extension of horizontal intersection lines

Single horizontal lines (such as end points of a gable intersection line) are extended along the intersection line to the map (partition) line if the endpoint is within a certain threshold distance. Figure 6-6 shows the working of extending an intersection line (cyan line) to map outlines (red line). In this case the intersection line ends inside the map polygon. If this is the case, the possibility to extend this line to the map polygon is activated. The map polygon is broken down in a sequence of line segments. Each of these line segments is intersected with the original intersection line. Intersection points near the original end point are shown as red, dark yellow and green dots in the figure. Dots are coloured red if the intersection point between a map line segment and the intersection line is located on the extension of the map line but at the original intersection line itself. Dark yellow means that the intersection point is in the extension of both the map line segment and the original intersection line. A green dot means that the intersection point is located at the map line segment and at the extension of the original intersection line. The user can specify by input parameters which considerations he prefers. Default settings are that if a point on the map polygon (green dot) is within one meter the intersection line is extended to the map.

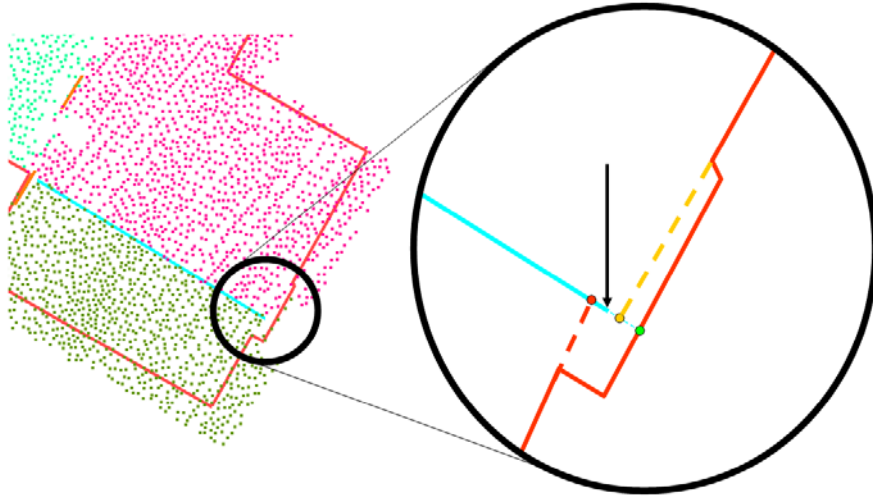


Figure 6-6 Extending an intersection line (cyan) to the map outline (red). Original end point is indicated by the black arrow, the preferred location is shown as green dot.

If no map segment is near the end of the intersection line, we propose to search for nearby intersection points on extensions of map segments (dark yellow). If none of these points are found, the location of this end point remains unchanged. Figure 6-7 shows an example where intersection lines are extended to the extension of a line segment of the map polygon. Note that the extended distance of the upper intersection line, is rather large as it has to bridge the gap of a chimney. In this case the extended distance is just below the threshold value of one meter.

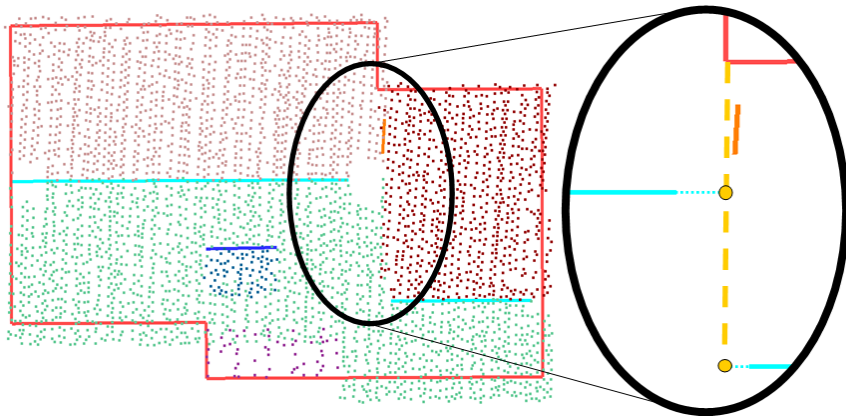


Figure 6-7 Two horizontal intersection lines extended to extension of map line.

6.5 Outer boundaries of roof faces

The task is to make a closed polygon for each of the roof faces. We have seen that a part of the polygon is covered by the interior skeleton. For each roof face we have an even number of outer points of the skeleton (see Figure 6-5), so the task is to make a logical connection between those outer points. These connections are at the outer boundary of roof faces and are called either eaves or gutters.

Several information sources can be invoked to propose the outer boundary of roof faces. The most data driven version is to use the outer boundary of segments to act as outer boundary of the roof face. However, outer boundaries of laser segments such as convex or concave hulls are rather noisy due to the relative arbitrary location of laser points on the edge of the segment. As our assumption is that roof edges show a more systematic man made pattern, this cannot be taken as fixed roof edge. Assumptions have to be added to generalize the outline. Dorninger and Pfeifer (2008) and Vosselman (1999) generalize the outer boundary of individual segments by enforcing orthogonality or parallelism to a dominant direction. Although this might work in most of the situations, we want to explore alternatives that do not rely on the outer boundary of individual segments.

Vosselman and Dijkman (2001) take the outline of ground plans as outlines of the roof faces. Intersection lines and step edges are used to subdivide the ground plan and assign heights to the bounds of the subdivisions. Also Brenner (2000) uses the ground plan as location of the walls. By choosing this approach, they accept to ignore overhanging parts, but in return they get at least a reliable approximation of the boundaries of roof faces.

In our approach, we choose to use the ground plan, but in a less strict sense than Vosselman and Dijkman (2001) and Brenner (2000). Our intention is that we will exceed the ground plan if we can reconstruct the overhang. In this section we will further explain the details for the reconstruction of outer boundaries.

6.5.1 Flat roof faces

For flat roof faces touching the map boundary, we will take the map boundary as roof boundary. In this paragraph we will explain why in laser scanner data it is hard to accurately determine the outer edges of flat roof faces automatically. Two reasons are listed here that complement each other:

- The direction and location of the outer boundary of flat segments cannot accurately be constrained in terms of function of the normal of the segment.
- Laser data on flat segments is influenced by the fact that laser pulses are not reflected if water stands on the surface. The outer boundary of the segment might not be the boundary of the object. Detection of holes in laser data is necessary in these cases. Propositions have to be made to check if these holes could be caused by non reflecting surfaces.

Taking into account that outer boundaries of flat segments cannot be reconstructed reliably and accurately plus the assumption that most flat objects do not exceed the wall, we propose to take the map outline as location of edges of flat roof parts.

6.5.2 Eave construction

Eaves are constructed at outer points that connect to horizontal skeleton edges. These outer points might be extended to the map outline as described in section 6.4. The eaves are created perpendicular to the intersection line, or parallel to the map outline, see Figure 6-8.

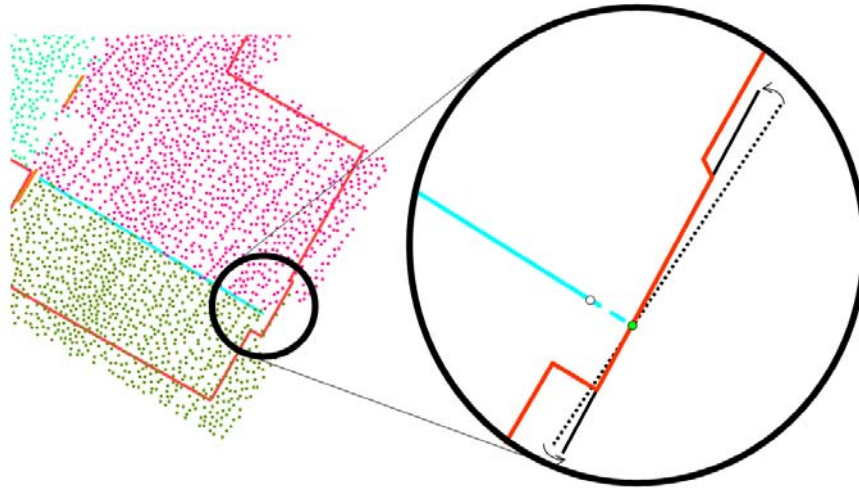


Figure 6-8 Adapting eave direction to map direction: default eave direction is perpendicular (dotted black line) to intersection line, but is adapted to map direction (black line) if within a certain angle threshold.

If an intersection line is extended to the map outline, the eaves at both sides of the intersection line are adjusted to the local direction of the map outline. Figure 6-8 shows an example where the direction of the map outline differs about five degrees from the perpendicular direction. If this difference is below 15 degrees, we take the direction of the map outline for the eave direction. The only parameter we now have to fix for the eaves is the end point. As the eave lies in the plane of the roof face, there is only one dimension to set to fix the 3D location of the eave's end point. For some situation the eave will connect to outer points of the inner skeleton. This is the case for the building shown in Figure 6-7. For most of the eaves, the end point is the corner point between eave and gutter.

6.5.3 Gutter construction

Map data represent locations of building walls, and cannot be taken as gutter location for tilted planes. Initially, gutters are created by calculating a horizontal line in the segment plane through the lowest laser point in the segment. Depending on the other edges this line intersects with either eaves or intersection lines. So, initially the gutter height is determined by the lowest laser point in the segment but the gutter heights are changed in the following situations:

- If the lower part of the segment is noisy. Histogram analyses are done to check if the lower part of the segment is sensitive to a few laser points. If the lowest 5% of the

- points reach more than 10% of the segment height, it indicates that that height is not very stable. If this is the case, the lowest 5% of the segment is removed, and the histogram analysis is repeated.
- Gutter heights at segments that have matched on the same target are made equal if the height is within a threshold (default: 0.5 m). The height of the lowest gutter is taken.
 - Gutter heights of tilted segments of the whole building are made equal if the height is within a threshold (default: 0.5 m).

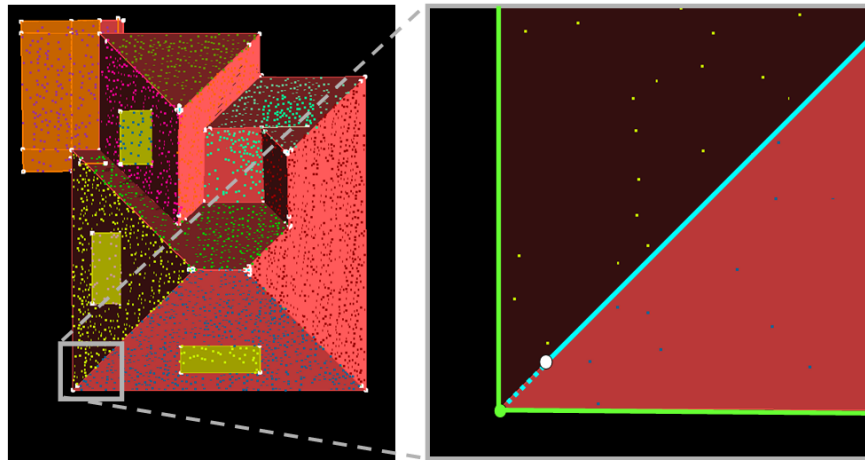


Figure 6-9 Situation where intersection line (cyan) is extended to the height of lowest point in segment. In this case all building gutters of tilted segments (green) are snapped to one equal height, as the lowest height of all segments is within 0.5m.

These rules imply that the gutter is always placed horizontal, at a height that is either determined by the lowest point in the segment, or snapped to another gutter height if they are close and related to each other in a certain way (via target or building number).

6.6 Dormers and step edges

So far, we have discussed how to deal with roof faces that shared at least one intersection line with another roof face, and matched with at least one target shape. The features that match with the simple dormer target are reconstructed independently, after the reconstruction of the main roof faces. This is mainly because, unlike other roof faces, the walls of the dormer roof do not reach to the ground but to the supporting roof face. An additional reason is that we can assign specific shape knowledge to reconstruct the dormer.

6.6.1 Simple dormers

In our definition simple dormers have a planar roof top that horizontally intersects the supporting roof face. Detection of these dormers was based on this single intersection line. These dormers are reconstructed by creating a rectangular shape around the dormer

segment. This rectangle is constructed by creating a line parallel to the intersection line at the end of the dormer segment (indicated with arrow 1 in Figure 6-10). Two additional perpendicular lines are added to create a polygonal face. Three dormer sides (two triangles and one rectangle) are constructed by taking the vertical face between the dormer face and the supporting roof face (arrow 2 in Figure 6-10).

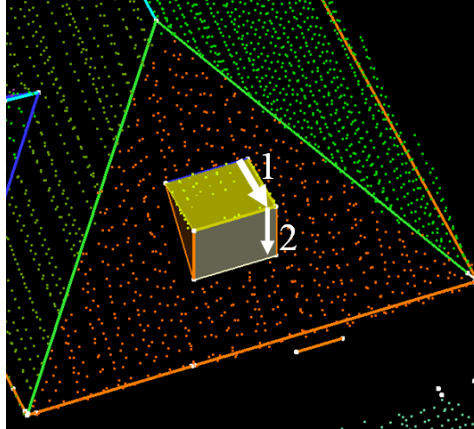


Figure 6-10 Reconstruction of dormer faces.

Figure 6-11 shows that the dormer top itself does not have to be horizontal, as long as the intersection line between the dormer top and supporting roof face is horizontal.

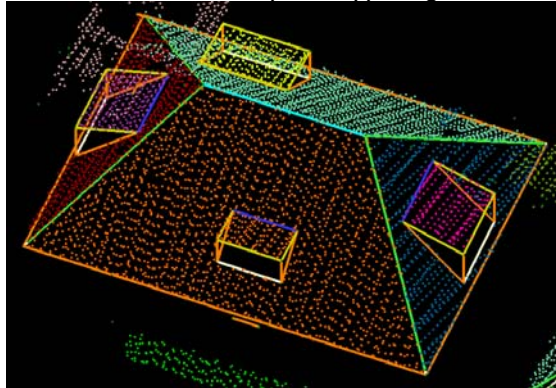


Figure 6-11 Our algorithm can handle dormer variations in size, location and inclination.

6.6.2 Step edges

Step edges are reconstructed after the initial construction of eaves and gutters. As described in 5.6.3 step edges are detected because of a vertical height difference between two segments. Therefore in 3D models their appearance can best be described by a vertical face. This vertical face is bounded by an upper and lower segment.

In general, the location of step edges cannot be detected reliably using only airborne laser data, because the location can not be determined by intersection of two faces. Exceptions are found when the vertical face is represented by a laser segment that could be intersected with the higher and lower segment. However, it can be expected that not all vertical segments can be found due to occlusions in the acquisition configuration. Even if the laser scanning system acquires in forward, nadir and backward configuration, only a part of the vertical walls can be detected (Rutzinger et al., 2009).

If the two segments concerned already are reconstructed as described in 6.5, we propose to make use of the location of their boundaries. These segments might have been reconstructed individually in the object driven approach described before. The location of the vertical face depends on the location of the edges of the reconstructed segments. We propose to take the location of the higher edge, as occlusion might affect the location of the lower segment. As the algorithm knows the approximate location by taking the laser points that detected the step edge in the first place, the nearest reconstructed edge of the higher segment is taken as location for the step edge. So, lower edges of the step edge will be snapped to the location of the higher edge, as visualised in Figure 6-12.

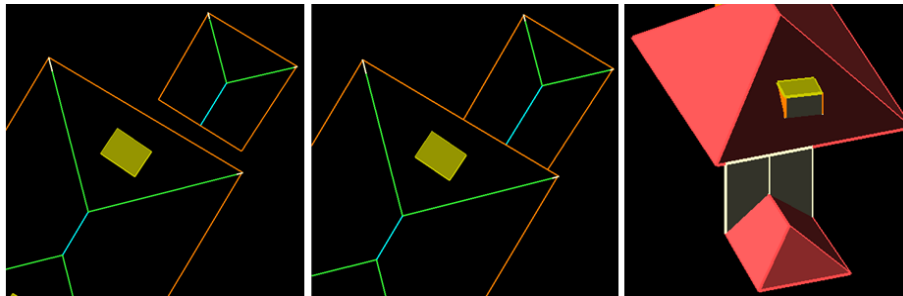


Figure 6-12 Reconstruction of individual roof parts (left), extended roof edges of faces that connect through step edges (middle), reconstructed step edge (right).

For step edges between segments that both have not been reconstructed yet, the location of the step edge is less reliable to determine. These cases occur when both segments are flat. The direction is determined by the normal direction of the (almost) vertical plane fitted through the laser points of both segments near the step edge. If we take the outer product of this normal vector with the zenith vector, we get the direction of the step edge. This method works well for step edges that have one straight direction.

6.6.3 Step edges for map subdivision

Figure 6-12 shows that step edges actually represent building walls, located inside the map polygon. In general, a step edge divides one building structure from another. At the same time, it defines the location where these two structures meet each other. We use this information for dividing the map polygon at step edge locations. At step edge locations the map outline has been split into two partitions, see Figure 6-13. If this split

line is close to a corner point in the map, the line will be snapped to the corner point. At the split line, we build two walls: one for the higher and one for the lower roof structure.

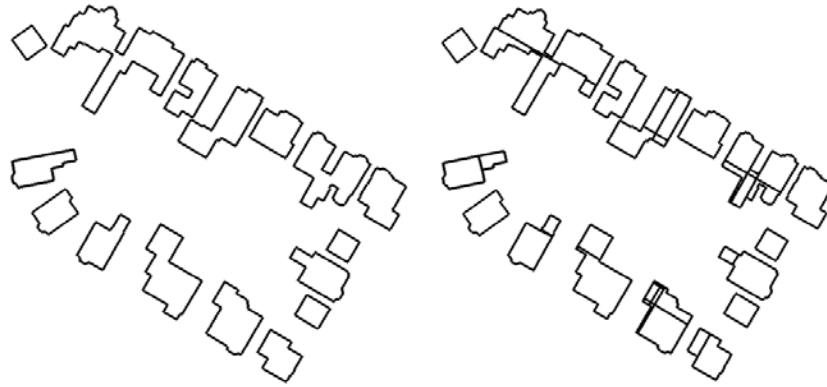


Figure 6-13 Left: Original map polygon. Right: subdivision of map line at step edge locations.

6.7 Reconstruction of walls

Our first algorithm at least builds walls for the first floor of a building, exactly at the location of the map polygon. On top of the first floor, walls are built until they reach the corresponding roof face. Therefore we take the location of the map vertices, added with the points of intersection between roof edges and the map outline. For each of these points the height is taken of respectively the roof and edge. This method works for roof faces that at least touch or show overhang on the roof outline.

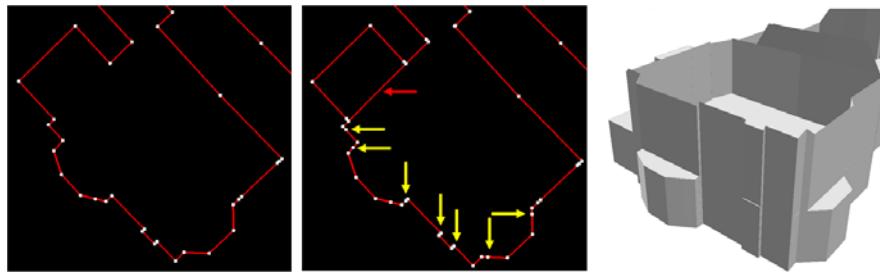


Figure 6-14 Map polygon with original map vertices (*left*), added vertices at locations where the roof intersect the map polygon (indicated by yellow arrows) plus partition caused by step edge (red arrow) (*middle*), and reconstructed walls and first floor (*right*).

For many roof faces the outer boundary is outside or on the map polygon. However, for some situations the outer bounds intersect the polygon, meaning the roof end is inside the building. We split the map polygon at the intersection points, to be able to reconstruct a wall to the roof face. The part of the polygon that has been cut off gets the height of the first floor. Most of these parts are bay extrusions, with no or little laser

points on top, as shown in Figure 6-15. If a laser segment is inside that part, the height is determined by fitting a plane through that segment.

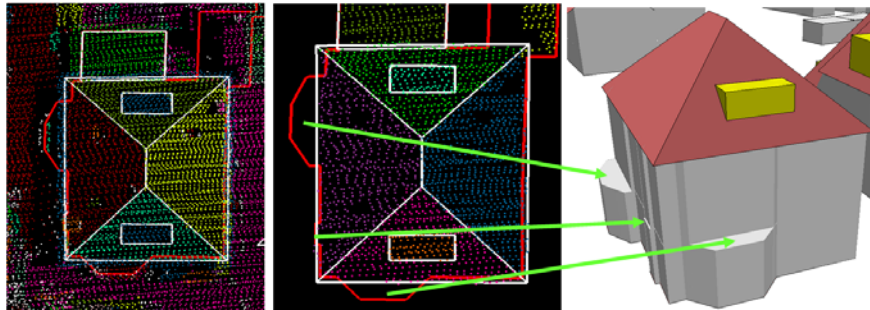


Figure 6-15 Extrusions without roof segments, get a fixed first floor height.

Remember from section 5.6.1 that we stored the ground floor height as an attribute value to each map polygon, at the data fusion step between laser data and map data. This ground floor height is taken as lower bounds for the walls.

6.8 Approach 2: reconstructed targets

To further emphasize the possibilities of using target knowledge in building reconstruction, we present a more model driven approach. Basic idea is that we fit a certain parametric model, using the data that we have found during the target based matching algorithm. Our input is the same as the data driven approach: we use the results of the target matching algorithm as described in chapter 5. Rather than trying to present the best method for a certain dataset and certain model requirements, we would like to emphasize on the flexibility to tune the reconstruction method according to the situation and user wishes. Depending on the data quality and user requirements the optimal relation can be determined by the user. Main differences with the more data driven method are:

- the reconstructed models are based on targets instead of individual segments;
- walls are based on the location of the roofs, instead of on the boundary of the map polygon. The location of the walls can be at the outer boundary (no overhang), or at a parameterised distance within the outer boundary (so including overhang).

Examples of model driven approaches can be found in 3D city reconstruction productions, where visual appearance of the 3D model is an important user requirement. Remaining challenge is to decide which parameters to estimate and how. To give an example, the height of a gable roof can be determined in many ways:

- by the highest point on the two gable segments,
- the highest point of the intersection line between the two segments, or
- in another combined parameter estimation where the height, slope, length and width are estimated simultaneously.

So, there are several ways to decide how building parameters are determined. Maas and Vosselman (1999) describe the use of moments to reconstruct simple roof types. The

length of a gable roof is therefore a function of the moments, which are again a function of the distribution of laser points. Verma et al (2006) also highlights the possibility to refine parametric models by properties of data features. For example individual roof faces on a gable roof can have their own slope. Their approach creates rectangular faces on gable roofs which eaves are passing through the outermost laser point; the gutter is parallel to the ridge. The height of the gutter is at the median height of points near the building outline. Brenner (2004) introduces ‘weak primitives’ to combine advantages of model driven parameterised models and data driven boundary representations. The advantage of weak primitives is that constraints on predefined models are written as a list of equations rather than static assumptions. Depending on which constraints are switched on/off the set of equations is solved. In his paper the author describes a theoretical, relatively simple, case how users can choose which constraints to activate and how interactive measurements influence the results. If we would like to implement weak primitives as proposed by Brenner (2004), we have to carry out two major changes. We have to automate the decision which constraints to enable/disable. Next, we have to replace the interactive measurements, which are assumed to be free of errors, by data features which have a stochastic character.

6.8.1 Parameterised target models

For each of our target shapes we have built a parameterised model. As we can decide for each target which data feature is the most valuable for estimating each of the parameters, we are able to combine strong elements of the data with strong elements of model information. In this section we highlight the situation of gable roofs, hip roofs and L-shaped buildings.

The ridge location of gable roofs is determined by the end point locations of the intersection line between the two faces. The ridge is made horizontal by taking the mean value of both points. The gutters are parallel to the ridge; one of them is passing through the lowest laser point of both segments. By default, both gutters have the same height. Note, that the difference with the data driven approach is that gutter heights are now determined by the lowest point of both segments of the target, instead of the lowest point in an individual segment. In addition, the inclination is taken from the segment that includes the lowest laser points, e.g. segment **a** in figure Figure 6-16. This is exactly what shows the flexibility of our target based matching approach: the details of the reconstructed model (for example the location of gutters) can be based on individual segments or a group of segments that belong to a specific target.

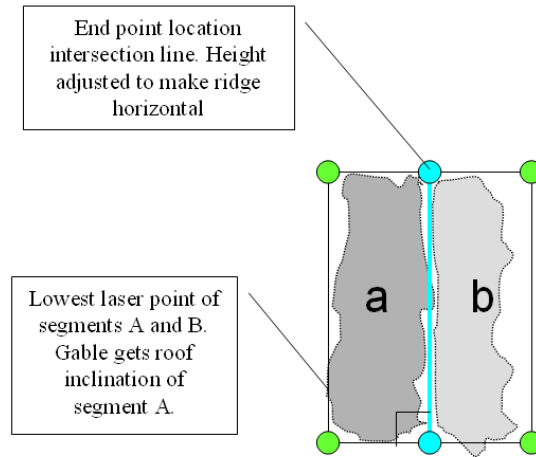


Figure 6-16 Assigning values to a gable roof, based on the intersection line (cyan) and lowest point in both segments.

The two end points of the hip roof ridge (cyan line in figure Figure 6-17) are determined by calculating the intersection points of the three surrounding roof segments (**abc** and **abd**). The height of the two points is averaged to enforce a horizontal top ridge. The width of the roof faces is defined by the parameter 'dist'. This parameter has been calculated by the perpendicular distance between the ridge line and lowest point in segments **a** or **b**. The height of the four gutter points (green dots) is defined by the height of the lowest laser point in segment **a** or **b**. Note that modelling an overhang is straightforward: the wall location is calculated with an adapted value for the 'dist' parameter. The location of the roof outline is not influenced by reconstructing the overhang: only the wall is shifted inwards the building.

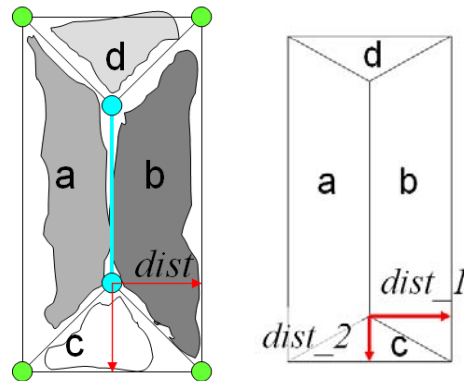


Figure 6-17 Assigning values to a hip roof with equal tilted roofs (left) and two different roof inclinations (right).

Our implementation is that for each target shape we decide which constraint(s) can be relaxed and which data features are assigned to that constraint. Figure 6-17 shows a hip roof and its parameters. By default, four sides of a hip roof target are reconstructed with equal inclination angle. However, if segments C and D have a significant different inclination angle, an extra parameter `dist_2` has been introduced and calculated. By setting a threshold value for the minimum angle difference, the user can decide when to reconstruct a hip roof with four equal inclinations or two different inclination angles. In Figure 6-18 the differences between the two options are clearly visible. On the top row, the hip roof has been reconstructed using the same inclination for all four roof faces, whereas on the bottom row the two side roof faces have another inclination angle. It is recommended to further analyse the decision to judge whether a discrepancy is significant or not.

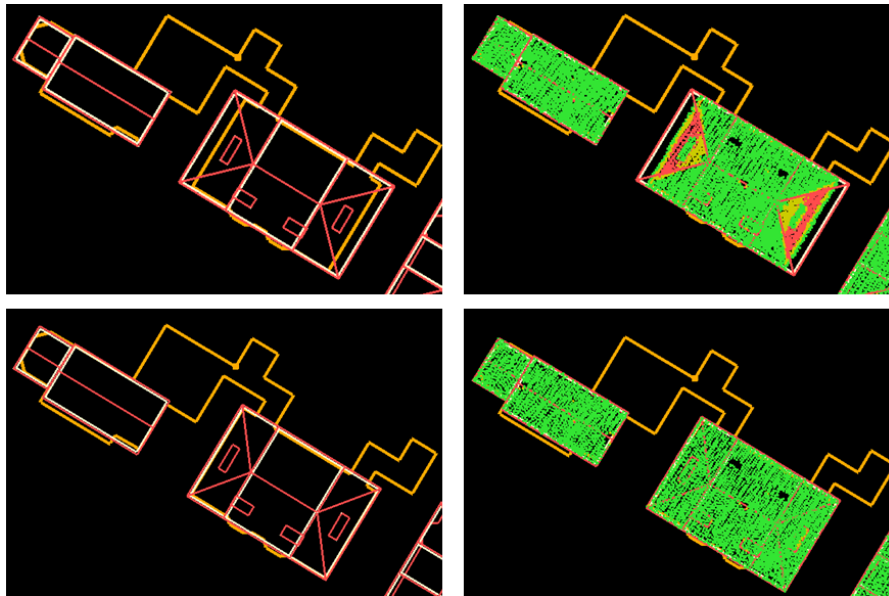


Figure 6-18 Top row: hip roof reconstructed with equal inclination angles. Right: laser point residuals superimposed. Bottom row: hip roof reconstructed with two different inclination angles. Right: as a result, the improvement on the laser point residuals is directly visible. Map polygon is shown as yellow polygon.

L-shapes do not have to have a straight angle between the two gabled parts (gable **ab** and gable **cd**). The orientations of the two gables are determined by the ridge direction of each of the gables. The height of the ridges is equalised by taking the average height of the largest gable ridge (**ab**). The height of the six gutter points (green dots) is defined by the height of the lowest laser point in segment **a** or **b**.

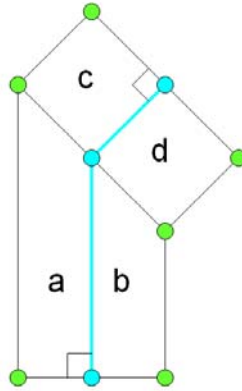


Figure 6-19 Structure of a L-shaped target.

As explained in the introductory of this section 6.8, our objective is not to present the best reconstruction method for a certain dataset, but to highlight the flexibility to assign parameter values in various ways.

6.8.2 Use of map data

The use of map data in this model driven approach is another interesting issue. The map polygon can be used to extend ridge lines such that they touch or extend the map polygon, similar to the data driven version. In our model driven approach we only use the map outline to extend horizontal ridges, see Figure 6-20. The walls have been constructed underneath the reconstructed roof. Therefore, the outline of the roof faces is taken, possibly shifted inwards if the overhang parameter is activated for that roof part.

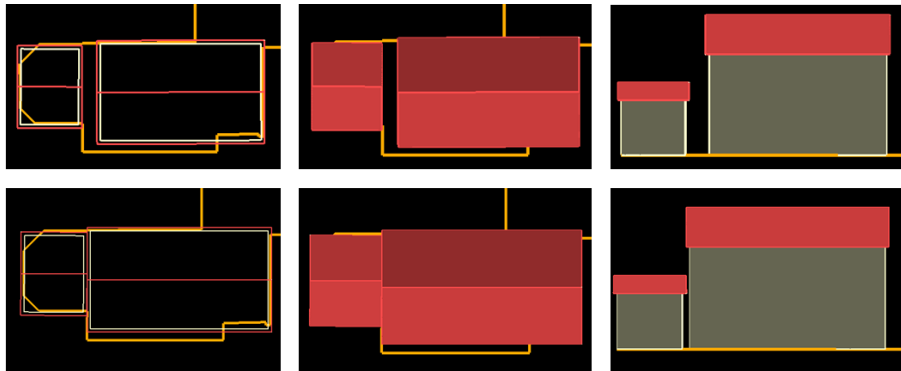


Figure 6-20 Top row: two gable roofs reconstructed based on the end point points of the ridge lines. Bottom row: ridge lines extended to (extensions of) the map polygon. Middle: top view with closed polygons. Right: side view to show overhang.

Below, a list of our implemented options is given. The list can be extended easily, and adapted for individual target shapes.

- Overhang: only reconstruct overhang if laser segments are used that partly fall outside the map outline.
- Extend ridge lines to the map polygon. By default, if the ridge line ends inside the map polygon, but within a certain specified distance (default 1.0 meter) the ridge line is extended to the map boundary.
- Symmetry on hip roof faces: if the two side faces show different slope angles than the main faces, allow for reconstruction of two different inclination angles.

6.8.3 Limitations

We did not implement algorithms that combine reconstructed target models. Milde et al. (2008) describe the grammar of combining such elementary roof shapes, including some basic rules. This grammar is currently under development, and is supposed to be finalised in the coming years. For future work, we recommend to analyse the rules proposed by Milde et al. (2008) and see of these can be included in the reconstruction algorithm. Kada and McKinley (2009) avoid an actual combination, by first splitting the map data into parts that contain a single (target) building model. In our approach, target models are reconstructed individually without grouping. As segments might be part of multiple targets, the reconstructed models contain overlapping roof faces. This can best be seen when visualising the wireframe representation of the reconstructed model, as shown on the right in Figure 6-21.

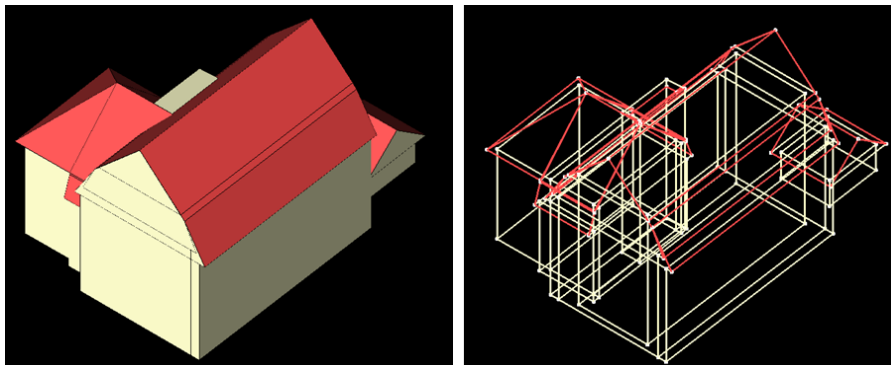


Figure 6-21 Reconstructed model containing multiple simple roof shapes and (right) its wire frame.

Also, we did not implement step edge reconstruction in this second approach. Amongst others, this means that small sheds next to or behind buildings are not reconstructed as the step edge between the shed and the main building is not used to partition the map outline.

6.8.4 Potential use

This model driven approach has great potential when reconstructing incomplete target matches. To make it effective we should incorporate probability values to data through the targets. For example, if one segment is missing on the lower part of a gambrel roof,

the other three segments match partly on the gambrel target. As it is very probable that the lower part of gambrel roof might be missing (Oude Elberink, 2008), it still can be assumed to be a gambrel roof. Future work includes the determination and embedding of probability values of (missing) roof parts into our reconstruction method.

When generalisation of 3D models is needed, this target based matching algorithm is useful. After the matching, it is known which segments match with which targets. Therefore it is also known on which target the most laser points match. This can be seen as the dominant roof structure for that building. It can be chosen to reconstruct that dominant roof structure using the corresponding laser points. As generalisation in 2D and in 3D is a complex procedure, that includes more than only showing more or less detail, we do not want to present this as solution for ‘the’ generalisation problem, but it certainly benefits to store realistic building shapes in various levels of details. In Figure 6-22 we have shown three situations that can be reconstructed from the target based matching results. On top, the target that matched with the highest number of laser points is reconstructed. In most of the cases, this target represents the main shape of that building. Exceptions are found on the double L-shaped (U-shaped) building in the lower corner of the area: only one L-shaped building is reconstructed as we do not have a U-shaped target. Also, when two buildings happen to be present in one map polygon, only the largest main building is represented, as shown in the middle grey ellipse. In the middle picture, a number of targets are reconstructed such that at least 75% of the laser points within that polygon are selected to reconstruct the building. This allows reconstructing more than one main shape per polygon. At the lower picture, all targets that had a full topological match with the data features are reconstructed.

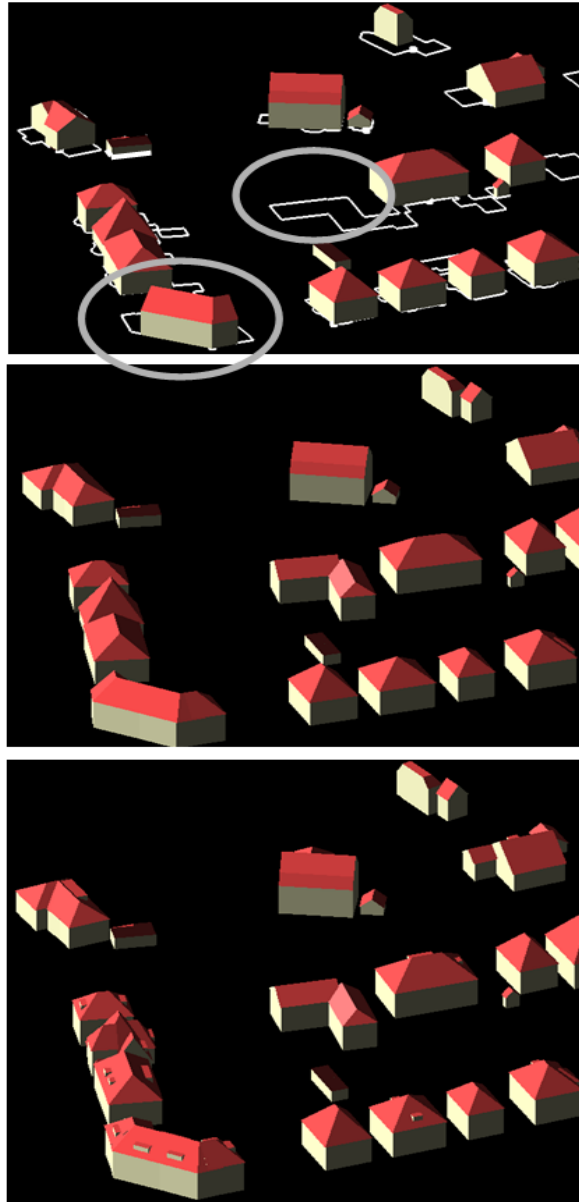


Figure 6-22 Various level of details can be reconstructed from the matching results. Top: only the target matched with the most laser points is reconstructed. Middle: targets are reconstructed until at least 75 % of the laser points have been used. Bottom: all complete targets have been reconstructed.

6.9 Summary

Our building reconstruction algorithm starts with laser data features that have been matched with target models. In general, the matched intersection lines represent the interior of the roof structure, so the task was to find an appropriate solution for the remaining roof edges, e.g. eaves and gutters. Map data and constraints inherited from the target models have been used in order to reconstruct a generalised roof model.

Constraints can be applied to a single roof face, e.g. horizontal gutter, a complete target match, e.g. symmetry in two faces of a gable roof, or to a complete building, e.g. all gutter heights are equal. In our combined features approach map data has been used for selection of roof segments and have been taken as location for walls. Therefore we needed to split up map polygons in order to build walls that distinguish various height levels, e.g. at step edge locations. The more model driven approach reconstructs parameterised building models. This approach relies more on geometric assumptions, such as roof symmetry, but the models can be refined if the data deviates significantly from the model. The target information includes the details on how these deviations are determined and on the thresholds to decide what is significant or not.

7 Results and evaluation¹

¹ This chapter contains content from:
Oude Elberink, S. and Vosselman, G., 2009. Building Reconstruction by Target Based
Graph Matching on Incomplete Laser Data: Analysis and Limitations. *Sensors*,
9(8): 6101-6118.

7.1 Introduction

In the previous chapters on building reconstruction the working of our algorithms has been explained, supported by showing the results of intermediate steps. In this chapter we present and analyse the end results of the reconstructed 3D models of the areas.

In our research data has been used from test areas in The Netherlands that are part of two different high density laser scanner datasets. Both datasets have been acquired by the FLI-MAP system of Fugro Aerial Mapping B.V.² In this chapter four areas are highlighted, called Ens 1 to 3 and Mid 4. These are abbreviations for three areas in Enschede and one in Middelburg, the Netherlands. Streetviews are given in Figure 7-1 for a first impression. In the following, specifications of the areas and datasets are listed.



Figure 7-1 Streetview of four areas. (Image courtesy © Enschede-stad.nl (Ens 1/2/3) and municipality of Middelburg (Mid4)).

For building reconstruction, the point density of the point cloud is the major factor that decides how the processing parameters have to be set. For the Enschede dataset the point density is on average about 20 points per square meter, but varies locally between 15 and 40 points per square meter, depending on whether the area is in a single or double coverage and on platform motions. Variations in point density are visualised in Figure 7-2, where the point density per square meter is shown in greyscale. Data ranges are between 0 points (black) and 180 points (white). Pixels with 0 laser points can be found on wet flat areas and occluded areas. Gaps larger than 20 m² are indicated with

² www.flimap.nl

white arrows. Three mean values are given in circles, showing average values in two single strips and the overlapping area in between. The strip in the lower part of the figure shows results of a typical swinging helicopter movement: some scan lines record the same area when the helicopter almost hangs still or bend over in flying direction. This results in point densities of up to 80 points per m². A few moments later the laser scan lines swing forward resulting in fewer points in along track direction (here indicated with 12 p/m²), compared to a normal single strip with about 20 p/m². As points on building walls are projected onto a horizontal plane, outlines of large buildings can be found just by analysing the (2D) point density (here 180 p/m²). The large point density at trees can be explained by the multiple returns recording. This results in more points per pulse, and can easily reach up to 90 p/m².

From the Enschede dataset three areas were selected. Criteria that were used for selection were the presence of various types of buildings within each area, and varying point density within the area. In order to process various building styles, we selected three regions within the city, built in their own style with their own characteristics. The first area (Ens 1) contains large residential buildings, built for the middle class. Roofs shapes are complex in the sense that there are many combinations of roof structures. The roofs shapes vary from building to building. Most of the building roofs contain overhanging parts. Ens 2 contains more buildings, but the roof sizes are smaller. There are many small extrusions at the roofs (e.g. dormers) and at the walls (bay windows). Ens 3 also contains smaller buildings, but the variety of building shapes is large.

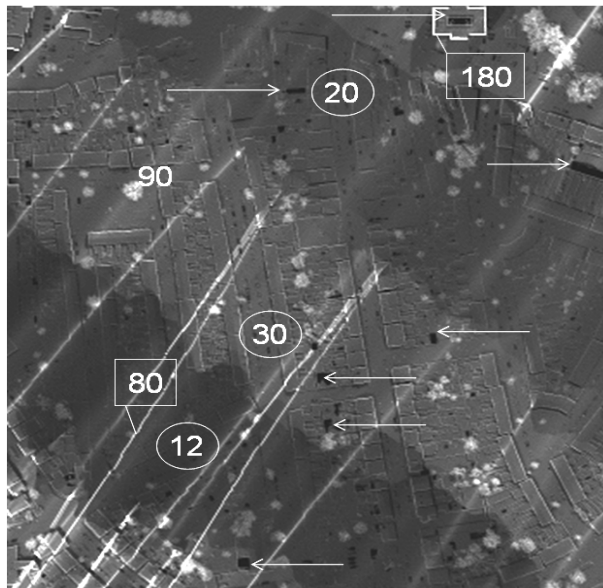


Figure 7-2 Number of laser points per square meter for Ens 3 area. Median values of single strips and overlapping area are circled, specific values are squared, and white arrows point at large data gaps.

In the Middelburg data set (Mid 4), usage has been made of the new national height model of the Netherlands, AHN-2. Laser point density is on average about 12 points per square meter, but in large areas of interest between 5-10 points per square meter. High point densities can be found in vegetated areas, where a great number of laser pulses returned as the systems records multiple returns per pulse. This increases the average of the point density in the area. At buildings, normally the pulse returns with a single echo except for the ones on the roof edges, partly hitting the roof and partly hitting the ground or wall. The area contains many data gaps due to flat roof parts at dormers, as can be seen in Figure 7-3. At the right the roof segments are given, showing that the roof faces are rather small and that for most buildings a clear main building shape is not clearly visible from the segments itself.

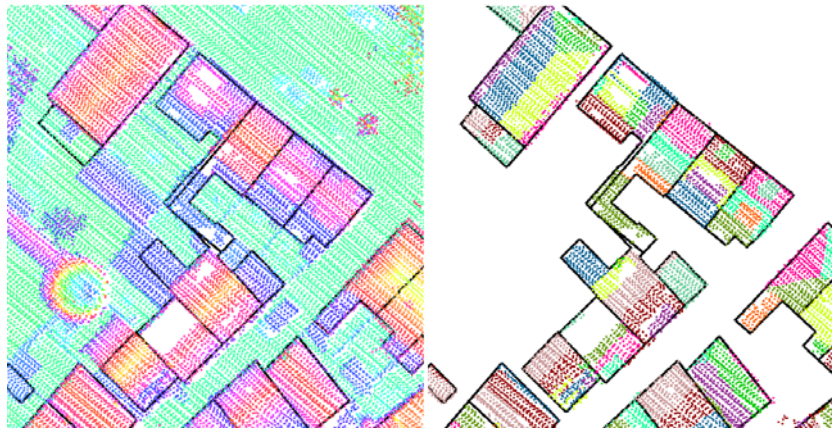


Figure 7-3 Left: AHN-2 data overlaid on the large scale topographic map. Right: selected roof segments per building.

We have taken map polygons from the cadastral map of Enschede and the large scale topographic map database GBKN from Middelburg. Both datasets contain building polygons at a map scale of 1:1000. In Table 7-1 various statistics are given of the data sets used in our research.

Table 7-1 Statistics on datasets of the four testareas.

Area ID	Ens 1	Ens 2	Ens 3	Mid 4
average # of laser points / m ²	20	20	20	8
# buildings	61	191	226	250
# roof segments	460	1570	1515	1081
# laser points in roof segments	176k	686k	598k	161k
Average # laser points per segment	382	437	395	149

In 7.2 we show results for both presented algorithms, followed by detailed evaluation on the quality of processing steps and the quality of the final results.

7.2 Results

7.2.1 Approach 1: Combined features

The first approach combines the features that were part of a complete match during the target based matching. For each of the segments the intersection lines are grouped and extended if necessary. Figure 7-4 shows results of area Ens 1 where our algorithm works well. Buildings in this area are characterised by various combinations of tilted roofs. The shapes of many buildings are quite unique in terms of shape and size; however they can be built by combining elements from basic roof types.



**Figure 7-4 Top: Variety of complex 3D building models in Zwik area (Ens 1).
Bottom: oblique image [bing.com].**

The majority of the buildings in this area contain overhanging roof parts. This means that the roof and walls can be reconstructed rather well, as the laser data is able to reconstruct roof faces that cover the total of the map polygon. The walls are then reconstructed by extrusion to the roof. The reason why this approach is able to reconstruct complex buildings is that it is able to capture complex shapes of individual roof faces. In Figure 7-5 roof faces of up to 7 intersection lines are reconstructed correctly. An imprecise step edge location leads to an incorrect wall location at one of the buildings at the bottom row, indicated by the red arrow.

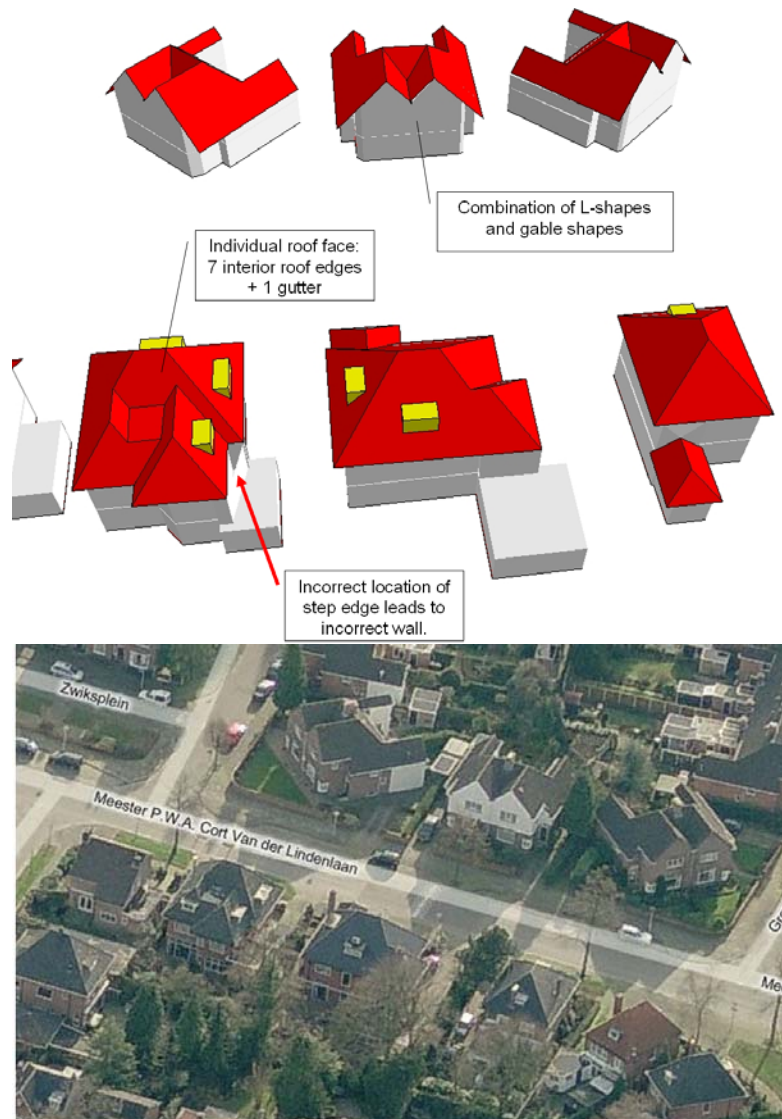


Figure 7-5 Top: Complex 3D building models by combination of complex roof shapes. Bottom: oblique image [bing.com].

Individual targets only have roof shapes up to three ridge lines per roof face. So the contribution of the combined feature approach is that with relative simple target shapes, complex roof faces can be captured. That is because the topology between roof faces allows extending intersection lines such that they intersect with each other at a corner point. By combining these individual complex roof faces, complex buildings can be reconstructed. Figure 7-6 shows the strength of the combining data sources. The map

data is responsible for the detailed construction of the walls, extension of the ridge line to the map outline and for giving direction to the eaves, whereas the laser points are responsible for the correctness of the roof shape. Figure 7-7 highlights the 3D impression of this approach: reconstructing the first floor according to the map outline definitively enhances the 3D model. The shape of the extrusions at ground level could not have been captured based on solely laser data. One gutter at the right hipped roof building is reconstructed too high as the corresponding segment does not contain laser points near the edge of this roof face.

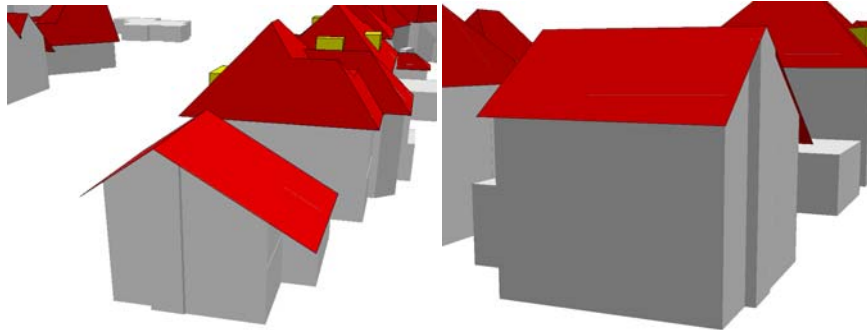


Figure 7-6 Walls at map location, roofs constructed by combining information from laser data, map data and roof shape assumptions.

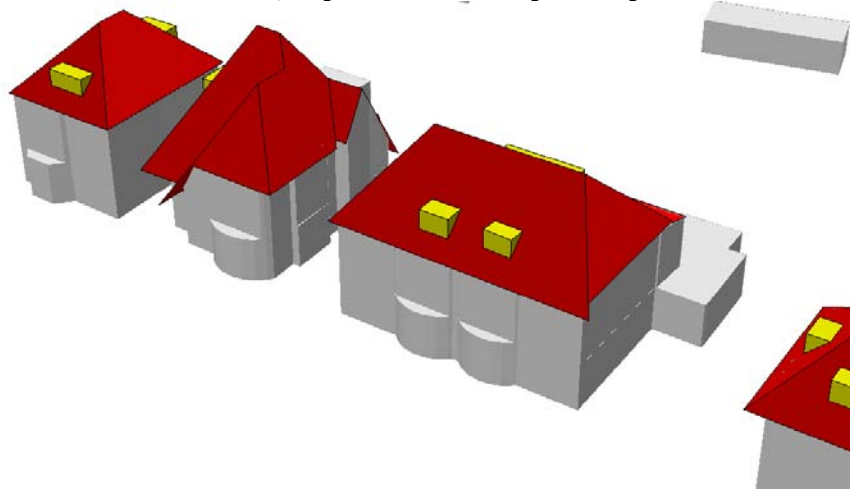


Figure 7-7 First floor at map polygon location. Upper floors reconstructed by extruding intersection of roof faces and map polygon.

In relation to the Enschede dataset, the point density of 5-10 p/m² of the Middelburg dataset is lower. The lower point density has an influence on the quality of extracted features, the optimal values of threshold parameters and on the quality of the final result. That is why we have to adapt the processing parameters and the expectations of the final results in terms of completeness and correctness of details. Remember that the minimum length to accept intersection lines was made dependent on the median point

distance. Therefore, with lower point density and increase of the point distance the minimum length threshold increases.

Due to the lower point density, the chance is higher that an intersection line ends inside the map polygon. Therefore extending ridge lines to the map data is important to avoid reconstructing too small roof faces.

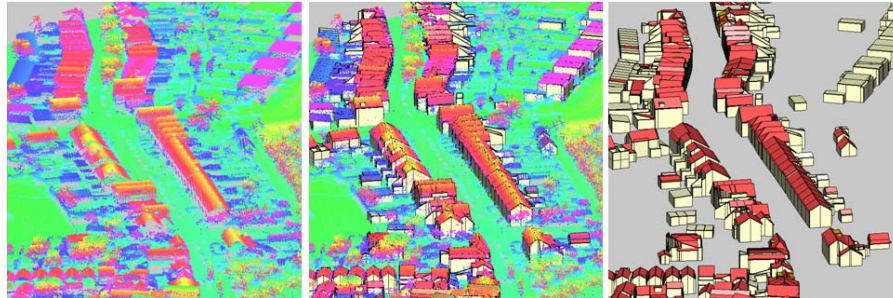


Figure 7-8 Laser data (left) and 3D reconstructed buildings (right). (Middle) Overlaying laser data on the reconstructed models.

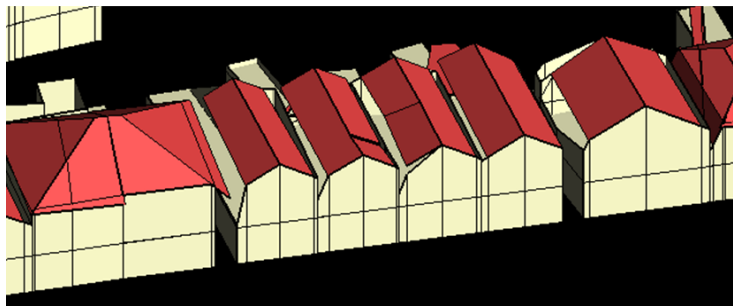


Figure 7-9 Incomplete roof models in Middelburg dataset.

The reason why the model is not complete (Figure 7-9) is that we reconstruct the roof and wall too independent, although we connect roofs and walls if intersection lines are close to the map polygon. In cases where the intersection line was not close enough to the map polygon, our algorithm does not extend this line further and reconstruct the roof based on the laser data only: the eaves are constructed perpendicular to the intersection line, and the gutters pass through the lowest point of the segment. If the segment is completely inside the map outline, the roof face is constructed inside the map polygon. This causes incomplete building models. For these cases, the method of Vosselman and Dijkman (2001) would give better results as all roof faces are bounded either by intersection line, step edge or map outline. However, the question is if the roof face should be extended to the map outline. There might be a reason why the segment ends inside the map polygon. In the Middelburg area, many gambrel roof buildings are present. Many of lower gambrel roof faces were not found, so the program handles the building as a gable roof. Future work is to extend our algorithm by detecting these

situations automatically, analyse the raw point cloud to hypothesize the actual shape of the building, and reconstruct these roof faces according to the hypotheses.

7.2.2 Approach 2: Reconstructed targets

In this section results are given for the four areas, first by showing an overview of all four areas in Figure 7-10, followed by four screenshots for each area. Main reason to show all results in one figure is to highlight the success of model driven reconstruction approaches: the results always seem to be correct, as they do not contain strange shaped models.

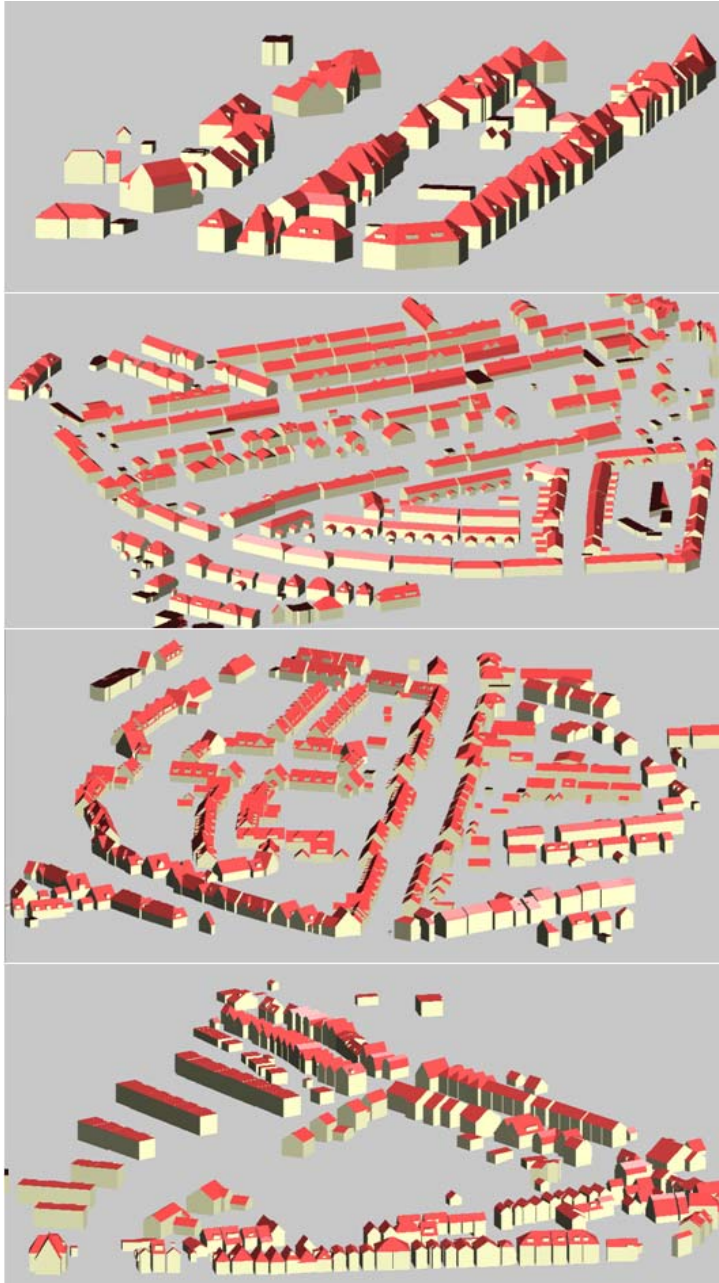


Figure 7-10 3D buildings reconstructed by the second approach for the four test areas.



Figure 7-11 Comparing oblique image of Indische buurt area with reconstructed models. Image taken from Bing.com.

In Figure 7-12 and Figure 7-13 the more model driven buildings are overlaid on the more data driven models, for two scenes in area Ens 1.

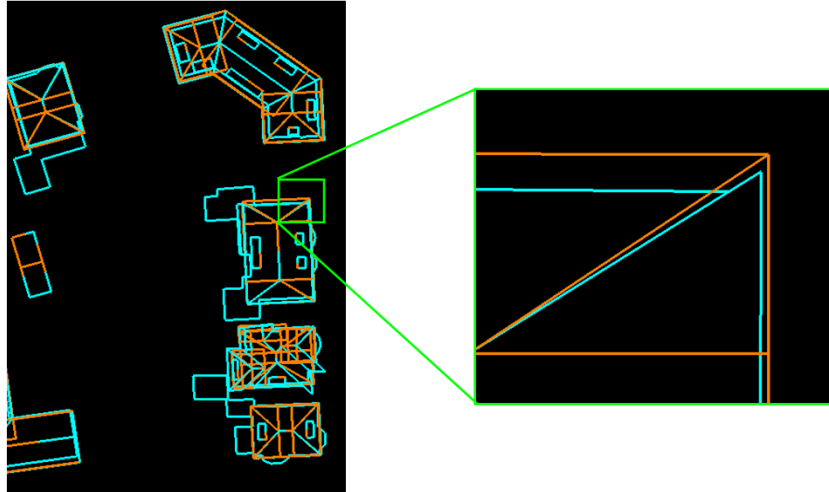


Figure 7-12 Overlay of data driven (cyan) and model driven (orange) building roof models. Left: overview wireframe representation; right: zoom on building corner to view difference.

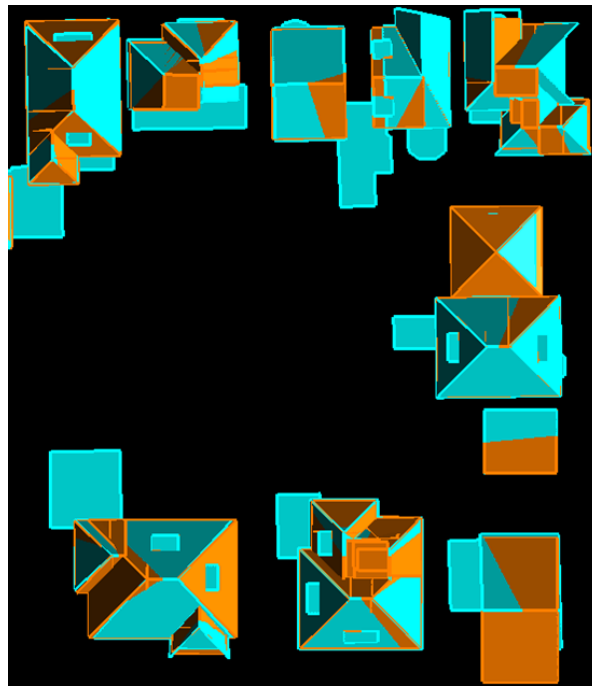


Figure 7-13 Boundary representation of overlaying data driven model (cyan) with model driven results (orange).

Figure 7-12 and Figure 7-13 show that the model driven approach contains more lines per roof face as the model faces have not been grouped for each of the segments. These figures show that both approaches have many similarities. That is because approach 1 is not completely data driven and approach 2 is not completely model driven. Both approaches are a mixture of data information and assumptions. Differences between the two approaches can best be seen at the sheds behind the building (not reconstructed in the model driven approach), the gutter locations and the roof face inclination. Figure 7-12 highlights the difference at a corner location (earlier discussed in Figure 7-7) where the more data driven approach incorrectly reconstruct one gutter. Another difference is in the reconstruction of walls, Figure 7-14. For approach 1 this is based on the map, subdivided by step edge locations and intersections with roof faces, whereas for approach 2 the walls are placed based on the outer edges of the reconstructed target models.

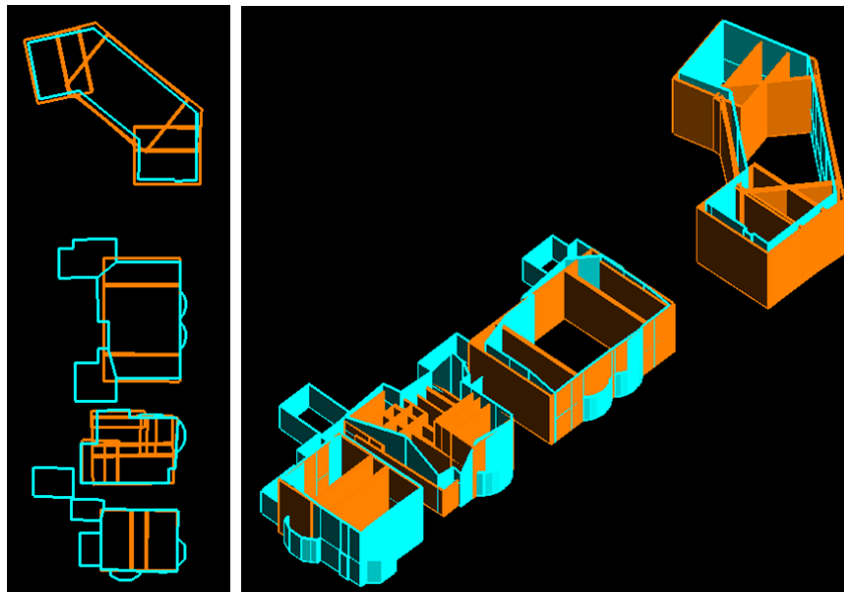


Figure 7-14 Left: top view on location of walls for data driven (cyan) and model driven (orange) approach. Right: oblique view on reconstructed walls.

7.3 Evaluation

Our evaluation is split up in three main parts:

1 Evaluating the laser data features (section 7.3.1)

The first quality section describes the quality of the laser data features, which are input for target based matching. These features are segments, intersection lines and the corresponding roof topology graph. This section shows that the quality of the final model is related to the quality of preceding steps. The consequences of threshold values along the workflow from laser points to final model are further explained.

2 Analysis on the result of the target based matching algorithm (section 7.3.2)

The quality of the target based matching has been examined by analysing the segments that are part of an incomplete target match. These segments indicate the success and the limitations of the target based matching.

3 Evaluation of the 3D building models (section 7.3.3)

We do not have accurate and complete reference data to check our final results. Despite the lack of independent reference data, we can evaluate our models in other ways. The reconstructed models are accompanied by three internal quality measures:

1. distance of laser points to roof faces,
2. distance from object point to nearest laser point,
3. not used laser segments.

7.3.1 Laser data features

Features found in the data are results of a chain of stochastic processes and deterministic assumptions. This makes the exact position and even the existence of a feature uncertain. In this section we discuss the quality of data features, and how that relates to the processing parameters.

7.3.1.1 Quality of laser segments

Finding planar segments for roof extraction is widely used in building reconstruction algorithms, (Brenner, 2000; Dorninger and Pfeifer, 2008; Hofmann, 2004; Jochem et al., 2009; Rottensteiner and Briese, 2003; Vosselman and Dijkman, 2001). As we have seen earlier section 5.3.1 one of the research problems is that some roof faces might not be detected in the laser data. *If* a segment is found, the quality of the plane parameters of the segment increases with the size and planarity of the segment. The other research problem was the quality of the outline of segments. Especially for steep, dark, flat and wet roof faces, the bounds of segments are rather noisy due to reflected or absorbed laser pulses. In general, it holds that for laser data that the pose of roof faces can better be determined than the outlines of the face.

7.3.1.2 Geometry of intersection lines and step edges

The quality of direction and position of an intersection line depends on the intersection configuration of the two segments. The position of the end point along the 3D line depends on the existence of nearby laser points in both segments. In our algorithm we assume that the geometric quality of the end points of intersection lines between two segments is in the order of the median point spacing. If this intersection line is again intersected with a third segment the quality significantly improves, as the position is determined by the intersection of three planes.

7.3.1.3 Roof topology graph

The quality of the roof topology graph can be described by the certainty that a segment (node) actually represents a roof face and that the intersection line (edge) represents an

interior edge of the roof boundary. Note that, this certainty value includes the risk that a segment or an edge is not present in the graph, but is in reality. At the moment, we do not calculate the quality of the elements of the roof topology graph. Setting a minimum segment size and minimum length of intersection lines, reduces the risk of erroneous nodes or edges. Future work includes calculating probability values to the elements of the graph, also taking into account the segment size and length of the intersection line.

7.3.1.4 Thresholds in laser data feature detection

To ensure a certain reliability to the features in the laser data, we specify threshold parameters to accept or reject features and their labels. We start by discussing segmentation parameters as these are in the early stages of feature extraction. Our segmentation algorithm is based on the surface growing algorithm as described in (Vosselman et al., 2004). Parameters have to be set that identify seeds and grow these seeds into segments.

Hough space bin sizes

Seed identification is done in Hough space. Each laser point defines a plane in Hough space, which is divided into discrete steps (bins). Every plane intersecting a bin, causes an increase in the counter of that bin. The bin sizes represent the size of the steps into which the Hough parameter space is divided. The bin size angle represents the minimum angle difference to discriminate between two planes. The bin size segment distance represents the minimum vertical distance to discriminate between two segments. Default values are 3° and 10 cm; this should be adapted if ‘objects to be found’ or ‘data to be used’ indicate otherwise.

Maximum distance to the plane

The decision to assign a point to a certain segment is based on the distance to the plane through the growing segment. This distance should include variations in height texture at the surface and laser point noise, and it is set on 10 cm by default.

Minimum segment size

The minimum segment size has been set in terms of number of laser points. This value can be determined by translating the desired level of detail to the expected number of points on the smallest object to be detected using the average/minimum/median laser point density. Our default minimum segment size is based on the aim to reconstruct roof faces larger than 2 m^2 . For each dataset the average point density is calculated, and scaled to the number of points per 2 m^2 . This can be the minimum segment size. However, some segments on roof faces of 2 m^2 will not be included as their point density might be lower than average. For those cases, one may want to add a buffer to the minimum segment size.

Minimum intersection line length

The minimum intersection line length depends on what can be found in the data in relation to the desired output. The larger the desired minimum ridge length, the more reliable is the intersection line that could be found in the laser data, but the higher the risk that small details can not be reconstructed.

Maximum distance between two neighbouring segments

This parameter defines the maximum distance between points of two segments to be considered as neighbouring segments. This value should be at least the median point distance otherwise segments might not be considered as neighbours because of the minimum distance between two points is just too large due to the distribution of laser points. On the other hand, the value should not be too large as this implies that two faces that aren't neighbours in reality might be considered as neighbouring segments in the data. This causes a distortion in the topological relations and thus the roof topology graph. In some cases the distance between two neighbouring segments is large, because of an occluded area between the two segments. Analysis of data gaps is necessary to locally increase the maximum distance, such that these neighbouring segments are correctly detected as neighbouring object faces. This data gap analysis is not incorporated in this research. Further research on this topic is needed, although some effort has been done by (Dharmapriya, 2009).

Intersection angle between two segments

Intersection lines are only determined if both segments intersect at a certain angle. Nearly parallel segments cause unreliable intersection lines, as they are highly sensitive to errors in the normal direction of the segments. The minimum difference between two normal directions is set on 20°.

Minimum height difference to label step edges

By default, the minimum height of a “step” has been set equally to the segmentation parameter of the bin size distance. This means that by default this is no extra threshold: any two segments that connect in 2D but not in 3D are considered as step edge.

Minimum number of points near step edge

At the detection stage, step edges are not represented by a line segment between two end points, unlike the extraction of intersection lines. Therefore we do not use the minimum length of the line, but the number of the laser points near the step edge. The minimum number is set on 15 points for each of the two segments.

7.3.1.5 The limits of threshold values

In this section we explain some dilemmas and inevitable problems when choosing threshold values. Within one building or region there may be a small variation in how similar objects appear in the data. Often, this is caused by irregularities in the acquisition configuration, but can also be caused by irregularities on the object itself.

In Figure 7-15 differences are shown between laser points and planes fitted through segmented laser points. The figure contains three components: on top a terrestrial photograph from two buildings, in the middle the differences between laser points and planes fitted through the segments of those two buildings, at the bottom the laser point height is replaced by the height difference and projected on a virtual vertical plane. The goal of Figure 7-15 is showing that roof planes in reality might show a small crack or bending, that also laser points might record that crack or bend, but that the processing parameters are responsible for neglecting details on the edge of threshold parameters.

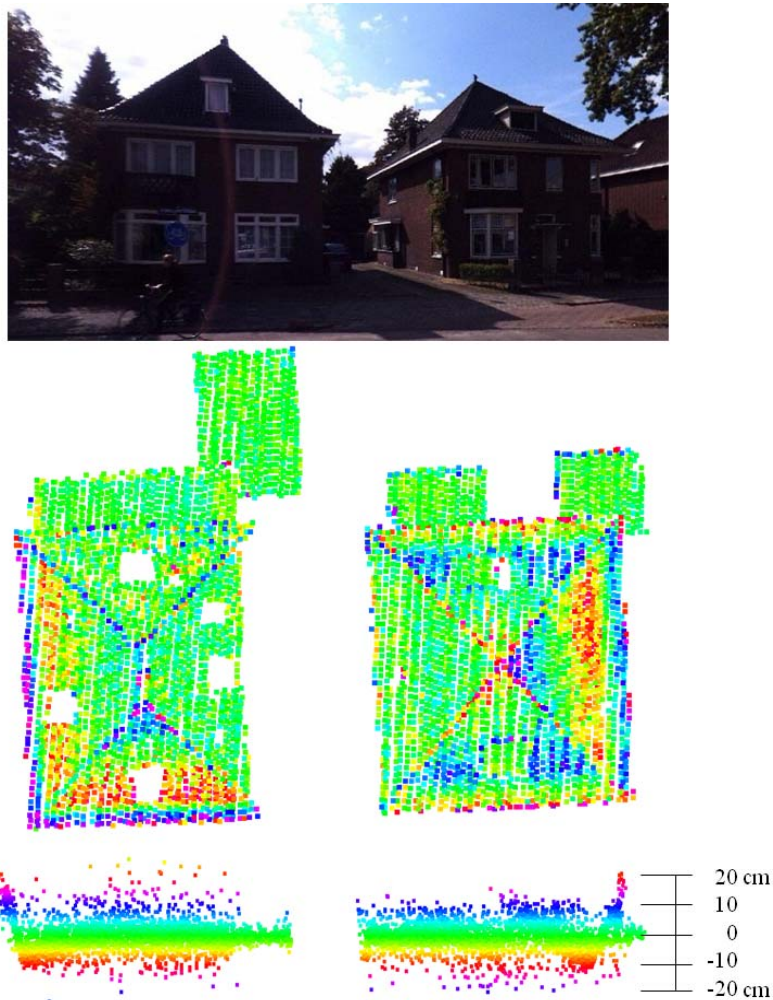


Figure 7-15 Deviations between laser points and planes through segments. Systematic patterns can be found at roof parts that slightly deviate from a planar surface.

To elaborate on the dilemmas of threshold values, we introduce Figure 7-16, handling the same two buildings as Figure 7-15, showing segmented laser points on the right hand side. The left building contains five dormers. Segments on these dormers are just too small to be handled as roof segments. A slightly larger dormer on the right building is extracted. Even more interesting is the detection (and the failure of detection) of roof segments at the lower sides of the roof faces. In reality, both buildings contain eight tilted roof segments each, as each roof side contains a change of angle at about 50 cm from the gutter. These lower roof faces are located partly inside the building outline, but also partly outside. The question is if this change of angle should be modelled or not. At

the left building, only one of the four lower roof faces is represented by a roof segment, two roof faces are under-segmented as they are merged with the higher ones, and one lower roof face is segmented, but the segment was removed as it was for more than 50% outside the map polygon. At the right hand building one lower roof face is represented by a roof segment, the other three are under-segmented. This is interesting, because it is expected that each of the buildings is more or less symmetric, that even the two buildings have about the same roof orientations and about the same roof face sizes. It means that the laser point distribution and the processing parameters just are not stable enough to get stable roof segments. In this case, a solution would be to narrow the maximum distance to a plane fitted through a segment in order to be added to that segment. At the other hand, the question could be posed if it is necessary to reconstruct the change of angle in the roof at all. Why not just reconstructing a simple hip roof on the left and a pyramid roof on the right? This turns around the problem and the solution: the detected segments on the lower roof faces can be considered as over-segmentation, so the parameter of maximum distance to the plane should be increased a little to let them merge with the higher roof part.

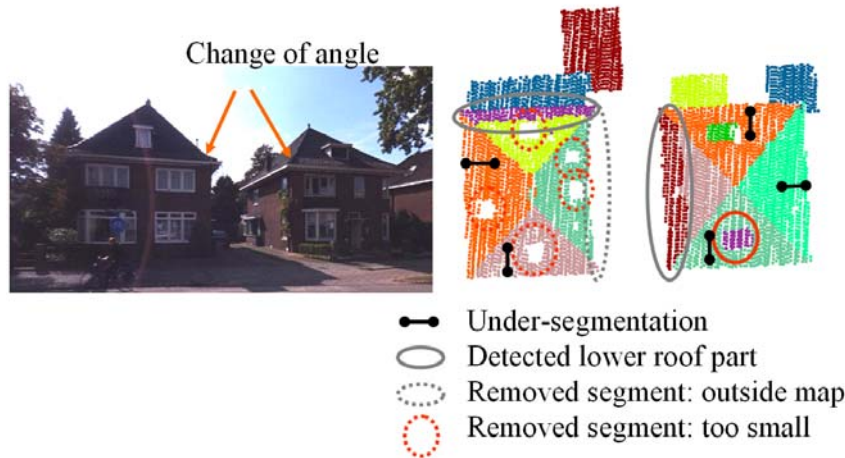


Figure 7-16 Objects on the edge of threshold values: small dormers and roof faces with a crack. Solid lines indicate that the objects are detected in the data, dashed lines indicate object parts that were not detected.

It is likely that flat roof buildings are not exactly flat. Especially for large industrial types of buildings (Figure 7-17), it is important that the roof can drain heavy precipitation. To carry the load and to drain the rain or snow, the surface of large flat buildings often bends. Planar segmentation of the laser point cloud will cause fragmentation when the thresholds are too strict.

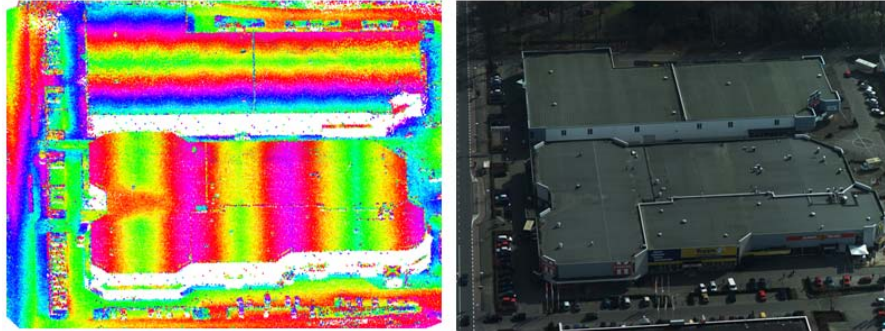


Figure 7-17 Large flat buildings show height variations up to 50 centimeters. Color cycle length adapted to show small height differences: one color cycle is one meter.

7.3.2 Evaluation on target based matching

The target based matching performs an important task in our reconstruction approach, as it decides which features belong to which target model. Based on this relation, the reconstruction is performed. That is why it is important to evaluate the working of the matching algorithm, starting with the features that did not match with a target model.

7.3.2.1 Incomplete match results

In Chapter 5, Figure 5-17 p91, several segments were not part of a complete match result. It is of high interest to examine these segments in order to detect incompleteness in the data or the target database. For our four areas we have listed the segments on incomplete match results. As can be seen in Table 7-2 this section deals with about 5% of the total number of roof segments, but these affect 19% of the buildings.

Table 7-2 Statistics on segments of incomplete match results.

Area ID	Ens 1	Ens 2	Ens 3	Mid 4	Total
# buildings	61	191	226	250	728
# laser points in roof segments	176k	686k	598k	161k	1621k
# roof segments	460	1570	1515	1081	4626
# roof segments not in complete match (%)	18 (4%)	64 (4%)	46 (3%)	71 (7%)	199 (4%)
# affected buildings	12 (20%)	37 (19%)	35 (15%)	55 (22%)	139 (19%)

For this evaluation, we removed segments containing less than 40 laser points from the analysing, so the table deals with segments on objects larger than about 2 m² for the dense dataset (Ens) and 4 m² for the AHN-2 dataset (Mid 4).

In Figure 7-18 segments from a small subset are superimposed to the automatically reconstructed building models. It is of interest to analyze these “left over” segments as these hold important information on the completeness of the match between laser data and model database. First question to be answered is why these segments are not part of a complete target match. As soon as this is known the question is if this should be avoided or solved. In the next section, an overview is given on the reasons why these segments are “left over”.



Figure 7-18 Segments of incomplete match results superimposed on 3D models.

7.3.2.2 Reasons for incomplete matches

For the four datasets, we have categorised the segments from incomplete matches according to six reasons, which are explained in this section. To each segment we manually assign one category. Results of this categorization are listed in Table 7-3. Although the individual numbers depend on local situations in the data and the real world, the table gives a general insight in how the reasons are distributed over the appearances. The first reason deals with segments that are not matched because they are not a roof face. The majority of the examined segments actually represent a real part of the roof. The reasons that they are not used in the reconstruction can be described by five categories, which are listed as reason 2 till 6.

Table 7-3 Reasons for segments being part of an incomplete match result.

Area ID	Ens 1	Ens 2	Ens 3	Mid 4	Total
# of segments leftover	18	64	46	71	199
1. Non building segment	3 (12%)	9 (14%)	9 (20%)	3 (4%)	24 (12%)
2. Absence of neighboring segments	7 (39%)	28 (44%)	16 (35%)	27 (38%)	78 (39%)
3. Disturbance of neighborhood relations due to over-segmentation	3 (17%)	5 (8%)	4 (9%)	3 (4%)	15 (8%)
4. Absence of neighborhood relations	3 (17%)	10 (16%)	4 (9%)	20 (28%)	37 (19%)
5. Target shape not in database	2 (11%)	7 (11%)	3 (7%)	14 (20%)	26 (13%)
6. Segment on border of dataset	0 (0%)	5 (8%)	10 (22%)	4 (6%)	19 (10%)

Non building segments

The first reason discussed here handles segments that actually should be removed for further processing. Planar laser segments can be found on objects that stand close to buildings but are not part of actual building, such as sun marquees and garden furniture. If these non building segments are located (partly) inside the building polygon, they are incorrectly taken as roof segments. The topology between these segments and neighboring roof segments may not match with a target roof model. So, the fact that they are left out from the automatic approach is in this case correct as they do not represent roof faces. These segments should be removed from further processing on building reconstruction. This group represents about 12% of examined segments.

Absence of neighboring segments

The major reason (39%) that a segment is not part of a complete match is that another segment, that would complete a certain target match, is missing. Often, this occurs when the missing segment is on a steep or small object face. For example, many segments in dataset 2 could not be found at one of the two sides of a gable shaped dormer, see the example of Figure 7-19. As can be seen at the scale bar, the missing segments should represent an object face of about 2 m². For this building 6 of the 8 gable shaped dormer faces could be segmented, and two are missing. Another common problematic case could be found on buildings with gambrel roof shapes where one segment on one of the lower steep roof faces is missing. As a direct result, the segment on the lower steep roof face that actually is found could not be part of a complete match.

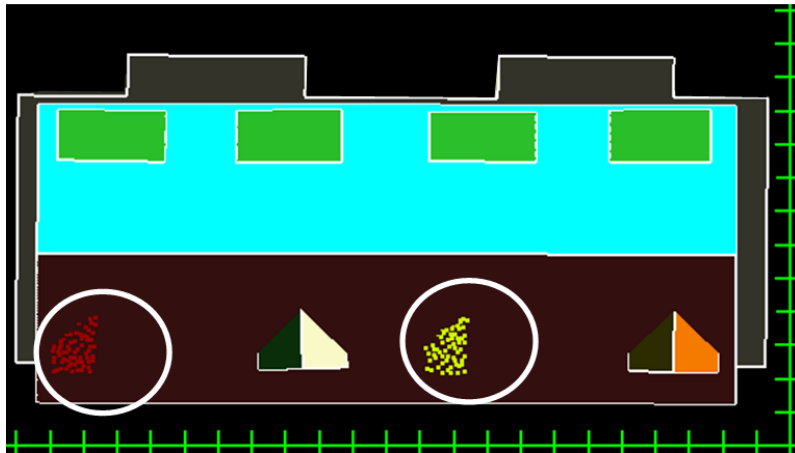


Figure 7-19 Segments are missing on one of the two sides of gable shaped dormers (white circles); resolution of the scale bar is 1 meter.

Disturbance of topologic relations due to over-segmentation

Another segmentation related reason is the disturbance of topological relations due to over segmentation. Over-segmentation occurs when one (planar) object face is represented by two or more segments. Segmentation errors are made if segmentation parameters locally do not fit to the data. Examples are in situations where platform movements cause large point spacing between two scan lines. If the distance between two scan lines exceeds the growing radius of the segmentation parameters, the segmentation algorithm will not bridge the data gap, splitting up laser points into multiple segments. These segments are treated as individual nodes in the topology graph. This break in the roof topology graph results in a distortion of the matching results.

Absence of topologic relations

Topological relations directly influence the matching results, as they are stored as edges in the roof topology graph. Relations can be absent due to a large distance between two neighbouring segments. Large distances can be found near occluded areas and regions with non reflecting surfaces. Examples are found at locations where solar cell collectors are placed near roof edges. The collectors cause local gaps in roof segments and not all intersection lines could be found.

Limitations of the target models

A roof topology graph might correctly describe a roof shape that is just not in the database. Examples in our dataset can be seen in Figure 7-20 on a five-sided hip roof and a five-sided pyramid roof. In these cases the limitations of the existing target models cause that the segments on the “fifth” roof face (grey circles) are left out from the automatic reconstruction.

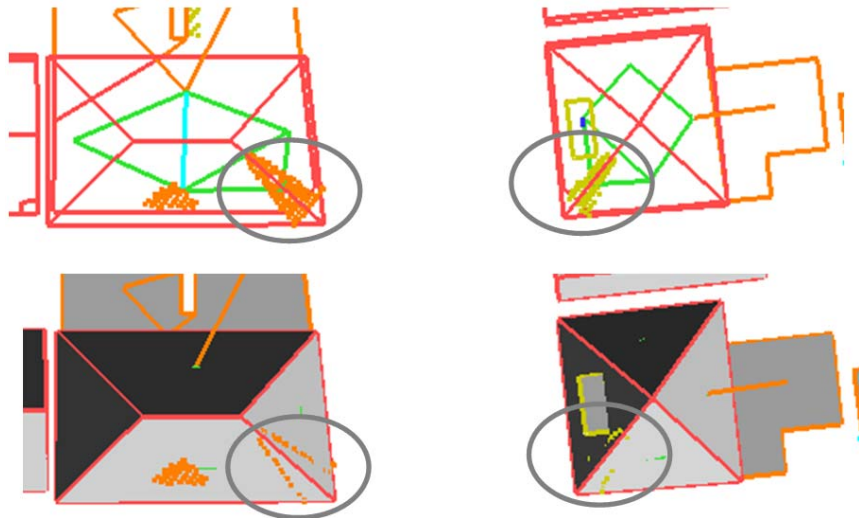


Figure 7-20 (Top) Segments left over superimposed on reconstructed models, including topological relations of all segments. (Bottom) As top, but for clarity reasons the reconstructed roof faces have been filled grey.

Border effects

For several segments on the border of the dataset no neighboring segments or relations could be found. Although this effect is obvious and scientifically not relevant, we mention this category for the completeness of our work.

7.3.2.3 Discussion on solving incomplete matches

Now the reasons have been analysed, the question is if this should and can be avoided or solved. Can this be avoided by changing the processing parameters? Or should the model database be extended to be able to include these segments such that they are part of a complete match?

First, we discuss the possibility to adapt the segmentation parameters to reduce the number of roof segments that are part of an incomplete match. In order to reduce the errors caused by missing roof segments, the segmentation algorithm should find roof segments at locations where previously the algorithm did not find segments. This can be done by decreasing the minimum of points in a segment in order to be taken as roof segment, or to loosen the acceptance criteria in the growing phase. However, an improvement to one error source might increase the errors from another problem, e.g. disturbance of topological relations. So our suggestion is to apply these changes locally, for example only to buildings that are affected by leftover segments. This can be done in an automated iterative way. The parameters are chosen such that the results that best fit to the user defined quality parameters.

The problem of limited number of target models can be avoided by adding new target models to the database. However, adding more target models that are less common may lead to false matches on other segments that are not part of a building and should be filtered out by the matching. Our goal is to relate object knowledge with features that

can be found in the data. To explain the complexity of finding a correct match, we take the situation of a five sided hip roof, as mentioned earlier in Figure 7-20. On the left in Figure 7-21 intersection lines and the roof topology graph are shown, on the right in target A and B two target roof shapes are represented as target graphs.

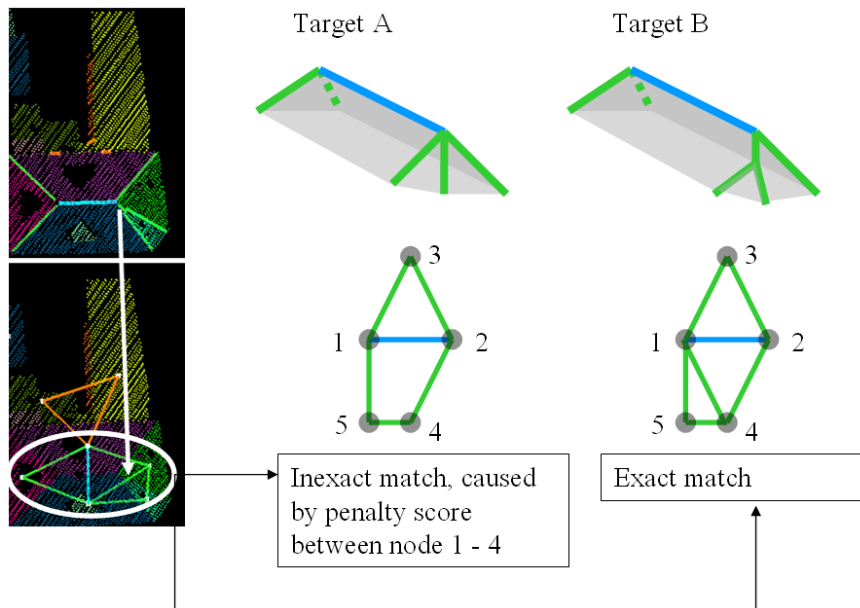


Figure 7-21 (Left) Intersection lines and roof topology graph of a five sided hip roof. (Middle) Most likely target A does not exactly match with roof graph. (Right) Exact match between data and (unlikely) target B.

Note that the topological relation indicated by the white arrow, is a result of intersection of two segments that are close to each other. The length of this intersection line can easily exceed the minimum length to be accepted, as is the case in our example. Therefore, from the data side the match with target B is more exact than a match with target A. Match results on target A include a penalty score for the presence of a topological relation in the data that is not in the target between node 1 and 4. However, from our object knowledge we might propose that it is more likely that face 1 and face 4 only meet in one point (target A) instead of sharing a line (target B). In this case our algorithm should ignore the intersection line that caused the penalty score and give preference to a more likely target shape A. This example shows the potential improvement of our target based graph matching by including likelihood estimators to the existence of an object face or a relation between two faces.

7.3.3 Reconstructed models

In the previous section we have evaluated the segments that did not completely match on a target. In this section we will examine the data features that were part of a complete match. These features have been used in the automatic reconstruction

algorithm, and therefore we can analyse the relation between input data and output model. Various indicators can be used to describe the quality of the reconstructed models. In this section we list a limited number of internal quality checks between laser scanner data and 3D model. Rather than to focus on the quality of the end product³, we would like to describe how to evaluate the processing steps and assumptions made. For end users as well as for researchers it is of interest to have insight in the consequences of successive reconstruction steps, in order to improve the 3D model or the reconstruction approach itself.

7.3.3.1 Residuals between model faces and laser data

The advantage of the having the relation between data and model is that we can check if individual model faces fit to the data. One of the quality checks is the perpendicular distance between 3D model faces and laser points, similar to the approach presented in (Dorninger and Pfeifer, 2008). Discrepancies between data and model can be visualised and quantified easily. Figure 7-22 shows the distance between laser points and its roof faces reconstructed by the more model driven approach, coloured in intervals < 20 cm (green), <50 cm (yellow) and >50cm (red). Segments that contain more than 20 laser points with a distance larger than 20 cm are written to an output file and shown to the user.

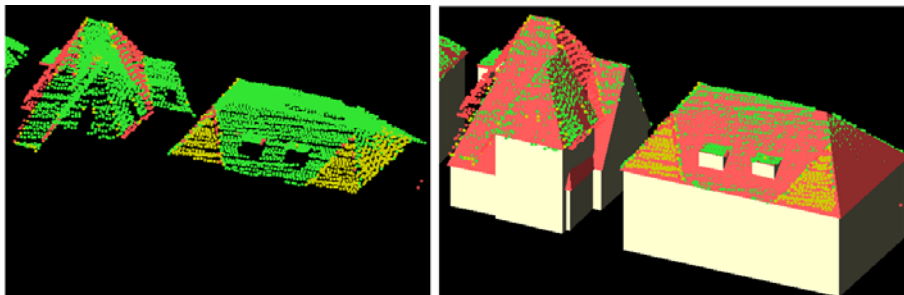


Figure 7-22 Laser points colored by residual value: the distance between a laser point and its projected position on the corresponding roof face.

It is expected in the more data driven approach that the majority of residuals is coloured green (within 20 cm, the acceptance height during planar surface growing in the segmentation step) as the model faces are constructed by least square fitting through the same laser points. Obviously, large residuals are found on segments that did not match completely, as these laser points are left out from the reconstruction step. However, we also find large residuals on some segments that are part of a complete matching result. It is of interest to elaborate on these data parts as it reveals information on the cases where the data does not fit to the assumptions of the algorithm.

We focus on residuals of segments that topologically matched completely on target objects. Large residuals on these segments imply that these segments geometrically do

³ to evaluate the absolute quality of the 3D model, the assessment would preferably be based on external 3D reference data

not fit to the constraints inherited from the target model, although the segments topologically fit. These situations indicate that the discrepancies are caused after segmentation, or at least that the laser points do not fit to the assumptions inherited from the target object. If during feature extraction errors are made that have caused a match with an incorrect target, the reconstructed roofs will show height differences on at least a part of the laser points. As in approach 1 each roof face is constructed by fitting a plane through a segment, large residuals are only caused by the fact that laser points are not within the reconstructed roof. In the more model driven approach differences between laser data and model can be caused by the fact that roof faces are not reconstructed by fitting through each segment, but on fitting a model on (part of) the data. Therefore, it is of interest to analyse laser points of segments that were part of a complete match, with residual values above 20 cm. These segments are detected automatically.

In Figure 7-23 examples are given of segments that do not exactly fit to the reconstructed roofs, although they were part of a complete match. They show the limitations of our automated reconstruction algorithm. On the left in Figure 7-23, the intersection line between two gable segments did not completely cover the actual gable ridge. Near the end of the ridge there were no laser points on the gable faces. In fact, a chimney was located at the ridge end. Outlines of these gable faces are constructed perpendicular to the ridgeline. This causes that a part of these segments falls outside the face outlines. On the right, a dormer face is missing due to a missing segment on the hipped part of the dormer. The two remaining segments correspond with a gable shaped dormer. Again, outlines of these segments are constructed perpendicular to the dormer ridgeline, cutting a part from both segments. These situations show that it is possible to detect incorrect assumptions. It is also possible to extend the ridgelines automatically until no more points fall outside the roof face. However, the situation on the right is then 'solved' incorrectly, because the correct solution would include the hipped roof face at the location of the missing segment.

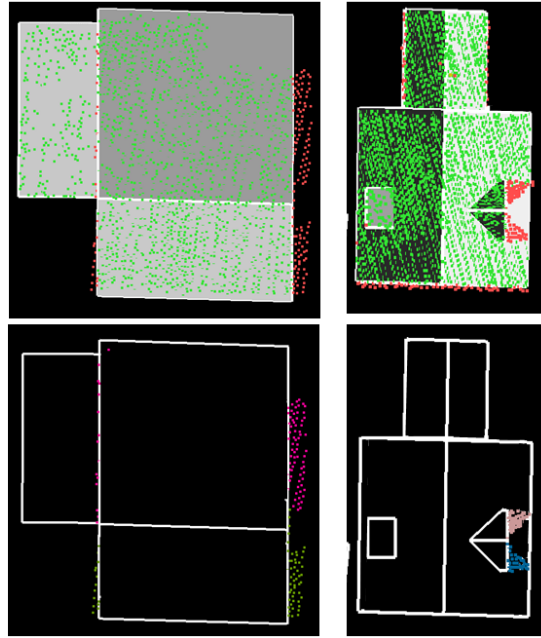


Figure 7-23 (Top) Laser points colored by residual value between laser point and reconstructed roof. (Bottom) Segment parts with high residuals due to incorrect assumptions on ridge length (left) and target shape (right).

7.3.3.2 Nearest distance between model points and laser data

The disadvantage of calculating the perpendicular distance between laser points and model faces is that it is not a fair quality check, as orientation of the model roof faces and the data are not independent at all. Especially for approach 1 which fits each individual roof face through a roof segment. Another quality measure is given by calculating the distance between 3D model points and the nearest laser point, as visualised in Figure 7-24. Although this is not an independent check either, it is of added value to the previous height check, because it holds information on how assumptions and constraints fit to the data. For example the reliability of the location of gutters can be determined.

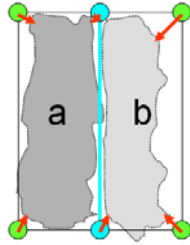


Figure 7-24 The distance between a model point and nearest laser point as a quality measure.

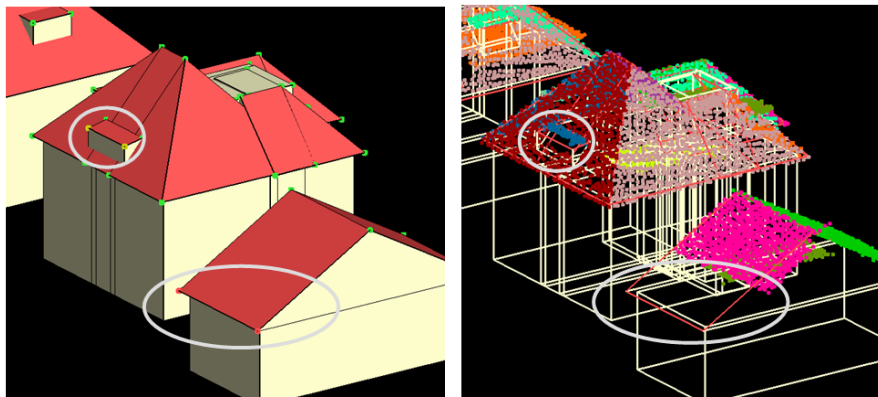


Figure 7-25 Nearest distance between 3D model points (reconstructed by approach 2) and laser points, coloured by residual value (<20 cm is green, <50 cm is yellow, > 50 cm is red). Right: Roof laser segments projected on wireframe.

As shown in Figure 7-25 there are two occasions where the nearest laser point is at a distance larger than 20 cm (yellow) or even 50 cm (red). These occasions can easily be selected automatically, based on parameters set by the user. One dormer face contains water, causing gaps in the laser segment, at the corners of the dormer face. This results in a reconstructed dormer that is too short. The other occasion can not be blamed on erroneous data, but at the wrong assumption that the gable would be symmetric. In Table 7-4 we have listed statistics of our four test areas from Enschede and Middelburg.

Table 7-4 Statistics on segments that do not exactly fit on reconstructed roofs.

Area ID	Ens 1	Ens 2	Ens 3	Mid 4
# buildings	61	191	226	250
# laser points in roof segments	176k	686k	598k	161k
# roof segments	460	1570	1515	1081

Approach 1				
# laser points with residual > 20 cm	3.1k (1.8%)	17.7k (2.6%)	11.9k (2.0%)	5.8k (3.6%)
# segments with more than 20 points with residual>20 cm	4	35	26	21
# affected buildings	3 (5%)	24 (13%)	18 (8%)	13 (5%)
# 3D object points with distance > 1 m to laser data	167	742	571	422
# segments not used	18	64	46	71
Approach 2				
# laser points with residual > 20 cm	8.5k (4.8%)	25.8k (3.8%)	18.8k (3.1%)	14.8k (9.1%)
# segments with more than 20 points with residual>20 cm	44	87	100	71
# affected buildings	21 (35%)	52 (27%)	62 (27%)	64 (25%)
# 3D object points with distance > 1 m to laser data	463	837	765	391
# segments not used	104	399	508	495

As expected the more data driven approach 1 better suits with the laser data. This is inherent to the algorithm, which fits a plane through segments for each roof face. For this approach, the number of affected buildings by segments that have a large number of laser points with large residuals varies between 5 and 13 percent of the total number of buildings. This variation can be explained by the variations of building parts between the four areas. For example assumptions on equal gutter heights and minimum segment size fit better in one situation than in others.

For the more model driven approach, we see that more deviations with the laser data occur. About 30 % of the buildings have laser segments with more than 20 points that have a distance larger than 20 cm to the roof plane. The number of segments that have not been used is higher in the model driven approach as a.o. small sheds attached to the

buildings have not been taken into account. This is because the integration of step edges is not implemented yet for the second approach. Therefore all segments that only have a connection through a step edge have not been reconstructed. Segments that only matched partly on a target are also included in this number of not used segments.

In order to support the interpretation of the models and the quality, delivering these quality measures is preferable been done both in numbers and in figures. In the following figures 7-26 to 7-29, the four screenshots represent the 3D model of the more model driven approach (upper left), the distance to nearest laser point (upper right), projected distance between laser points and roof faces (lower left) and the laser segments that were not used as they were part of an incomplete target match (lower right).

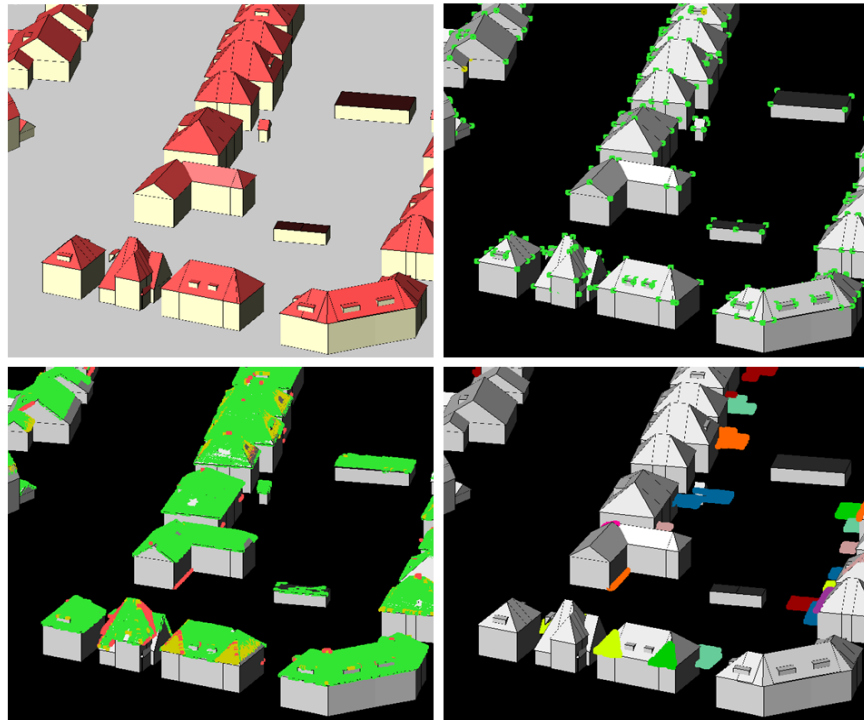


Figure 7-26 Area Zwik (Ens 1).

In Ens 1 relatively large and complex buildings are present. In general these buildings are modelled well (upper right) as the roof sizes are rather large. Exceptions are found at the hip roof at the front row where two roof extensions were not modelled, caused by missing data connections in between the triangular extension and the main hip roof shape. Many sheds behind buildings are not reconstructed (lower right) in the more model driven approach.

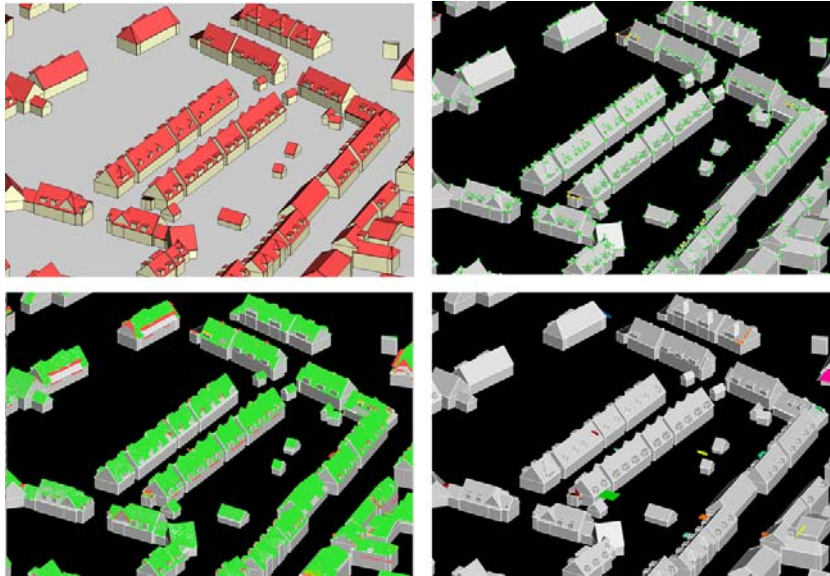


Figure 7-27 Area Pathmos (Ens 2).

The second area in Enschede (Figure 7-27) consists of relatively simple buildings with many roof extensions. The model driven approach is suitable for this area as data and buildings reasonably fit to target models.

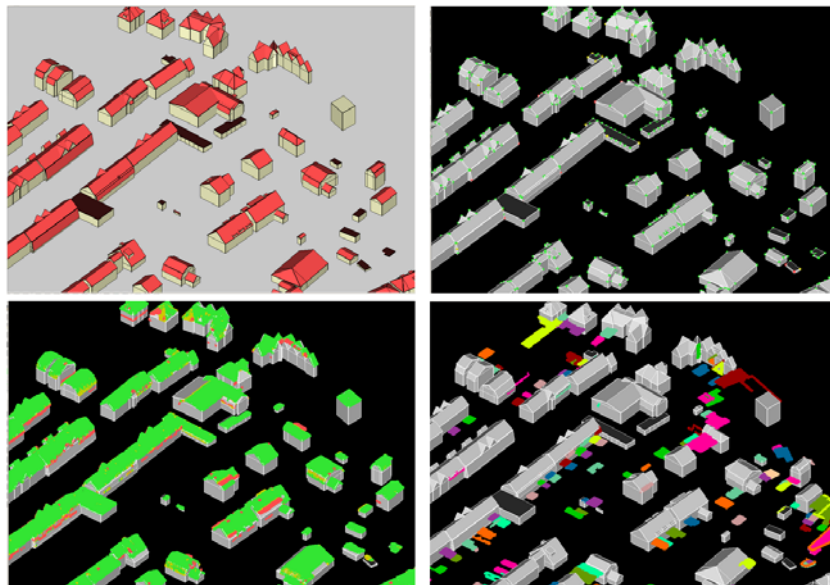


Figure 7-28 Area Indische buurt (Ens 3).

Area Ens 3 contains various building types (Figure 7-28). About a third of the gambrel roof types are not detected as such but as gable roof as one or both of the lower roof faces is not present in the laser segments. However, the main shape of the building is still covered by the gable roof part. Many segments on small sheds are left out from the reconstruction (lower right) in the second approach. This can partly be avoided by adding the first floor at the map polygon location, but then a solution has to be found for the merging of the model driven walls and these first floor walls.

For the Middelburg data set (Figure 7-29) the more model driven approach is visually more attractive than the more data driven approach (Figure 7-9) as the walls are placed underneath the reconstructed roofs. However, Table 7-4 shows that the quantitative precision of the model did not improve. In the Middelburg dataset nearly horizontal roofs are represented by exactly horizontal roofs, causing small deviations at object point locations (yellow dots on left side of upper right screenshot). The difficulty is to judge whether the discrepancy is acceptable or not. Remember that an important motivation to reconstruct buildings in a more model driven approach is that the data can be missing or erroneous. So, the inflexibility of model driven results will also cause differences between model and data. Hence, differences between data and reconstructed model are subject to considerations. Other information sources or probability values should be incorporated to judge the optimal solution for these situations.

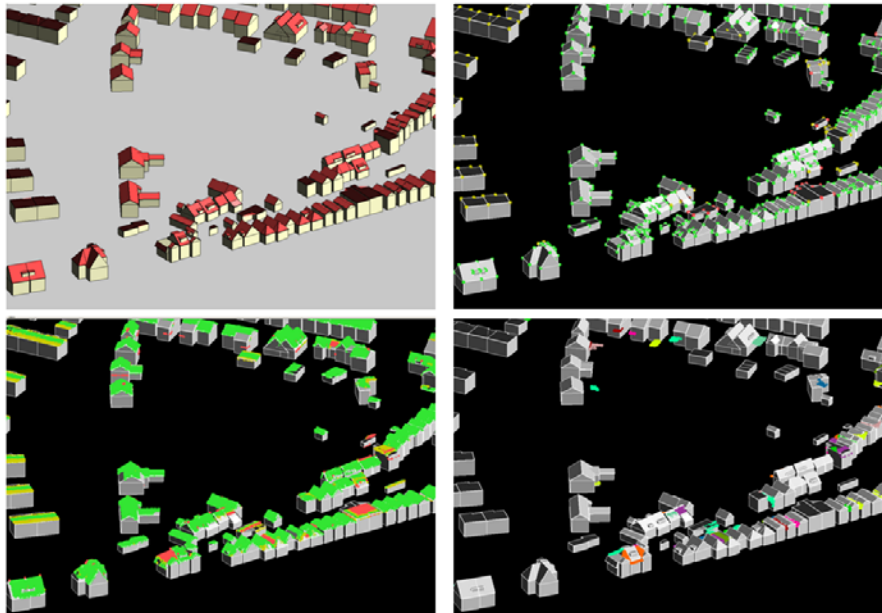


Figure 7-29 Mid 4 area from the Middelburg AHN-2 dataset.

7.3.4 Problematic situations

In this section, we describe the situations that can not be reconstructed by both our algorithms. The first problematic situation is when buildings contain complex height

jumps. In Figure 7-30 such a building is shown. Although the building does not seem to be that complex, the combination of flat roof parts and complicated height jumps makes this building problematic to reconstruct using our approach. The exact reason is that our algorithm cannot reliably locate all edges of flat roof segments, and therefore the locations of corner points inside the map polygon are not found. Solutions for these flat roof buildings can be found in subdividing the map polygon in many partitions, merging neighbouring partitions containing the same segment, and reconstruct flat roof parts individually, see Figure 7-30. The correct subpartition is the most challenging part. Next to a cell decomposition algorithm as proposed by Kada and McKinley (2009), the polygon has to be partitioned at height jump locations where the map partitioning did not give hints for roof edges. The latter algorithm should be an extension of the refinement step in (Vosselman and Dijkman, 2001) as it should include step edges that have multiple directions and therefore cannot be represented by a single straight line. The difficulty is to find a stable method for finding and processing the outlines of segments. The point density within these segments varies from zero or a few points per m^2 , due to occlusion and gaps due to water surfaces, to full point density, as can be seen in Figure 7-30.

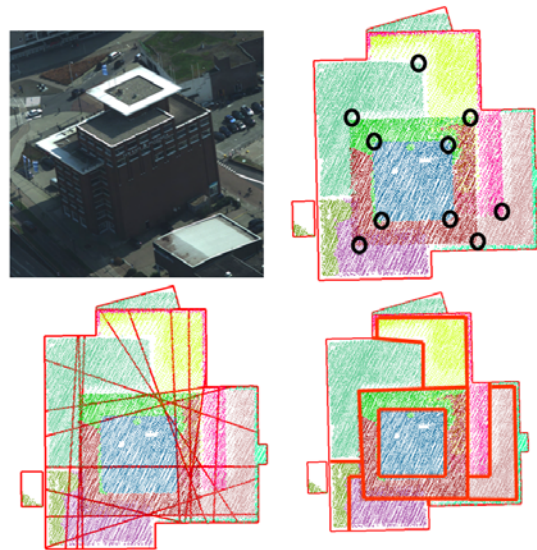


Figure 7-30 Upper left: oblique image of building with complex height jumps. Upper right: corner points (black circles) that should be detected reliably. Bottom left: automatic partition results. Bottom right: proposed subpartition. Partition manually determined.

In line with the above mentioned problem, we see that inner city buildings often show complex height jump situations within the map polygon. As long as the height jump has one direction, we can split the map line along that direction. However, in many cases the height jump contains multiple directions, which we do not detect, and therefore our reconstruction method fails for such locations. In Figure 7-31 our reconstructed inner city model of Enschede is shown, that highlights the problematic situations. More than

30% of the buildings contain segments that were not part of a complete target match. Using the segments that actually were matched complete, more than 35% of the buildings have segments with more than 20 points with large residuals to the reconstructed face. This means that the assumptions on the outline of these roof faces are not correct. Three land mark buildings are left out from the dataset. These are the city hall and two churches. This dataset was originally prepared for the production of a 3D city model of Enschede with multiple levels of detail. The land mark buildings are processed using a manual reconstruction technique mainly based on terrestrial data.

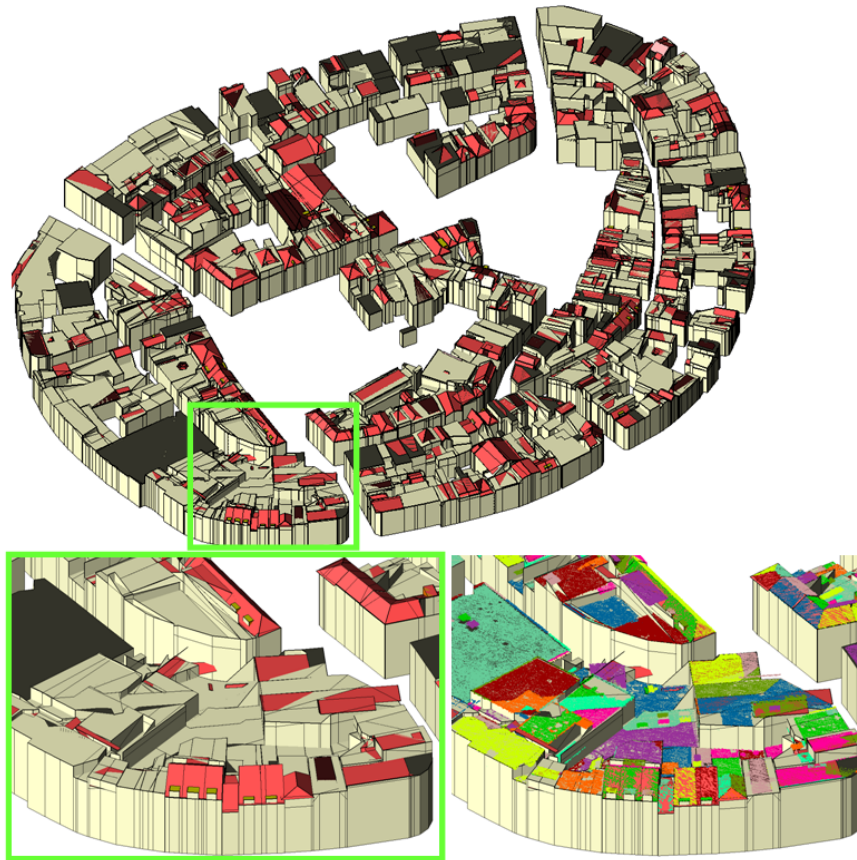


Figure 7-31 (Top) Automatic reconstruction results of innercity area, success rate about 50 %. (Bottom Left) Zoomed in. (Bottom right) Segmented laser data superimposed on the model.

In Figure 7-32 residuals of laser points are visualised for the inner city area. Although the general impression might be that the quality is reasonable due to the majority of low residual values, one has to keep in mind that about 30% of the buildings contain at least one segment that has not been used. In addition to that, 35% of the buildings have large segments with high residual values.



Figure 7-32 Residual values between laser data and reconstructed roof faces.

On the left in Figure 7-33 laser segments are shown that are left out from the reconstruction, superimposed on the model reconstructed from the accepted laser segments. This object is definitively a too big challenge to reconstruct automatically, at the moment. Underlying reasons are that:

- the segmentation is not complete due to the steep roof faces;
- the segmentation is not correct as the curvature in the roof face either causes over- or under-segmentation, depending on the desired model structure;
- relations are missing between two roof faces due to the upper two reasons;
- even if the segmentation is perfect, it would not match with a target graph as there is no six sided “tipi” shaped building target in our database.

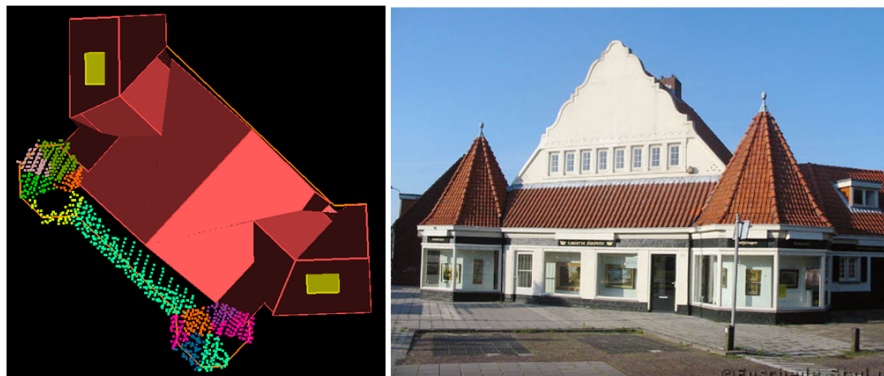


Figure 7-33 (Left) Reconstructed model and segments left out from the automated algorithm. Photo explains the challenging situation: roof faces are

slightly curved and steep, roof shape is irregular and not in target database.

7.3.5 Performance in time

As the focus of our algorithm was on the methodological level, rather than on the computational level, improvements can be made to speed up the algorithm. We listed our computing time per process in Table 7-5. As the processing time depends on both the number of buildings and the number of laser points, we added the size of the input data for each of the four test datasets. The numbers in the table are best interpreted by relatively comparing the computing time, rather than looking at absolute values.

Table 7-5 Performance, expressed in computing time per process.

	Ens 1	Ens 2	Ens 3	Mid 4
# laser points	2.49 million	5.71 million	2.78 million	1.92 million
# buildings	61	191	226	250
# roof segments	460	1570	1515	1081
# p/m ²	20	20	20	8
	Time in minutes			
Segmentation	2	10	2	1
Assign laser segments to map polygons, DTM height to map polygons	20	115	69	29
Intersect roof segments	<1	12	4	<1
Target based matching	<1	2	2	<1
Data driven method, including quality measures	4	68	17	2
Model driven method, including quality measures	<1	3	3	<1
Total (minutes)	29	210	97	35
Average per building (sec)	29 sec	66 sec	26 sec	9 sec

Improvements can be made to speed up the total time of processing. For example, when assigning the laser data to map polygons, we do not make use of any indexing algorithm that speed up locating areas of interest. This is especially true for dataset Ens 2, where there are many segments on relatively many buildings. Including a spatial indexing function would reduce the number of potential buildings where the laser point potentially falls inside. The data driven method contains several loops over the buildings and its features, to group and merge intersection lines, to intersect with the map polygon and to integrate the step edges after the roof reconstruction. This reflects on the large computation time on dataset Ens 2 with many features and buildings. The more model driven approach is faster but it has to be noted that both the grouping of target models and integration of step edges is not implemented yet.

Our algorithms have been built including several optional processing steps and threshold values, for example how to use the information from map data to reconstruct building walls. These parameter values depend on the user requirements and the data properties. The problem with lists as given in Table 7-5 is that it does not indicate the time that the user is analysing the (intermediate) results and the quality of the models. Even more important than the length of that time component, is the fact that the user actually should spend time on translating user requirements into processing parameters.

7.4 Potential for nation wide 3D building database

Now that we have seen the results and limitations on our test dataset, we can discuss what is the potential use of our algorithms in case of upgrading 2D building maps to 3D building models. It is expected that in the near future, nation wide height models will become available with more than 5 points per m². For example, in the Netherlands the AHN-2 is currently built with point densities of more than 8 points per m².

We have seen that our algorithm is capable of reconstructing complex buildings, as long as:

- the data is complete, and
- the complex building topologically can be described by a combination of target graphs.

Furthermore, our algorithm can detect situations automatically that need more attention from the user. The thresholds that describe which situations are shown to the user can be set up by the user at forehand.

Our algorithm is not able to reconstruct complex flat roof structures, which might be frequently present in industrial areas and inner city areas. This is because we cannot reliably determine multiple directions in height jumps between two flat roof faces. In these cases, the best solution is to subdivide the map outline in an algorithm that is able to split and merge the map outline, even at locations where there is no hint from the outline itself.

Estimations based on datasets of various municipalities (Middelburg, Enschede and Rotterdam) are that the number of building polygons (including industrial buildings) is about a third of the number of inhabitants. For the Netherlands (16.5 million inhabitants) we estimate that there are about 5.5 million buildings to be reconstructed. If we take the rough estimation that 20% of the buildings cannot completely be reconstructed due to an incomplete match result and that another 10% of the buildings contain complex height jumps, about 30% of the buildings are affected by errors. This means over 1.5 million buildings cannot be reconstructed automatically, using our reconstruction approach. We estimate that when using a semi-automatic reconstruction approach, one person can process about 500 buildings per day. Using this value we can calculate that it would take 3000 days for one person to process the 1.5 million buildings. As this is still a huge amount of work (15 man years when working 200 days a year), the necessity of further research is obvious in order to reduce the number of

buildings that has to be processed semi-automatically. Proposals for further research are explained in chapter 8.2.

7.5 Summary

We have shown results of 3D reconstructed models, including several quality checks. These quality measures describe the completeness of the match results plus the correctness of assumptions to the roof outline.

About 20% of the buildings are affected by segments that did not completely match with the target graphs. In a few of these cases, this was correct because the segment was not representing a roof face. However, in about 40% of these cases, a neighbouring segment that would complete a target match was missing. Adapting processing parameters, such as minimum segment size, might improve the result but it may also disturb other topological relations.

Setting the parameters is therefore an important task for the operator. Specially, parameters that define the segmentation algorithm are crucial as the segment is the key data feature in our algorithm.

In order to improve our matching algorithm, the likelihood of relations between segments could be included in the attribute list of edges in the roof topology graph. At the moment only information on the geometric appearance of the intersection line is given as attribute value to the corresponding graph edge. Future work includes defining likelihood functions for graph edges and analysing the effect of likelihood attributes.

Part IV: Conclusions and recommendations

8 Conclusions and recommendations

8.1 Conclusions

We have presented methods for automated reconstruction of 3D roads and 3D buildings. Although both methods are designed on using map data and airborne laser scanning data, the essence in the research activities on roads differs basically from those on buildings. For roads the focus has been on reconstructing the edges' height of the objects, whereas for buildings the challenge is to reconstruct the 3D shape inside the building edges. That is why the conclusions are split into general 3D topographic object reconstruction (8.1.1) and specific conclusions for 3D road reconstruction (8.1.2) and building reconstruction (8.1.3).

8.1.1 3D Topographic object reconstruction

Reconstructing topographic objects needs a careful tuning between the real object properties, the objects' appearance in the data and the properties of the modelled object.

We have shown the use of general object properties in each of the reconstruction algorithms, such as:

- Highways are smooth surfaces, in both planimetry and height.
- Buildings consist of a combination of planar roof faces.

Both reconstruction algorithms need a segmentation step in an early stage of processing. For road reconstruction the main reason is to remove points on small objects. For the 3D reconstruction itself, the shape of the segment does not have an influence as a nearby selection of points is taken to fit a plane through. For building reconstruction the segmentation results have a larger impact on the final results as our assumption is that each segment represents one roof face. This means that the shape and neighbourhood relations of the segment have a direct influence on the final results. Careful tuning of the segmentation parameters is therefore essential for building reconstruction.

The use of maps in object reconstruction has proven helpful to select relevant laser data, to assign land use information to laser data and to determine planimetric positions of specific 3D objects, such as roads and flat roof types.

8.1.2 3D Road reconstruction

Automated 3D road reconstruction is feasible. We have presented an approach that can assign laser data on various height levels to the correct height level of interchanges. A combined map-growing and laser-growing algorithm has been developed to correctly assign laser points to 2D map polygons. We showed that if we add knowledge about the direction of roads (to connect small road parts) and knowledge about the situation of the road in the height dimension (to select laser data), we are able to correctly assign laser data to map data. Polygons that are connected in 3D are merged. Accompanying laser points are assigned to that polygon. By performing this step correctly, we are able to connect road parts without laser points to other road parts which do contain laser points. Occluded road polygons are created automatically when two roads cross in 3D. The correct assignment of laser points to map polygons is proven to be the crucial part in 3D road reconstruction. As soon as the assignment has been done, the task is to

calculate the height at the points of the road boundaries. This has been done by selecting nearby laser points that have been assigned to that polygon, followed by a plane fitting algorithm to transfer the height from the laser points to the boundary. For road reconstruction we assumed that the geometric modelling was basically limited to triangulating the 3D boundary of road polygons. These 3D boundaries are represented by 3D map points and their topological relations. After the fusion of laser and map data we have shown that the predicted quality of the final model can be determined. Precision of the map points have been calculated by error propagation of laser point noise and the configuration of the laser points used for plane fitting. Influences of model uncertainty have been taken into account. Average predicted standard deviation of map point heights is about 10 cm.

Our method combines a 2D topographic data set with an airborne laser scanner dataset (2.5-3D). Even at locations where locally no height information is available, our method can reconstruct 3D roads with a height precision in the order of 10-15 cm. Conditions are that the gap should not exceed more than about 100 meter and the road follows a (nearly) planar pattern. Input data sets used in this project are parts of national databases. Now that we can predict quality of 3D roads, we can predict the height quality for all roads in the national database without actually having to reconstruct them, and without testing them with reference data.

At this stage, the user is able to decide if he can use the two datasets for reconstructing roads that meet his requirements. We have shown that the predicted quality was a realistic measure when we compared our 3D model with reference data.

Our algorithm assumes that the laser data and map data are registered correctly or at least in the order of the map precision. Parameters have to be set that represent the size of objects that need to be filtered out, the expected maximum curvature of roads and maximum slope variations. If these are set correctly, our algorithm runs automatically, without the need of editing. If a national 3D road model is made, our algorithm is capable of reconstructing situations that fulfil the abovementioned conditions. For a complete automatic reconstruction of a nationwide database, it is necessary that the parameter values are set correctly for each of the situations. This latter activity is subject to further research in order to automatically determine the correct parameter values for road reconstruction.

8.1.3 3D Building reconstruction

Fully automated 3D building reconstruction remains a challenging research topic. The handling of the complexity of roof structures and how they appear in the data is not completely solved in this thesis.

When reconstructing the topology of a building roof, laser data provides information on what could be roof part (in terms of segments) and how these roof parts connect (in terms of intersection lines and height jumps). We have presented a target based graph matching algorithm that relates topology of common building models with the topology found in the laser data.

The quality of the input data and their processing steps still has a significant influence on the quality of the graph matching. Errors in the segmentation step, e.g. caused by

highly varying point density, disturb topological relations between segments. As our matching algorithm is based on these topological relations, errors in these relations have a direct consequence for the matching results. The positive aspect is that our algorithm detects problematic situations for automated building reconstructions, although we did not present an automated solution for these situations. Problematic areas are found in cases where both laser data and model information are weak. This occurs at complex roof structures where data is missing or erroneous and the roof shape is not in the data base. About 20% of the buildings are affected by segments that did not completely match with the target graphs. In a few of these cases, this was correct because the segment was not representing a roof face. However, in about 40% of the cases, a neighbouring segment that would complete a target match was missing.

The contribution of our building reconstruction algorithm is that we have presented an approach that relates data features with model information. This relation enables transferring general object knowledge to the data. This knowledge can be in terms of deciding what the optimal height for a gutter is, or what other constraints affect the data. The advantage of this relation is that the actual reconstruction can be either more data or more model driven. The choice of those two depends on the application, data quality and scene properties. The orientation of roof faces reconstructed by the more data driven approach better fits to the laser data, due to the implementation that each of the roof faces is on a plane fitted through the corresponding roof segment. The interior edges of the roof are based on intersection lines between accurately defined planes. The outer edges of roof faces, e.g. gutters and eaves, are reconstructed by applying constraints to the direction of those roof edges: gutters are made horizontal, passing through the height of the lowest laser point of the roof segment and eaves are created perpendicular to the connected ridge point or their direction is adapted to the direction of the nearby line segment of the map polygon. The reconstruction of walls is based on the intersections of roof faces or step edges with the map polygon. The success of this data driven approach depends on how realistic these assumptions actually are. These assumptions get more realistic for denser laser data sets and residential areas with buildings containing overhanging roof parts. Besides this, it is expected that the map polygon accurately represent the location of the building walls. As the reconstructed roofs and the walls are mainly based on two different data sources the registration between the two data sources should be correct.

The more model driven approach is less dependent on the map data as the walls of the reconstructed models are constructed, based on the reconstructed roofs. By definition the roofs connect to (with or without overhang) the walls. This means that the more model driven reconstructed buildings are not exactly at the map polygon location, but in return they deliver a topological closed model. For visualisation purposes this approach is attractive as it does not contain strange shaped results. Interior edges of the more model driven approach do not exactly coincide with the intersection lines, although the object points defined by three planes are forced to have the planimetric location of the intersection point of the three planes.

Target based (graph) matching can be applied to other topographic objects as well, as it just can be seen as a pattern recognition tool. If part of a predefined pattern can be seen

in the data, it can be detected by our matching algorithm. Our targets are defined in a simple nodes and edges structure, accompanied by labels for each of the edges.

8.2 Recommendations

For both road and building reconstruction, automated parameter value determination is subject for future research. When extending the area size to be processed, e.g. when reconstructing 3D models at a national level, it is important that the processing parameters are valid for the local situation. Default parameter values are supposed to be valid in most of the cases, but in specific situations changes have to be made. These changes depend on either specific situations in the area or the configurations in the data. It is of great interest to analyse the possibilities to automatically determine the correct parameter values. For example, if part of the input laser data happens to be noisy, the segmentation parameters should be changed in order to get better segmentation results.

Our roof detection approach is based on a labelled graph matching algorithm. The graph holds information on the existence of roof faces and their possible intersections. The existence of a roof and roof intersection is represented by a node and an edge in the graph; the label indicates the geometry of the intersection. The label can be determined reliably, but the reliability of the existence of a graph edge could be further examined. Our recommendation is to calculate and integrate probability values for these graph edges. It would mean a different storage of the roof graph, but also a change in acceptance of matching results. This acceptance should be based on probability values that are stored in the target graphs, for each of the edges individually. To start collecting statistical values for the existence of roof faces and edges, it is recommended to store information of 3D buildings that are being built.

The algorithm can automatically reconstruct buildings using data features that topologically matched with target models. Some of the features, e.g. segments and intersection lines, have not been used in our algorithm. Reasons why they were excluded have been examined and described. Results of the target based matching could be analysed more thoroughly. Incomplete matching results are a huge information source for solving problematic situations, as they directly highlight discrepancies between data and target models. If situations are near threshold values, e.g. segments just too small to be recognised as roof segment, our algorithm is not capable of adapting the processing parameters. Therefore, a broader scene understanding should be integrated with our algorithm, which can decide on why in certain cases the threshold values should be increased or decreased. This broader scene understanding is recommended for further research. This broader interpretation should be able to detect the optimal situation automatically. To give an example, integrating information of the building construction style or roof material would be of help to predict the shape of buildings or to predict the absence of data. Using that information, the program can decide how to proceed.

Future research is needed to reconstruct complex height jumps. The challenge is to reliably detect corner points of flat roof faces, located inside the map polygon. Polygons have to be partitioned at height jump locations where the map polygon may not give hints for roof edges.

Conclusions and recommendations

As mentioned in our chapter on the use of 3D topography, user requirements iterate after using data. In the next few years 3D models will be used more and more. It is of interest to monitor the quality and the requirements of 3D models, during the same period. This information can be used to adapt the reconstruction parameters.

List of publications

- Oude Elberink, S. and Vosselman, G., 2006a. 3D Modelling of Topographic Objects by Fusing 2D Maps and Lidar Data, International Archives of Photogrammetry, Remote Sensing and Spatial Information Sciences, XXXVI part 4, Goa, India, on CD-ROM.
- Oude Elberink, S. and Vosselman, G., 2006b. Adding the Third Dimension to a Topographic Database Using Airborne Laser Scanner Data. International Archives of Photogrammetry, Remote Sensing and Spatial Information Sciences, XXXVI part 3, Bonn, Germany, pp. 92-97.
- Oude Elberink, S. and Vosselman, G., 2007. Quality analysis of 3D road reconstruction, Laserscanning 2007. International Archives of Photogrammetry, Remote Sensing and Spatial Information Sciences, XXXVI, part 3/W52, Espoo, Finland, pp. 305-310.
- Oude Elberink, S. and Vosselman, G., 2008. Quality analysis of 3D road reconstruction. The Photogrammetric Journal of Finland, Vol. 21 (No. 1): 51-60.
- Oude Elberink, S., 2008. Re - using laser scanner data in applications for 3D topography. In: Advances in 3D geoinformation systems / ed. by P. van Oosterom, S. Zlatanova, F. Penninga and E. Fendel. Berlin: Springer. pp. 87-99.
- Oude Elberink, S., 2008. Problems in Automated Building Reconstruction based on Dense Airborne Laser Scanning Data. International Archives of Photogrammetry, Remote Sensing and Spatial Information Sciences, XXXVII, part 3A: pp. 93-98.
- Oude Elberink, S., 2009. Target Graph Matching for Building Reconstruction. International Archives of Photogrammetry, Remote Sensing and Spatial Information Sciences, XXXVIII, 3 / W8: pp. 49-54.
- Oude Elberink, S. and Vosselman, G., 2009a. 3D information extraction from laser point clouds covering complex road junctions. The Photogrammetric Record, 24(125): 23-36.
- Oude Elberink, S. and Vosselman, G., 2009b. Building Reconstruction by Target Based Graph Matching on Incomplete Laser Data: Analysis and Limitations. Sensors, 9(8): 6101-6118.

Bibliography

- Abo Akel, N., K. Kreimeike, S. Filin, M. Sester and Doytsher, Y., 2005. Dense DTM Generalization Aided by Roads Extracted from LiDAR Data. In: *International Archives of Photogrammetry, Remote Sensing and Spatial Information Sciences*, XXXVI, 3/W19: pp. 54-59.
- Alharthy, A. and Bethel, J., 2002. Heuristic Filtering and 3D Feature Extraction from Lidar Data. In: *International Archives of Photogrammetry, Remote Sensing and Spatial Information Sciences*, XXXIV, part 3a: pp. 23-28.
- Baarda, W., 1968. A Testing Procedure for Use in Geodetic Networks. New Series 2. Netherlands Geodetic Commission, Delft, the Netherlands.
- Bengoetxea, E., 2003. Inexact Graph Matching Using Estimation of Distribution Algorithms. PhD Thesis, Ecole Nationale Supérieure des Télécommunications, Paris, France.
- Brenner, C., 2000. Towards fully automatic generation of city models. In: *International Archives of Photogrammetry, Remote Sensing and Spatial Information Sciences*, XXXIII, part B3: pp. 85-92.
- Brenner, C., 2004. Modelling 3D Objects Using Weak CSG Primitives. In: *International Archives of Photogrammetry, Remote Sensing and Spatial Information Sciences*, Vol. XXXV, part B3: pp. 1085-1090.
- Bretar, F., M. Chesnier, M. Roux and Pierrot-Deseilligny, M., 2004. Terrain Modeling and Airborne Laser Data Classification Using Multiple Pass Filtering. In: *International Archives of Photogrammetry, Remote Sensing and Spatial Information Sciences*, XXXV, part B3: pp. 314-319.
- Clode, S., Kootsookos, P. and Rottensteiner, F., 2004. The Automatic Extraction of Roads from Lidar Data. In: *International Archives of Photogrammetry, Remote Sensing and Spatial Information Sciences*, Vol. XXXV, Part B3: pp. 231-236.
- Crombaghs, M., Oude Elberink, S., Brugelmann, R. and de Min, E., 2002. Assessing height precision of laser altimetry DEMs. In: *International Archives of Photogrammetry, Remote Sensing and Spatial Information Sciences*, XXXIV, part 3a: pp. 85-90.
- Dharmapriya, G., 2009. Classification of gaps in laser scanner data. MSc Thesis, International Institute for Geo-Information Science and Earth Observation, Enschede, 49 pp.
- Dorninger, P. and Pfeifer, N., 2008. A Comprehensive Automated 3D Approach for Building Extraction, Reconstruction, and Regularization from Airborne Laser Scanning Point Clouds. *Sensors*, 8(11): 7323-7343.
- Durupt, M. and Taillandier, F., 2006. Automatic building reconstruction from a digital elevation nodel and cadastral data: an operational approach. In: *International Archives of Photogrammetry, Remote Sensing and Spatial Information Sciences*, XXXVI, part 3: pp. 142-147.
- Elaksher, A. and Bethel, J., 2002. Reconstructing 3D Buildings From Lidar Data. In: *International Archives of Photogrammetry, Remote Sensing and Spatial Information Sciences*, XXXIV, part 3a: pp. 102-107.
- Haala, N. and Brenner, C., 1997. Generation of 3D city models from airborne laser scanning data, EARSEL Workshop on LIDAR remote sensing of land and sea, Tallinn, Estonia, pp. on CD-rom.

- Haala, N., C. Brenner and Anders, K.-H., 1998. 3D Urban GIS From Laser Altimeter and 2D Map Data. In: *International Archives of Photogrammetry, Remote Sensing and Spatial Information Sciences*, 32, part 3: pp. 339-346.
- Hatger, C., 2005. On the use of Airborne Laser Scanning Data to Verify and Enrich Road Network Features. In: *International Archives of Photogrammetry, Remote Sensing and Spatial Information Sciences*, XXXVI, 3 /W19: pp. 138-143.
- Hatger, C. and Brenner, C., 2003. Extraction of Road Geometry Parameters From Laser Scanning and Existing Databases. In: *International Archives of Photogrammetry, Remote Sensing and Spatial Information Sciences*, XXXIV, 3/W13: pp. on CD-ROM.
- Hofmann, A., 2004. Analysis of TIN-Structure Parameter Spaces in Airborne Laser Scanner Data for 3-D Building Model Generation. In: *International Archives of Photogrammetry, Remote Sensing and Spatial Information Sciences*, XXXV, part B3: pp. 302-307.
- Hofmann, A., Maas, H.-G. and Streilein, A., 2002. Knowledge-Based Building Detection Based on Laser Scanner Data and Topographic Map Information. In: *International Archives of Photogrammetry, Remote Sensing and Spatial Information Sciences*, XXXIV, part 3A: pp. 169-175.
- Hu, X., C. Tao and Hu, Y., 2004. Automatic Road Extraction from Dense Urban Area by Integrated Processing of High Resolution Imagery and Lidar Data. In: *International Archives of Photogrammetry, Remote Sensing and Spatial Information Sciences*, Vol. XXXV, part B3: pp. on CD-ROM.
- Jochem, A., Hoefle, B., Rutzinger, M. and Pfeifer, N., 2009. Automatic Roof Plane Detection and Analysis in Airborne Lidar Point Clouds for Solar Potential Assessment. *Sensors*, 9(7): 5241-5262.
- Kada, M. and McKinley, L., 2009. 3D Building Reconstruction From Lidar Based on a Cell Decomposition Approach. In: *International Archives of Photogrammetry, Remote Sensing and Spatial Information Sciences*, XXXVIII, 3 / W4: pp. 47-52.
- Koch, A., 2004. An Approach for the Semantically Correct Integration of a DTM and 2D GIS Vector Data. In: *International Archives of Photogrammetry, Remote Sensing and Spatial Information Sciences*, 35, part B4: pp. 523-528.
- Kolbe, T., Groeger, G. and Pluemer, L., 2005. CityGML – Interoperable Access to 3D City Models. In: P.v. Oosterom, S. Zlatanova and E. Fendel (Editors), *Int. Symposium on Geo-Information for Disaster Management*. Springer Verlag, Delft, The Netherlands.
- Maas, H.-G. and Vosselman, G., 1999. Two Algorithms for Extracting Building Models from Raw Laser Altimetry Data. *ISPRS Journal of Photogrammetry and Remote Sensing*, vol. 54(no. 2-3): 153-163.
- Matikainen, L., J. Hyypä and Hyypä, H., 2003. Automatic Detection of Buildings from Laser Scanner Data for Map Updating. In: *ISPRS*, vol. 34, part 3/W13: pp. on CD-ROM.
- Mayer, H., Hinz, S., Bacher, U. and Baltsavias, E., 2006. A Test of Automatic Road Extraction Approaches. In: *International Archives for Photogrammetry, Remote Sensing and Spatial Information Sciences*, XXXVI, part 3: pp. 209-214.

- Mikhail, E.M., Bethel, J.S. and McGlone, J.C., 2001. Introduction to modern photogrammetry. Wiley, New York, USA.
- Milde, J., Zhang, Y., Brenner, C., Pluemer, L. and Sester, M., 2008. Building Reconstruction using Structural Description based on a Formal Grammar. In: *International Archives of Photogrammetry, Remote Sensing and Spatial Information Sciences*, XXXVII, part 3B: pp. 227-232.
- Morgan, M. and Habib, A., 2002. Interpolation of Lidar Data and Automatic Building Extraction, ASPRS/ACSM Conference. ASPRS, Washington, D.C., USA, pp. on CD-ROM.
- Oude Elberink, S., 2008. Problems in Automated Building Reconstruction based on Dense Airborne Laser Scanning Data. In: *International Archives of Photogrammetry, Remote Sensing and Spatial Information Sciences*, XXXVII, part 3A: pp. 93-98.
- Oude Elberink, S. and Maas, H.-G., 2000. The use of Anisotropic Height Texture Measures for the Segmentation of Airborne Laser Scanner Data. In: *International Archives of Photogrammetry, Remote Sensing and Spatial Information Sciences*, XXXIII, Part 3B: pp. 678-684.
- Pfeifer, N., Gorte, B. and Oude Elberink, S., 2004. Influences of Vegetation on Laser Altimetry Analysis and Correction Approaches. In: *International Archives of Photogrammetry, Remote Sensing and Spatial Information Sciences*, 36, 8-W2: pp. 283-287.
- Pu, S., 2010. Knowledge based building facade reconstruction from laser point clouds and images (in print). PhD Thesis, International Institute for Geo-Information Science and Earth Observation, Twente University of Technology, Enschede, The Netherlands.
- Rottensteiner, F., 2006. Consistent Estimation of Building Parameters Considering Geometric Regularities by Soft Constraints. In: *International Archives of Photogrammetry, Remote Sensing and Spatial Information Sciences*, 36, part 3: pp. 13-18.
- Rottensteiner, F. and Briese, C., 2002. A New Method for Building Extraction in Urban Areas from High-Resolution Lidar Data. In: *International Archives of Photogrammetry, Remote Sensing and Spatial Information Sciences*, XXXIV, part 3A: pp. 295-301.
- Rottensteiner, F. and Briese, C., 2003. Automatic Generation of Building Models from Lidar Data and the Integration of Aerial Images. In: *International Archives of Photogrammetry, Remote Sensing and Spatial Information Sciences*, XXXIV, part 3/W13: pp. on CD-ROM.
- Rottensteiner, F., J. Trinder, S. Clode and Kubik, K., 2005. Automated Delineation of Roof Planes from Lidar Data. In: *International Archives of Photogrammetry, Remote Sensing and Spatial Information Sciences*, 36, 3/W19: pp. 221-226.
- Rutzinger, M., Oude Elberink, S., Pu, S. and Vosselman, G., 2009. Automatic Extraction of Vertical Walls from Mobile and Airborne Laser Scanning Data. In: *International Archives of Photogrammetry, Remote Sensing and Spatial Information Sciences*, XXXVIII, part 3a: pp. accepted for publication.
- Sampath, A. and Shan, J., 2004. Urban Modeling Based on Segmentation and Regularization of Airborne Lidar Point Clouds. In: *International Archives of Photogrammetry, Remote Sensing and Spatial Information Sciences*, Vol. XXXV, part 3B: pp. 937-941.

- Simonse, M., Verbree, E., Asperen, P.v. and Vegt, J.-W.v.d., 2000. Construction of the 3D TOP10 - Integration of Countrywide Planimetric Data and Laseraltimetry Data to Support 3D-Visualisation and Analysis. In: *International Archives of Photogrammetry, Remote Sensing and Spatial Information Sciences*, XXXIII: pp. 995-2002.
- Sithole, G. and Vosselman, G., 2004. Experimental Comparison of Filter Algorithms for Bare Earth Extraction From Airborne Laser Scanning Point Clouds. *ISPRS Journal of Photogrammetry and Remote Sensing*, 59((1-2)): 85-101.
- Sithole, G. and Vosselman, G., 2005. Filtering of airborne laser scanner data based on segmented point clouds, Workshop Laserscanning 2005. *International Archives of Photogrammetry, Remote Sensing and Spatial Information Sciences*, Enschede, the Netherlands.
- Suveg, I. and Vosselman, G., 2004. Reconstruction of 3D building models from aerial images and maps. *ISPRS Journal of Photogrammetry and Remote Sensing*, 58(3-4): 202-224.
- Taillandier, F. and Deriche, R., 2004. Automatic Building Reconstruction from Aerial Images: a Generic Bayesian Framework, *ISPRS Congress. International Archives of Photogrammetry, Remote Sensing and Spatial Information Sciences*, Istanbul, Turkey.
- Teunissen, P., 1991. An integrity and quality control procedure for use in multi sensor integration., ION GPS-90. *Proceedings of ION GPS-90*, Colorado Springs, USA, pp. 513-522.
- Tóvári, D. and Pfeifer, N., 2005. Segmentation based robust interpolation - a new approach to laser data filtering, *Laserscanning 2005. International Archives of Photogrammetry, Remote Sensing and Spatial Information Sciences*, Enschede, the Netherlands.
- Verma, V., Kumar, R. and Hsu, S., 2006. 3D Building Detection and Modeling from Aerial LIDAR Data, *IEEE Computer Society Conference on Computer Vision and Pattern Recognition (CVPR'06)*. IEEE Computer Society, Washington, DC, USA, pp. 2213-2220.
- Voegtle, T., Steinle, E. and Tovari, D., 2005. Airborne laserscanning data for determination of suitable areas for photovoltaics. *International Archives of Photogrammetry, Remote Sensing and Spatial Information Sciences*, Enschede, The Netherlands, pp. 215-220.
- Vosselman, G., 1999. Building Reconstruction Using Planar Faces in Very High Density Height Data. In: *International Archives of Photogrammetry, Remote Sensing and Spatial Information Sciences*, XXXII, part 3/2W5: pp. 87-92.
- Vosselman, G., 2003. 3D Reconstruction of Roads and Trees for City Modelling. In: *International Archives of Photogrammetry, Remote Sensing and Spatial Information Sciences*, XXXIV, part 3/W13: pp. 231-236.
- Vosselman, G., 2008. Analysis of Planimetric Accuracy of Airborne Laser Scanning Surveys. In: *International Archives of Photogrammetry, Remote Sensing and Spatial Information Sciences*, XXXVII, part 3A: pp. 99-104.
- Vosselman, G., B. Gorte, G. Sithole and Rabbani, T., 2004. Recognising Structure in Laser Scanner Point Clouds. In: *International Archives of Photogrammetry, Remote Sensing and Spatial Information Sciences*, XXXVI, part 8 / W2: pp. 33-38.

- Vosselman, G. and Dijkman, S., 2001. 3D Building Model Reconstruction from Point Clouds and Ground Plans. In: *International Archives of Photogrammetry, Remote Sensing and Spatial Information Sciences*, 34, 3/W4: pp. 37-43.
- Vosselman, G., Kessels, P. and Gorte, B., 2005. The utilisation of airborne laser scanning for mapping. *International Journal of Applied Earth Observation and Geoinformation*, 6(3-4): 177-186.
- Vosselman, G. and Maas, H.-G., 2001. Adjustment and filtering of raw laser altimetry data. In: *Proceedings of OEEPE Workshop on Airborne Laserscanning and Interferometric SAR for Detailed Digital Terrain Models*, OEEPE Publication No. 40: pp. on CD-ROM: 11p.
- Wang, O., Lodha, S. and Helmbold, D., 2006. A Bayesian Approach to Building Footprint Extraction from Aerial LIDAR Data, Third International Symposium on 3D Data Processing Visualization Transmission Chapel Hill, USA, pp. 192-199.
- Zhang, C., 2003. Towards an operational system for automated updating of road databases by integration of imagery and geodata *ISPRS Journal of Photogrammetry and Remote Sensing*, 58(3-4): 166-186.

Summary

Introduction and research goal

Our research covers the automation in acquiring three dimensional (3D) topographic objects. The research tasks focus on two specific objects: roads and buildings. These objects are of high importance in 3D city models as they are two major topographic classes in the urban environment.

Our activities are located between:

1. how topographic objects exist in reality;
2. how they are captured in the data, and
3. how they appear in a modelled/virtual world.

To accomplish an automated approach, existing 2D topographic maps are upgraded to 3D using airborne laser scanner data. 3D topography also includes multiple heights or even multiple objects on top of each other at a certain location.

The essence in the research activities on roads differs basically from those on buildings. For roads the focus is on reconstructing the edges' height of the objects, whereas for buildings the challenge is to reconstruct the 3D polyhedral roof shape inside the building edges.

3D Road reconstruction

When examining 3D road objects, we can expect that multiple road objects cross at a certain location. An automated method for 3D modelling of complex highway interchanges is presented. Laser data and 2D topographic map data are combined in an innovative 3D reconstruction procedure. Complex situations demand for knowledge to guide the automatic reconstruction. This knowledge is used in the fusion procedure to constrain the topological and geometrical properties of the reconstructed 3D model. Laser data has been segmented and filtered before it is fused with map data. In the surface-growing algorithm combining map and laser points, the laser data is assigned to the corresponding road element. Elevations of map points are determined by least squares plane fitting through a selection of neighbouring laser points. Although results are shown using two specific data sources, the algorithm is designed to be capable of dealing with any polygon-based topographic map and any aerial laser scanner data set.

Quality analysis is essential for developing a reliable reconstruction process and for a proper use of 3D data. The quality of 3D reconstructed roads strongly depends on accuracy and type of input data and the reconstruction processing steps. We predict the precision of reconstructed map elevations by propagating errors in the input data through the processing steps. Besides this quality prediction, we test the reconstructed model against independent reference data. Differences between these two datasets are explained by the predicted uncertainty in the model. Map point heights can be reconstructed with an average precision of 10 to 15 cm, depending on the laser point configuration.

3D Building reconstruction

The building reconstruction task contains three main goals:

1. to select laser points belonging to building roofs,
2. to detect the roof structure of that building, and
3. to reconstruct the outlines of the roof.

We present a building reconstruction approach, which is based on a target graph matching algorithm as intermediate step to relate laser data with building models. Establishing this relation is important for adding building knowledge to the data. Our targets are topological representations of the most common roof structures which are stored in a database. Laser data is segmented into planar patches. The segments that are selected in the segment-in-polygon algorithm are considered initial roof segments. Topological relations between segments, in terms of intersection lines and height jumps, are represented in a building roof graph. These relations are labelled according to their geometry and that of the segments (e.g. same/opposite normal direction, convex/concave, tilted/horizontal). This graph is matched with the graphs from the target database. Matching results describe which target objects appear topologically in the data.

Our target based graph matching algorithm supports the first two goals. The matching algorithm performs a filtering task: data features that topologically correspond with common roof structures are considered to be part of the roof structure of that building. These data features will be transferred to our automated building reconstruction, where the outlines of the roof faces have to be reconstructed. Segments and intersection lines that do not fit to an existing target roof topology will be removed from the further automated reconstruction approach. The reconstruction algorithm covers the third main goal of our building reconstruction task.

For the geometric reconstruction, we present two approaches that vary in the amount of information they take from the data.

- The first, more data driven approach starts with laser data features that have been matched with target models. In general, the matched intersection lines represent the interior of the roof structure, so the task is to find an appropriate solution for the remaining roof edges, e.g. eaves and gutters. Map data is used for selection of roof segments and is taken as location for walls. Therefore we need to split up map polygons in order to build walls that distinguish various height levels, e.g. at step edge locations.
- The second, more model driven approach reconstructs parameterised building models. This approach relies more on geometric assumptions, such as roof symmetry, but the models can be refined if the data deviates significantly from the model. The target information includes the details on how these deviations are determined and on the thresholds to decide what is significant or not.

We present results of 3D reconstructed models, including several quality checks. These quality measures describe the completeness of the match results plus the correctness of assumptions to the roof outline. About 20% of the buildings are affected by segments

that did not completely match with the target graphs. In a few of these cases, this is correct because the segment is not representing a roof face. However, in about 40% of these cases, a neighbouring segment that would complete a target match is missing. Adapting processing parameters, such as minimum segment size, may improve the result but it may also disturb other topological relations. Setting the parameters is therefore an important task for the operator. Specially, parameters that define the segmentation algorithm are crucial as the segment is the key data feature in our building reconstruction algorithm.

In order to improve our matching algorithm, the likelihood of relations between segments could be included in the attribute list of edges in the roof topology graph. At the moment only information on the geometric appearance of the intersection line is given as attribute value to the corresponding graph edge. Future work includes defining likelihood functions for graph edges and analysing the effect of likelihood attributes.

Samenvatting

Introductie en doel van het onderzoek

Het promotieonderzoek behandelt de geautomatiseerde inwinning van drie dimensionale (3D) topografische objecten. We richten ons daarbij op de 3D reconstructie van wegen en gebouwen. Deze objecten zijn belangrijke elementen in digitale 3D modellen.

De onderzoeksactiviteiten verbinden drie versies van topografische objecten met elkaar:

1. hoe de objecten er in werkelijkheid uitzien;
2. hoe ze gerepresenteerd worden in de data, en
3. hoe ze gemodelleerd moeten worden in een 3D model.

Om een geautomatiseerde inwinning mogelijk te maken, is uitgegaan van bestaande 2D topografische bestanden. Deze worden geconverteerd naar 3D door laseraltimetriegegevens toe te voegen. In 3D modellen kunnen meerdere hoogtes op dezelfde locatie voorkomen en er kunnen zelfs meerdere objecten boven elkaar liggen.

Het onderliggende principe om van 2D wegen naar 3D wegen te komen, is wezenlijk anders dan het principe om 3D gebouwen uit 2D gebouwen te verkrijgen. Dat komt omdat voor wegen het doel is om de zijkanten van de weg in 3D vast te leggen, en de weg zelf als een (getrianguleerd) vlak te beschouwen tussen de 3D zijkanten. Voor 3D gebouwen is het juist van belang te kijken naar wat de 3D vorm is van dakdelen binnen de omlijning (muren) van het gebouw.

3D wegen

Kijkend naar de aansprekende 3D situaties voor wegobjecten, dan komen we al snel uit bij viaducten en complexere knooppunten. Op die locaties bevinden zich meerdere wegdelen boven elkaar. Ons onderzoek richt zich op deze situaties. Om een goede combinatie van laseraltimetriegegevens en 2D topografie mogelijk te maken, is gekeken naar algemene kennis over hoe de weg in werkelijkheid verloopt. Deze kennis is geïntegreerd in onze automatische reconstructiemethode. Een voorbeeld van deze kennis is dat een weg een glad, niet abrupt, hoogteverloop kent. Daarom zijn kleine objecten uit de laser data gefilterd (bijvoorbeeld data op auto's en verkeersmeubilair) om zo alleen de laser data van de wegvlak over te houden. Aan de hand van deze punten kan beredeneerd worden hoe de weg lokaal verloopt. Deze gefilterde data wordt samengevoegd met 2D topografische objecten op basis van de horizontale en de verticale positie. Dit laatste is noodzakelijk om een goede samenvoeging te krijgen op de plekken waar wegen elkaar kruisen. Laserdata op het bovenliggende wegvlak, dient immers niet samengevoegd te worden met het onderliggende wegvlak. De hoogte van de zijkanten van de weg wordt verkregen door een mathematisch vlak te berekenen door de laserpunten in de buurt van die zijkant. De hoogte van het vlak op de positie van de zijkant van de weg wordt vastgelegd als 3D positie.

Een goede kwaliteitsbeschrijving is belangrijk, zowel tijdens de opbouw van het algoritme als tijdens het gebruik van de 3D data. De kwaliteit van de berekende 3D

posities is afhankelijk van de input data en de verwerkingsstappen. We berekenen de precisie van de gereconstrueerde hoogtes door middel van de foutenvoortplanting van de precisie van de input data. Dit wordt de geschatte precisie genoemd. Naast deze schatting, zijn de hoogtes ook getoetst aan de hand van referentiemetingen. Verschillen tussen de referentiemetingen en de gereconstrueerde hoogtes kunnen worden verklaard aan de hand van de geschatte precisie van ons model. Afhankelijk van de configuratie van de laser punten ligt de gemiddelde precisie van de gereconstrueerde hoogte van de zijkanten van de weg tussen de 10 en 15 centimeter.

3D gebouwen

De 3D gebouwreconstructie bestaat uit drie hoofdtaken:

1. selecteren van laser data die op dakvlakken liggen,
2. detecteren van dakvormen van elk gebouw, en
3. reconstrueren van de dakomlijning.

Onze gebouwreconstructie is gebaseerd op een zogenaamde ‘target graph matching’ algoritme. Dat betekent dat we kenmerken die in de laserdata gevonden kunnen worden, gerelateerd (gematched) worden met gebouwmodellen (targets) uit een database. Deze relatie is belangrijk om kennis over gebouwen toe te voegen aan de corresponderende laserdata. De targets zijn topologische beschrijvingen van de meest voorkomende dakvormen, die worden vastgelegd in een graaf. Elke graaf bestaat uit knopen (dakvlakken) en lijnen. Elke lijn beschrijft een relatie (bijvoorbeeld snijlijn) tussen twee dakvlakken. De laserdata wordt gesegmenteerd. Ieder segment bestaat uit laserpunten die in een bepaald 3D vlak liggen. De segmenten die zich (grotendeels) binnen een gebouwpolygoon bevinden worden geselecteerd als voorlopig daksegment. De daksegmenten vormen samen met de snijlijnen en hoogtesprongen tussen twee naburige segmenten, een graaf van dakvlakken. Deze graaf bestaat dus uit knopen (de segmenten) en lijnen (de relatie tussen twee segmenten). De lijnen zijn gelabeld aan de hand van de geometrie van de relatie tussen twee segmenten en van de segmenten zelf. Bijvoorbeeld krijgen alle horizontale snijlijnen tussen daksegmenten met tegengestelde richting hetzelfde label. Deze graaf wordt gematched met de topologische beschrijvingen van de meest voorkomende dakvormen, ofwel de targetgraaf. Het resultaat van het matchingalgoritme beschrijft welke dakvormen voorkomen en welke data daaraan gerelateerd is.

De matching is van belang voor de uitvoering van de eerste twee hoofdtaken. Ten eerste worden segmenten die niet tot een bepaald dakmodel horen, eruit gefilterd. De overgebleven segmenten hebben allen een bepaalde relatie met een bestaand dakmodel. Deze segmenten gaan naar de automatische dakreconstructiemodule, waar de omlijning van elk daksegment bepaald wordt. Dit wordt de geometrische reconstructie van de omlijning van gebouwdaken genoemd. De geometrische reconstructie is het derde deel van de gebouwreconstructie en hebben we op twee manieren bepaald.

- De eerste, meer datagestuurde aanpak combineert alle segmenten en snijlijnen die gematched zijn met één of meerdere targetmodellen. Over het algemeen representeren de snijlijnen tussen twee daken de interne structuur van het dak (bijvoorbeeld de noklijn), dus de taak is om de buitenkant van het dak (bijvoorbeeld de goot) te reconstrueren. De gebouwpolygoon uit de 2D

topografische kaart worden gebruikt voor de locatie van de muren van het gebouw. De polygonen worden gesplitst als er een hoogtesprong binnen het gebouw optreedt om op die locatie een muur neer te kunnen zetten.

- De tweede, meer modelgestuurde aanpak gaat uit van een geparаметeriseerd model van de target die gematched zijn met de data. Deze aanpak is meer gebaseerd op geometrische aannames, zoals de aanname dat een dak symmetrisch is, maar kan worden aangepast als de data daar aanleiding toe geeft. Het targetmodel bevat informatie over de wijze waarop omgegaan moet worden met verschillen tussen data en een gereconstrueerd model.

In dit proefschrift beschrijven wij het opbouwproces en de resultaten van 3D gebouwreconstructies. Deze modellen worden ook voorzien een kwaliteitsbeschrijving. Deze beschrijven de volledigheid van het matchingsproces en de kwaliteit van de aannames over de omlijning van de daken. Ongeveer 20% van de gebouwen bezit een segment dat niet gerelateerd kan worden aan een targetmodel. We noemen deze segmenten onderdeel van een niet volledige match. In enkele van deze gevallen is dat een goed teken, omdat dat segment daadwerkelijk geen deel uitmaakt van een dakvorm. Echter, in ongeveer 40% van deze gevallen is een gebrek aan een ander segment, de oorzaak van de niet volledige match. Aanpassen van de verwerkingsparameters, bijvoorbeeld de segmentatieparameters, zouden de resultaten kunnen verbeteren, maar kan voor andere situaties de resultaten verslechteren. Daarom is het van belang om de goede verwerkingsparameters vast te stellen. Vooral de segmentatieparameters zijn belangrijk omdat elk segment behandeld wordt als dakvlak en daarom als belangrijk element fungeert in de gehele gebouwreconstructie.

Een mogelijkheid om ons matchingalgoritme te verbeteren is het toevoegen van waarschijnlijkheden aan de elementen in het target model. Op dit moment wordt alleen de geometrische informatie van een snijlijn vastgelegd als label van de bijbehorende lijn in een graaf. Toekomstig onderzoek bevat het vaststellen van waarschijnlijkheden van snijlijnen en het analyseren van het effect van deze waarschijnlijkheden op het matchingsresultaat en op het uiteindelijke 3D gebouwmodel.

ITC Dissertation List

http://www.itc.nl/research/phd/phd_graduates.aspx

Curriculum Vitae

Sander Oude Elberink (Almelo, The Netherlands, 1976) graduated as Geodetic Engineer from Delft University of Technology in 2000. His master research was on classification of airborne laser scanner data using anisotropic texture measures, performed in the Section of Photogrammetry and Remote Sensing. At that same Section, he joined as researcher on 3D reconstruction from line scanner imagery. From 2001 till 2005 he worked as research consultant and project manager at the Survey department of Rijkswaterstaat in Delft. His tasks were to assess and to improve quality for airborne, terrestrial and hydrographic data acquisition projects.

September 2005 Sander started his PhD research on “Acquisition of 3D topography” at the International Institute for Geo-Information Science and Earth observation (ITC) Enschede. His research was part of the project ‘3D Topography’ which received the RGI Innovation Award in the category science in 2007. He received a young author’s award for best paper at the ISPRS congress in Beijing, China in 2008. In 2009 Sander received the ITC research award for best ISI paper. The paper, co-authored by George Vosselman, was about 3D road reconstruction and published in the Photogrammetric Record. From September 2009 Sander holds a position of assistant professor at the department of Earth Observation Science at ITC. His main research and educational responsibilities are (semi-) automated acquisition of (3D) geo-information.